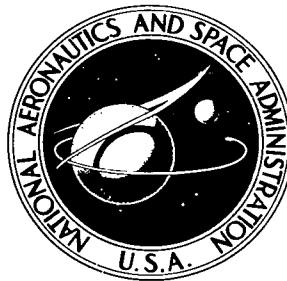


NASA TECHNICAL NOTE



NASA TN D-6480

C.1



LOAN COPY: RETUR
AFWL (DOUL)
KIRTLAND AFB, N. M.

NASA TN D-6480

COMPARISONS OF THEORETICAL AND
EXPERIMENTAL PRESSURE DISTRIBUTIONS
OVER A WING-BODY MODEL
AT HIGH SUPERSONIC SPEEDS

by Lloyd S. Jernell

*Langley Research Center
Hampton, Va. 23365*

1. Report No. NASA TN D-6480		2. Government Accession No.		0133321	
4. Title and Subtitle COMPARISONS OF THEORETICAL AND EXPERIMENTAL PRESSURE DISTRIBUTIONS OVER A WING-BODY MODEL AT HIGH SUPERSONIC SPEEDS		5. Report Date September 1971		6. Performing Organization Code	
7. Author(s) Lloyd S. Jernell		8. Performing Organization Report No. L-7881		9. Performing Organization Name and Address NASA Langley Research Center Hampton, Va. 23365	
10. Work Unit No. 136-13-01-05		11. Contract or Grant No.		12. Sponsoring Agency Name and Address National Aeronautics and Space Administration Washington, D.C. 20546	
13. Type of Report and Period Covered Technical Note		14. Sponsoring Agency Code		15. Supplementary Notes	
16. Abstract An investigation has been conducted to determine the effectiveness of various theoretical methods in predicting the pressure distribution over a wing-body configuration at high supersonic speeds. Theoretical pressure coefficients are compared with experimental values obtained on a delta planform wing-body model in the Langley Unitary Plan wind tunnel at Mach numbers from 2.30 to 4.63 and angles of attack to approximately 11°.					
17. Key Words (Suggested by Author(s)) Pressure distribution Wing-body configuration Prandtl-Meyer expansion Shock-expansion method Linear-theory methods		18. Distribution Statement Unclassified - Unlimited			
19. Security Classif. (of this report) Unclassified		20. Security Classif. (of this page) Unclassified		21. No. of Pages 83	
				22. Price* \$3.00	

COMPARISONS OF THEORETICAL AND EXPERIMENTAL
PRESSURE DISTRIBUTIONS OVER A WING-BODY MODEL AT
HIGH SUPERSONIC SPEEDS

By Lloyd S. Jernell
Langley Research Center

SUMMARY

An investigation has been conducted to determine the effectiveness of various theoretical methods in predicting the pressure distribution over a wing-body configuration at high supersonic speeds. Theoretical pressure coefficients are compared with experimental values obtained on a delta planform wing-body model in the Langley Unitary Plan wind tunnel at Mach numbers from 2.30 to 4.63 and angles of attack to approximately 11° .

For bodies of fineness ratio similar to the fuselage forebody of the present investigation, the data indicate that at Mach numbers near and above 4.63 the conical-shock-expansion method may be considered accurate enough for many engineering purposes.

At Mach numbers of 3.95 and 4.63 the experimental pressure distributions over the wing surfaces affected by expanded flow are essentially constant.

The linear-theory methods used to predict the wing pressures are in reasonable agreement with the experimental data throughout the test Mach number range.

At the higher Mach numbers the Prandtl-Meyer expansion method (from free-stream conditions) affords good agreement with the experimental data over the wing upper surfaces at angle of attack.

Although some pressure gradient exists over each of the flat lower wing surfaces at angle of attack at Mach number equal to 4.63, the two-dimensional shock-expansion method provides an accurate estimate of the average pressure coefficient for each surface.

INTRODUCTION

In the field of aeronautical research there is a continuous effort toward the development of new methods with greater reliability for predicting the aerodynamic characteristics of flight vehicles. Considerable progress has been made in recent years utilizing various theories and numerical procedures in conjunction with the electronic computer to provide methods by which the engineer can make quicker and more precise evaluations of

relatively complex configurations (refs. 1 to 3). To date most of the computer programs dealing with supersonic aerodynamics have been based on the linear theory. Due to its basic assumption of small perturbations (pressure disturbances small in comparison with static pressure) this theory would be expected to be most effective in the lower supersonic speed range and to exhibit a decrease in reliability at the higher Mach numbers. It is understandable, therefore, that most of the work based on this theory has been concentrated in the lower supersonic speed range to Mach numbers of about 3.

There presently exists the need to determine the effectiveness of these and other theoretical methods in predicting the aerodynamic characteristics of flight vehicles in the high supersonic speed range. The data of reference 4 indicate that for some wing planforms the computerized lift program (based on linear theory, see ref. 2) used in that investigation provides good agreement with experiment for Mach numbers to 4.63. Also, data from previous investigations, such as those of references 5 to 7, indicate that the pressure distribution over essentially flat lifting surfaces at moderate angles of attack becomes relatively constant as hypersonic speeds are approached; and in many instances, the pressure distribution may be approximated by theories based on two-dimensional or conical flows. With regard to the fuselage, several methods which have been considered for predicting the flow fields about slender bodies of revolution at high supersonic speeds are discussed in references 8 to 10.

The purpose of the present investigation is to determine the effectiveness of various theoretical methods in predicting the pressure distribution over a wing-body configuration at high supersonic speeds. Theoretical pressure coefficients are compared with the experimental values obtained on a delta planform wing-body model at Mach numbers from 2.30 to 4.63.

SYMBOLS

b	wing span
c	local wing chord
C_p	pressure coefficient, $\frac{p_l - p_\infty}{q_\infty}$
l	body length
M	Mach number
p_l	local static pressure

p_{∞}	free-stream static pressure
q_{∞}	free-stream dynamic pressure
x	longitudinal distance measured from body nose or wing leading edge
y	lateral distance measured from body center line
α	angle of attack measured from body center line, deg
ϕ	body meridian angle measured from top, deg

Subscripts:

b	body
w	wing

APPARATUS AND METHODS

Model

A drawing of the model is presented in figure 1. The forward 70 percent of the fuselage was contoured according to the method described in reference 11, which predicts the profile required for minimizing the wave drag (in this case for a body of specified length and base diameter). The remaining aft section of the fuselage was cylindrical. The wing had a delta planform of 65° leading-edge sweep and a symmetrical double-wedge airfoil section of 6-percent thickness. Pressure orifices were located along the surface of the upper left quadrant of the fuselage and on the upper surface of the left wing. Thus, since the configuration was symmetrical with respect to the horizontal plane, pressure measurements could be obtained over the entire configuration by the appropriate selection of the test angles of attack.

Tunnel

The investigation was conducted in the high Mach number test section of the Langley Unitary Plan wind tunnel, which is a variable-pressure continuous-flow facility. The test section is approximately 1.2 meters square by 2.1 meters long. The nozzle leading to the test section is of the asymmetric sliding-block type, which permits a continuous variation in Mach number from 2.3 to 4.7.

Measurements, Corrections, and Tests

The pressures were measured with the use of two multi-channel electrical transducers having a maximum variation of 34 475 N/m² and an accuracy within 345 N/m². Boundary-layer transition strips approximately 1.6 mm wide were placed 10 mm rearward (streamwise) of the wing leading edge and 30.5 mm rearward of the nose apex. The strips were composed of No. 40 carborundum grains embedded in a plastic adhesive.

The test angle-of-attack range was approximately $\pm 10^\circ$. The angles of attack have been corrected for tunnel flow angularity and for deflection of the model support system due to load. The tests were conducted at Mach numbers from 2.30 to 4.63 and at a Reynolds number of 9.84×10^6 per meter. The dewpoint was maintained below 239 K to prevent moisture condensation effects.

PRESENTATION OF RESULTS

The results of this investigation are presented in the following figures:

	Figure
Experimental pressure coefficients over body; $M = 2.30$	2
Experimental pressure coefficients over body; $M = 2.96$	3
Experimental pressure coefficients over body; $M = 3.95$	4
Experimental pressure coefficients over body; $M = 4.63$	5
Comparison of body experimental data with conical-shock-expansion method; $\alpha = 0$	6
Comparison of body experimental data with conical-shock-expansion method; $\alpha = 6.2^\circ$; $M = 4.63$	7
Experimental pressure coefficients over wing; $M = 2.30$	8
Experimental pressure coefficients over wing; $M = 2.96$	9
Experimental pressure coefficients over wing; $M = 3.95$	10
Experimental pressure coefficients over wing; $M = 4.63$	11
Comparison of wing experimental data with linear-theory method; $\alpha = 6.7^\circ$; $M = 2.30$	12
Comparison of wing experimental data with linear-theory method; $\alpha = 6.5^\circ$; $M = 2.96$	13
Comparison of wing experimental data with linear-theory method; $\alpha = 6.4^\circ$; $M = 3.95$	14
Comparison of wing experimental data with linear-theory method; $\alpha = 6.2^\circ$; $M = 4.63$	15
Comparison of wing experimental data with various theories; $\alpha \approx 6^\circ$	16
Comparison of wing experimental data with various theories; $\alpha \approx 11^\circ$	17

DISCUSSION

The experimental pressure coefficients measured over the body are shown in figures 2 to 5. The data over the nose section forward of the wing generally exhibit the expected higher values near the nose, followed by a decrease in C_p as the flow expands rearward. For $\frac{x_p}{l} \geq 0.5$ the effects of wing interference become noticeable, particularly over the lower body surface at angle of attack.

For the Mach numbers and angles of attack considered in this investigation, the most accurate technique for predicting the pressure coefficients over the forebody likely would be that of reference 8, which utilizes the method of characteristics. However, due to the relatively large amount of time required to employ that procedure, recourse was made to the comparatively simple conical-shock-expansion method considered in reference 10 wherein it is assumed that the flow at the nose apex is conical and expands two-dimensionally along the body meridian lines. In figure 6 the pressure coefficients predicted by this method are compared with experimental values at zero angle of attack for Mach numbers of 2.30 and 4.63. It should be pointed out that no attempt was made to account for the effects of wing interference which begin at $\frac{x_p}{l} \approx 0.5$. As expected, the agreement is relatively poor at $M = 2.30$ but improves considerably as Mach number is increased to 4.63. A comparison of theory with experiment at $M = 4.63$ and $\alpha = 6.2^\circ$ is shown in figure 7. As expected, the theoretical data predict a relatively low pressure at $\phi = 0$ and an increase in C_p as ϕ is varied to 180° ; however, the experimental data indicate a higher pressure at $\phi = 0$ than would be expected in comparison with the other experimental data and theory. It is believed that this increased static pressure may be attributed to the merging of the crossflow at the $\phi = 0$ meridian plane. For bodies of fineness ratio similar to that considered herein (≈ 8.4), these data indicate that at Mach numbers near and above 4.63 the conical-shock-expansion method may be considered accurate enough for many engineering purposes.

The experimental data for the wing are presented in figures 8 to 11. At the lower Mach numbers the data exhibit considerable variation of pressure coefficient in both the chordwise and spanwise directions. However, these gradients diminish as Mach number is increased. At Mach numbers of 3.95 and 4.63 the pressure distributions over the wing surfaces affected by expanded flow are essentially constant.

Comparisons of the wing experimental pressure coefficients with the linear-theory method are shown in figures 12 to 15 for an angle of attack of approximately 6° . The lift-induced pressure was calculated with the use of a computer program based on the method described in reference 2. In that approach the model is described to the computer as a plate the planform of which is representative of the configuration. The curvature of the plate is determined by the mean camber of the wing, the fuselage curvature, and the

vertical position of the wing relative to the fuselage. To account for the effects of wing thickness, an incremental pressure was added to the lift-induced pressure. The procedure is based on the application of supersonic sources to thin wings, as described in reference 12. As previously mentioned, the theoretical data would be expected to become less effective as Mach number is increased. However, for this particular configuration at least, the combination of the two methods produces results which are in reasonable agreement with the experimental data throughout the test Mach number range.

Comparisons of the wing experimental pressure coefficients with the predictions of various other theories are shown in figure 16 for an angle of attack of approximately 6° . The effects of body interference have been neglected in the theoretical calculations. As expected, none of these methods is effective in predicting the pressure coefficients at $M = 2.30$. Especially noteworthy in the disagreement are the relatively large experimental pressure gradients over the wing surfaces, in contrast to the constant values (per flat surface) predicted by the theoretical methods. As previously mentioned, the experimental pressure gradients over the wing surfaces greatly decrease as Mach number is increased. At the higher Mach numbers the Prandtl-Meyer expansion from free-stream conditions (P-M expan. from free stream) affords good agreement with the experimental data over the upper surfaces. Although a considerable gradient remains over the lower forward wing surface at the higher Mach numbers, the tangent-wedge (or oblique-shock) method provides a good estimate of the average pressure coefficient. At $M = 4.63$ the Prandtl-Meyer expansion from the tangent-wedge value of the forward surface (commonly referred to as the shock-expansion method) provides good agreement of theory with the average experimental pressure coefficient over the lower rearward surface. Figure 17 presents a comparison of these theories with the experimental data at an angle of attack of approximately 11° . The relationship between the theoretical and experimental values is very similar to that at $\alpha \approx 6^\circ$.

CONCLUSIONS

An investigation has been conducted to determine the effectiveness of various theoretical methods in predicting the pressure distribution over a wing-body configuration at Mach numbers from 2.30 to 4.63. The results are summarized as follows:

1. For bodies of fineness ratio similar to the fuselage forebody considered herein the data indicate that at Mach numbers near and above 4.63 the conical-shock-expansion method may be considered accurate enough for many engineering purposes.
2. At Mach numbers of 3.95 and 4.63 the experimental pressure distributions over the wing surfaces affected by expanded flow are essentially constant.

3. The linear-theory methods used to predict the wing pressures are in reasonable agreement with the experimental data throughout the test Mach number range.

4. At the higher Mach numbers the Prandtl-Meyer expansion method from free-stream conditions affords good agreement with the experimental data over the wing upper surfaces at angle of attack.

5. Although some pressure gradient exists over each of the flat lower wing surfaces at angle of attack at Mach number equal to 4.63, the two-dimensional shock-expansion method provides an accurate estimate of the average pressure coefficient for each surface.

Langley Research Center,
National Aeronautics and Space Administration,
Hampton, Va., August 12, 1971.

REFERENCES

1. Carlson, Harry W.; and Middleton, Wilbur D.: A Numerical Method for the Design of Camber Surfaces of Supersonic Wings With Arbitrary Planforms. NASA TN D-2341, 1964.
2. Middleton, Wilbur D.; and Carlson, Harry W.: A Numerical Method for Calculating the Flat-Plate Pressure Distributions on Supersonic Wings of Arbitrary Planform. NASA TN D-2570, 1965.
3. Carmichael, Ralph L.; and Woodward, Frank A.: An Integrated Approach to the Analysis and Design of Wings and Wing-Body Combinations in Supersonic Flow. NASA TN D-3685, 1966.
4. Jernell, Lloyd S.: Longitudinal Aerodynamic Characteristics of Wing-Body Models With Arrow, Delta, and Diamond Planforms at Mach Numbers from 2.30 to 4.63 and Comparisons With Theory. NASA TM X-1522, 1968.
5. Murray, William M., Jr.; and Stallings, Robert L., Jr.: Heat-Transfer and Pressure Distributions on 60° and 70° Swept Delta Wings Having Turbulent Boundary Layers. NASA TN D-3644, 1966.
6. Bertram, Mitchel H.; and Everhart, Philip E.: An Experimental Study of the Pressure and Heat-Transfer Distribution on a 70° Sweep Slab Delta Wing in Hypersonic Flow. NASA TR R-153, 1963.
7. Dorrance, William H.: Two-Dimensional Airfoils at Moderate Hypersonic Velocities. J. Aeronaut. Sci., vol. 19, no. 9, Sept. 1952, pp. 593-600.
8. Ferri, Antonio: The Method of Characteristics for the Determination of Supersonic Flow Over Bodies of Revolution at Small Angles of Attack. NACA Rep. 1044, 1951.
9. Van Dyke, Milton D.: A Study of Hypersonic Small-Disturbance Theory. NACA Rep. 1194, 1954.
10. Eggers, A. J., Jr.; and Savin, Raymond C.: A Unified Two-Dimensional Approach to the Calculation of Three-Dimensional Hypersonic Flows, With Applications to Bodies of Revolution. NACA Rep. 1249, 1955.
11. Haack, W. (K. W. Mosauer, transl.): Projectile Forms of Minimum Wave Resistance. Douglas Aircraft Co., Inc., #288, May 7, 1946.
12. Jones, Robert T.: Thin Oblique Airfoils at Supersonic Speed. NACA Rep. 851, 1946.

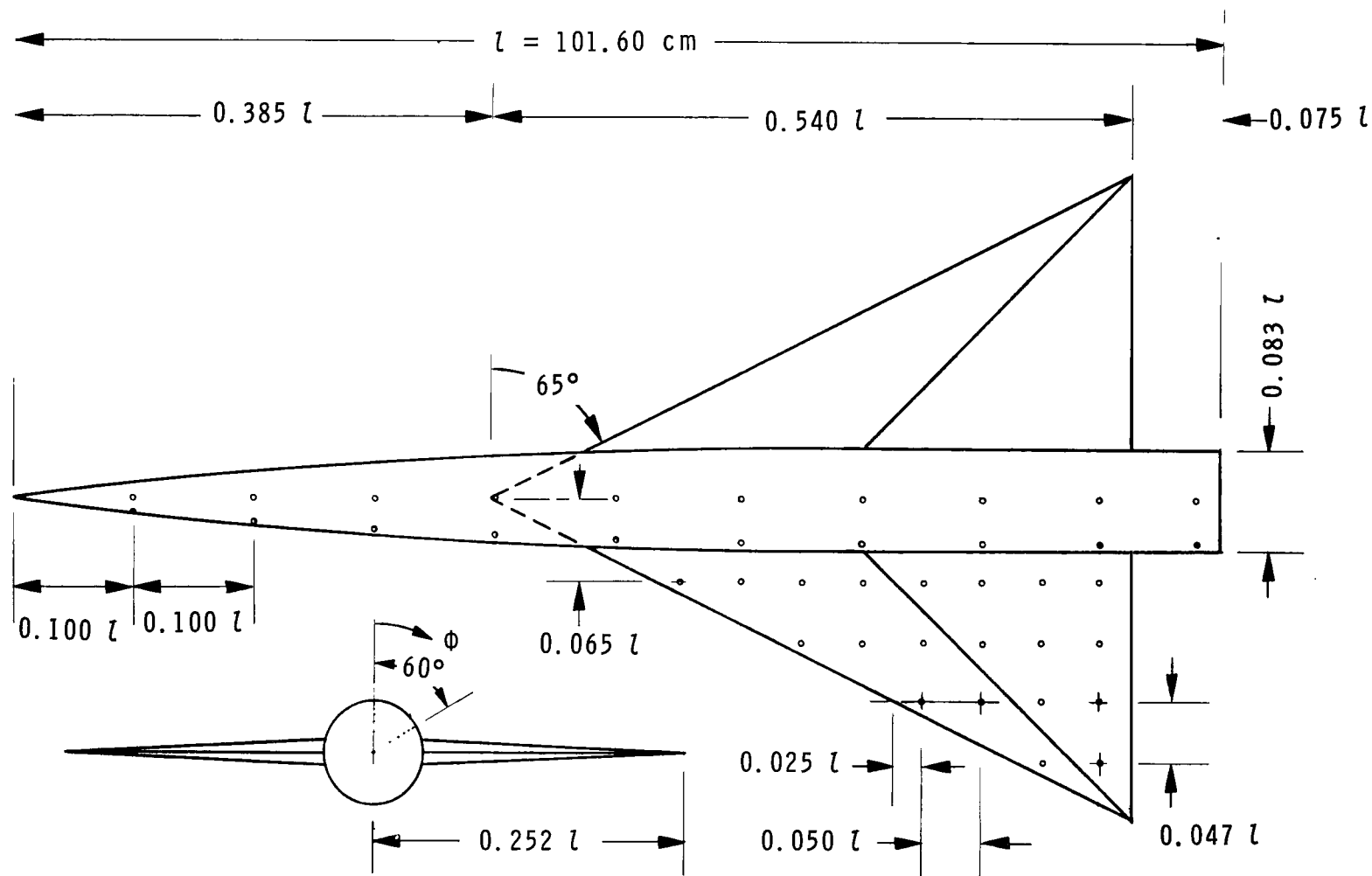


Figure 1.- Sketch of model showing location of pressure orifices.

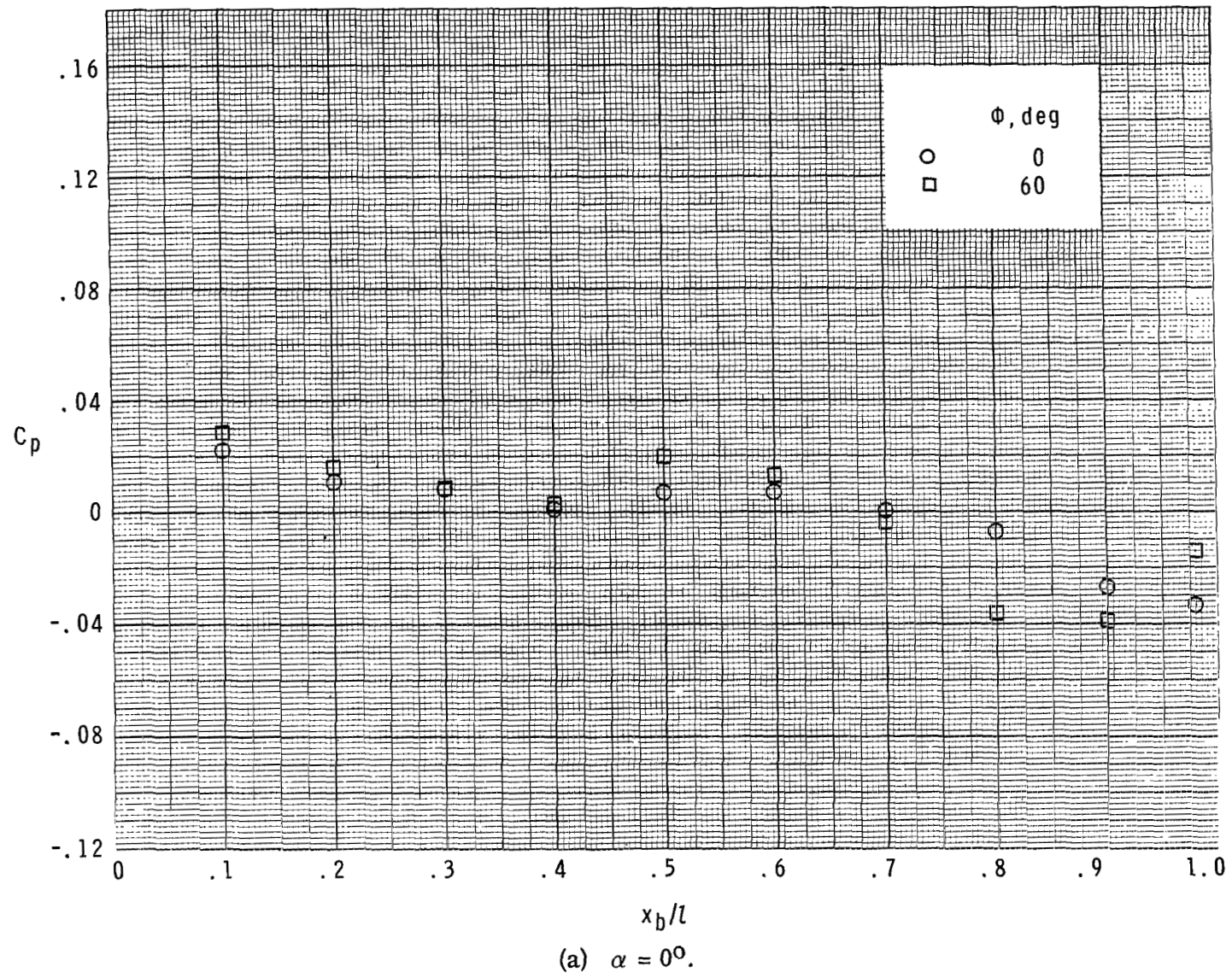
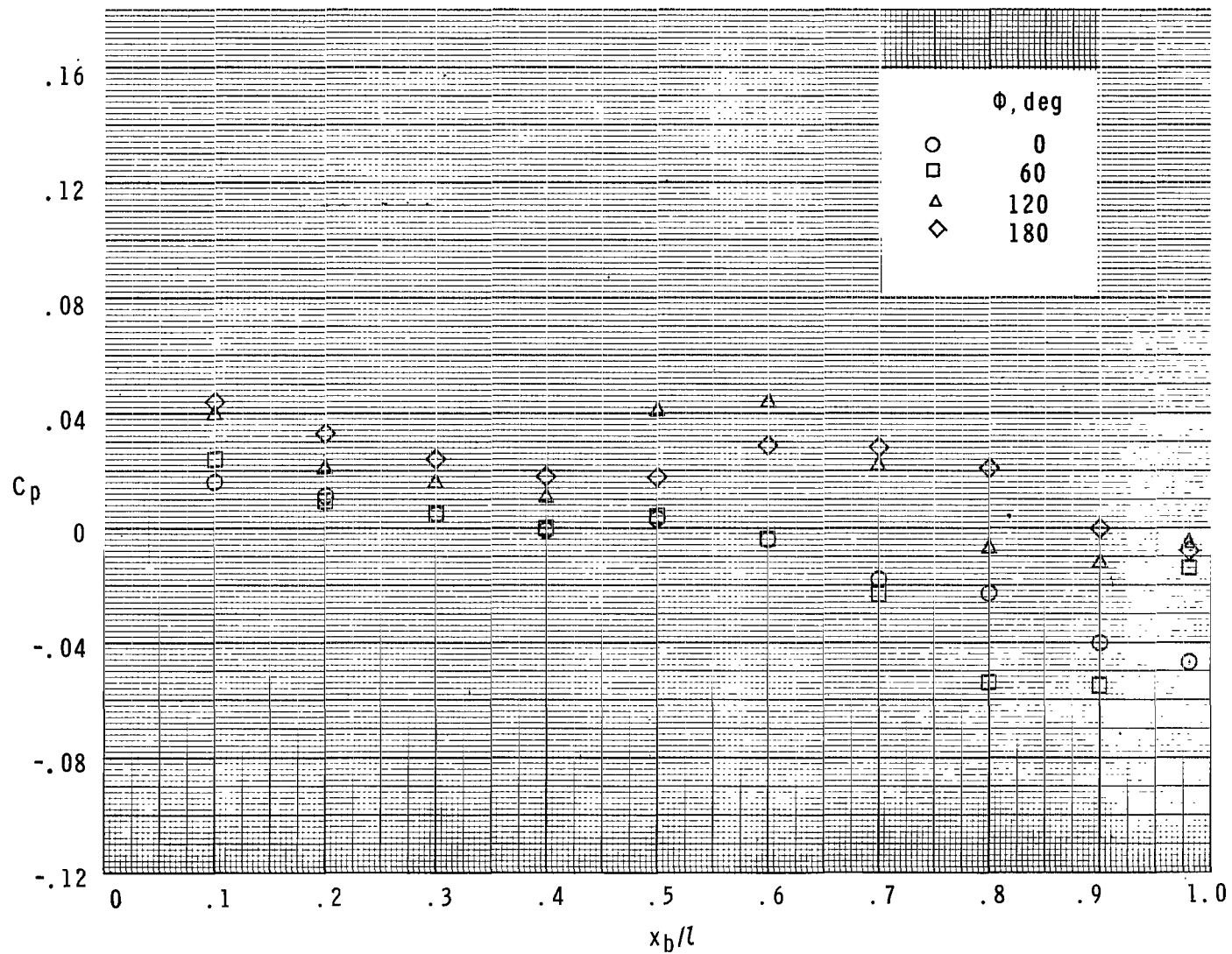
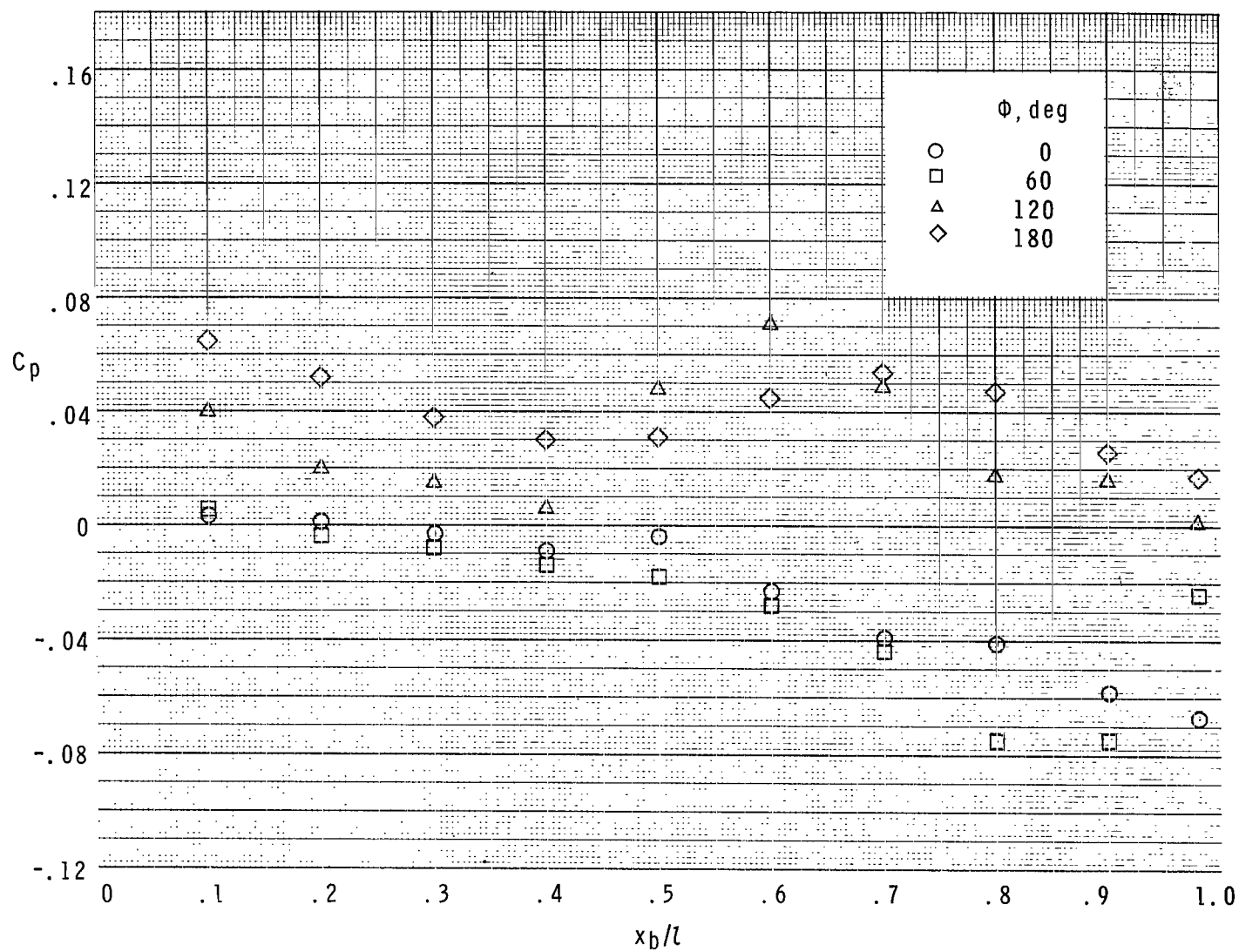


Figure 2.- Experimental pressure coefficients over body; $M = 2.30$.



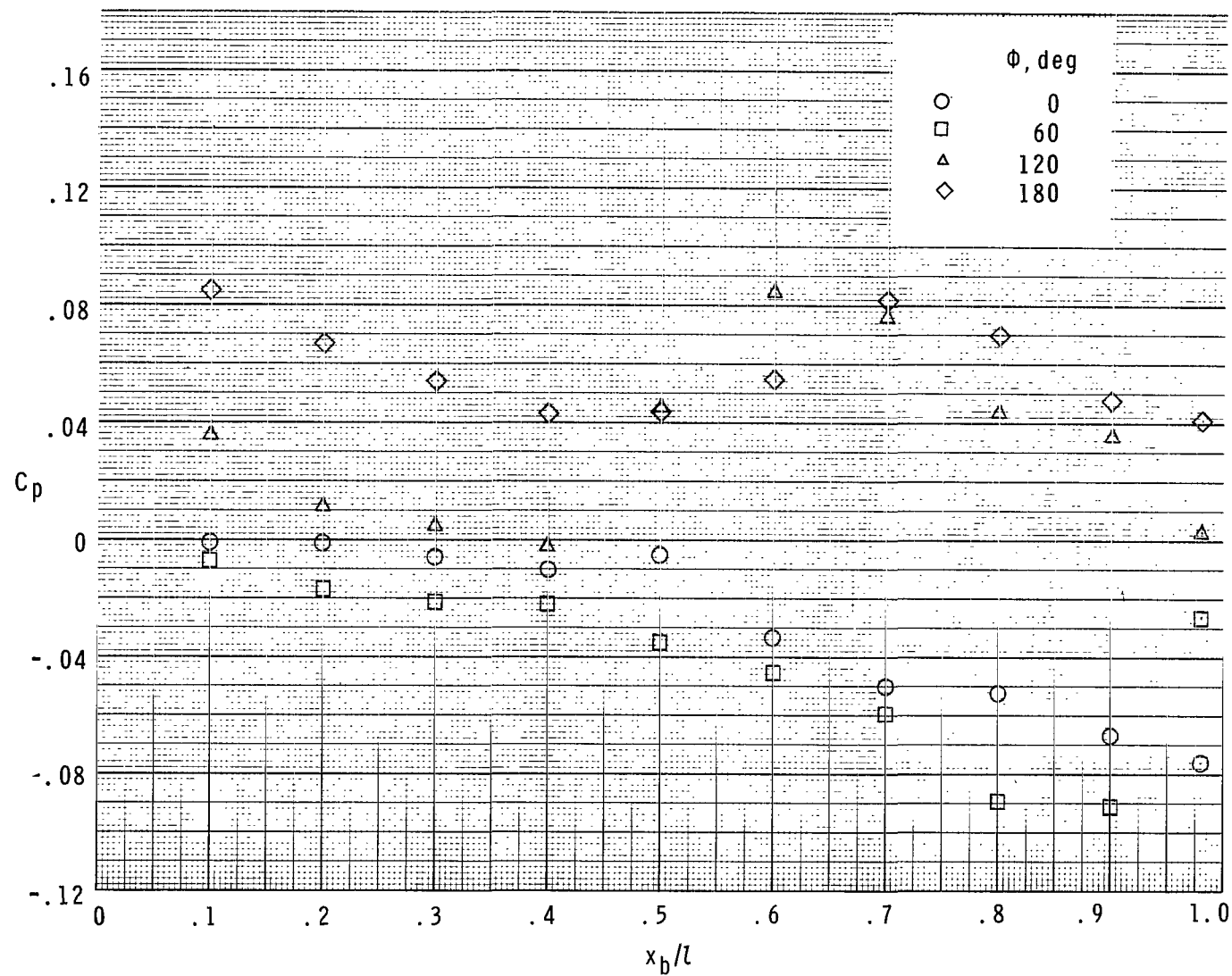
(b) $\alpha = 2.2^\circ$.

Figure 2.- Continued.



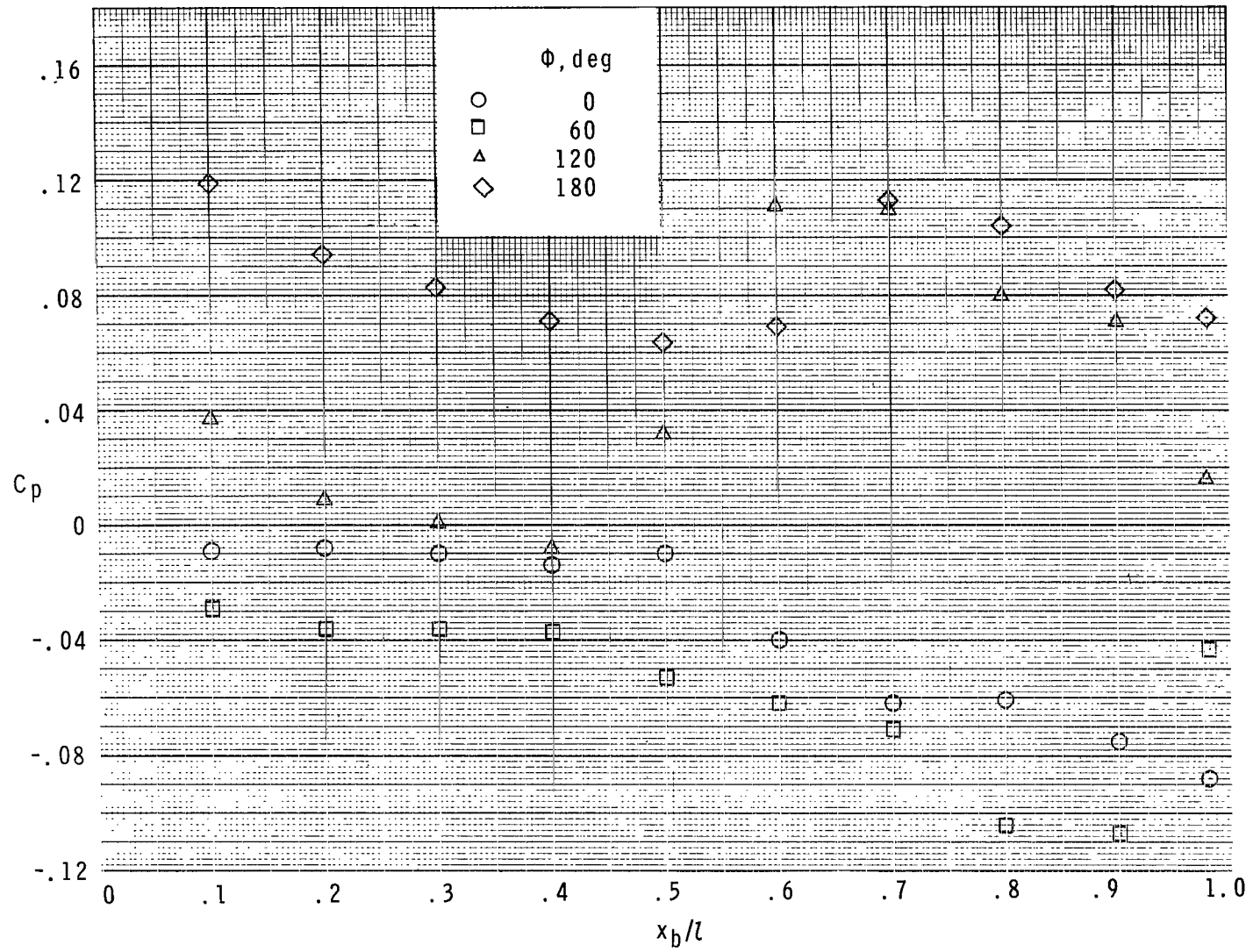
(c) $\alpha = 4.5^\circ$.

Figure 2.- Continued.



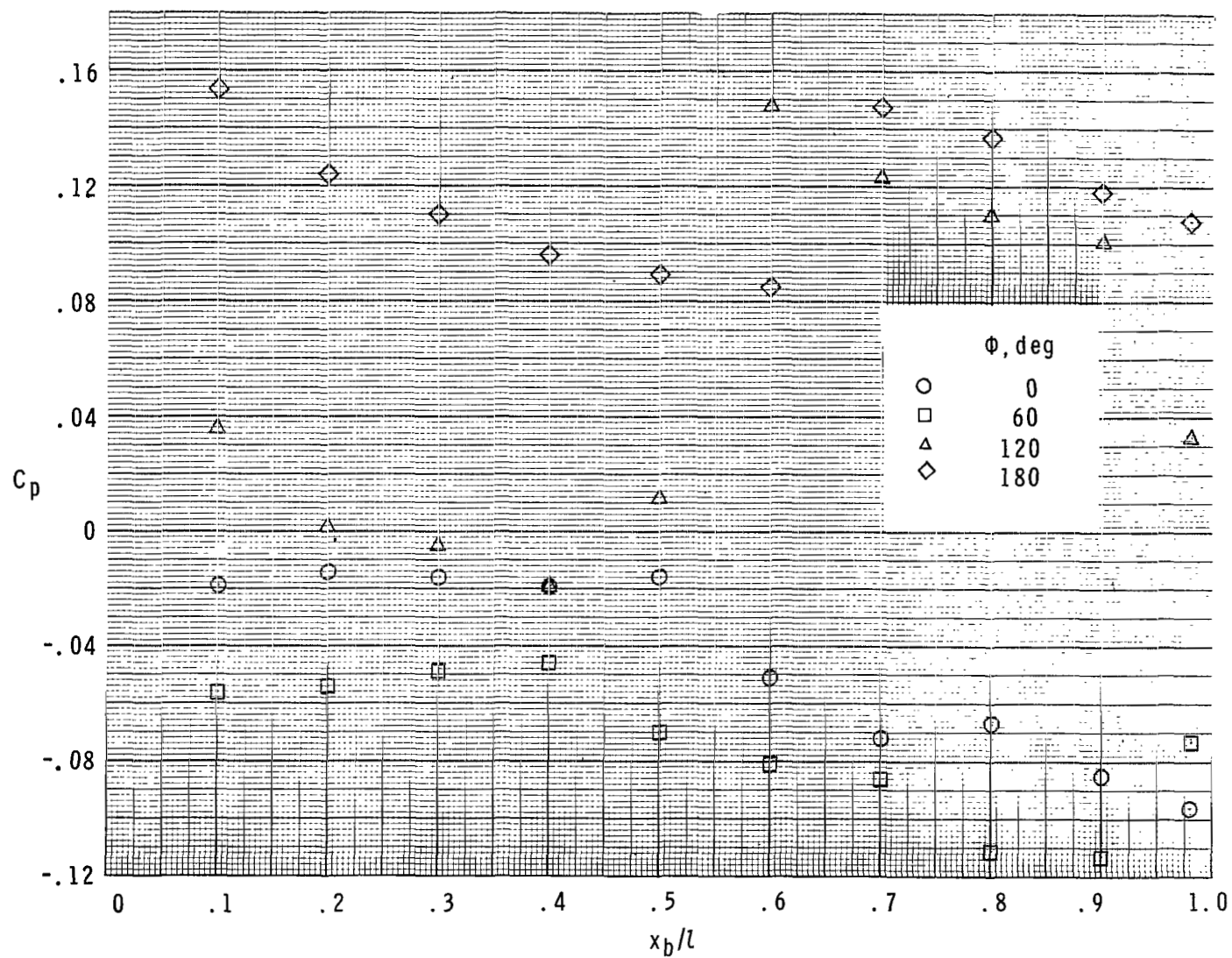
(d) $\alpha = 6.7^\circ$.

Figure 2.- Continued.



(e) $\alpha = 8.8^\circ$.

Figure 2.- Continued.



(f) $\alpha = 11.1^\circ$.

Figure 2.- Concluded.

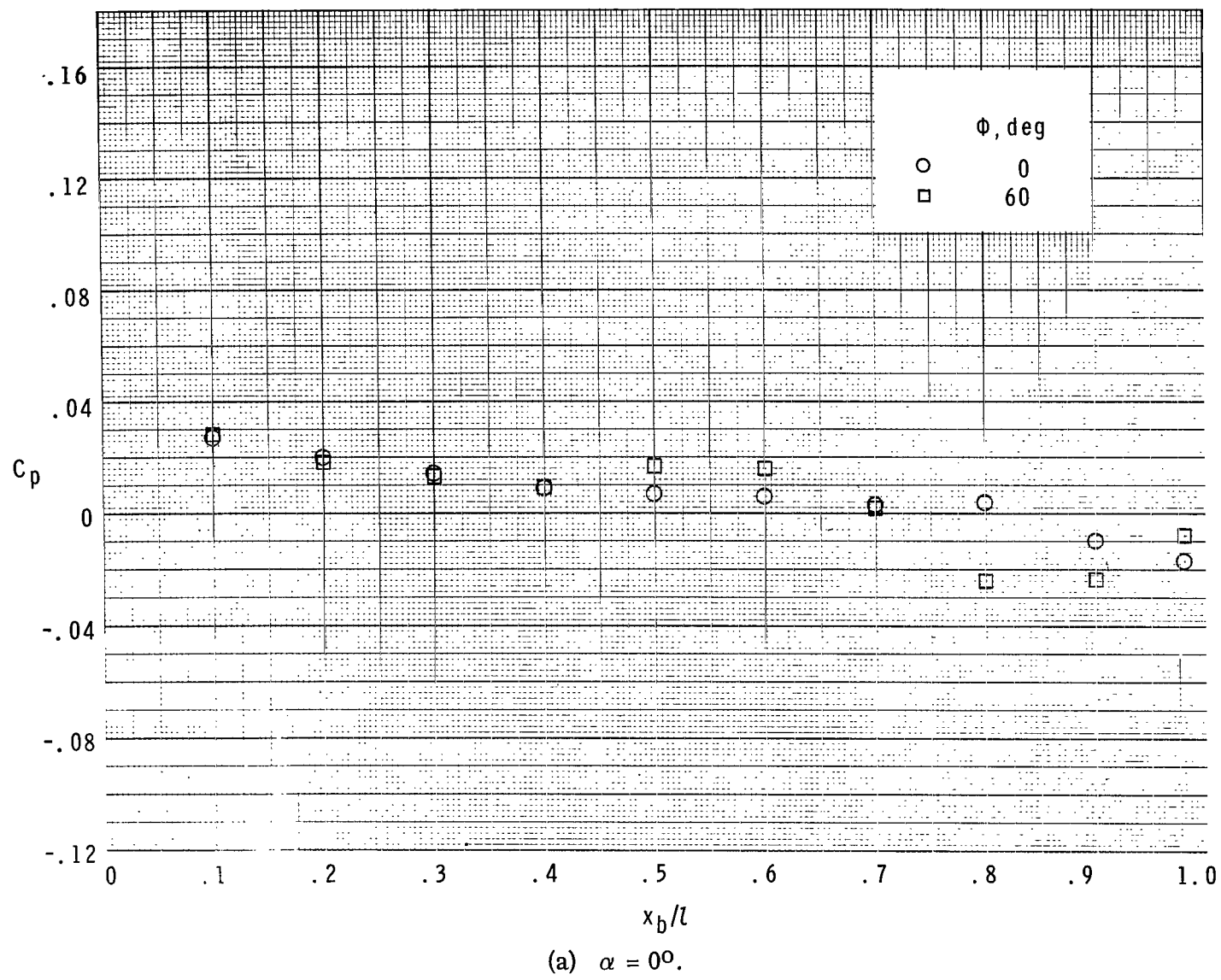
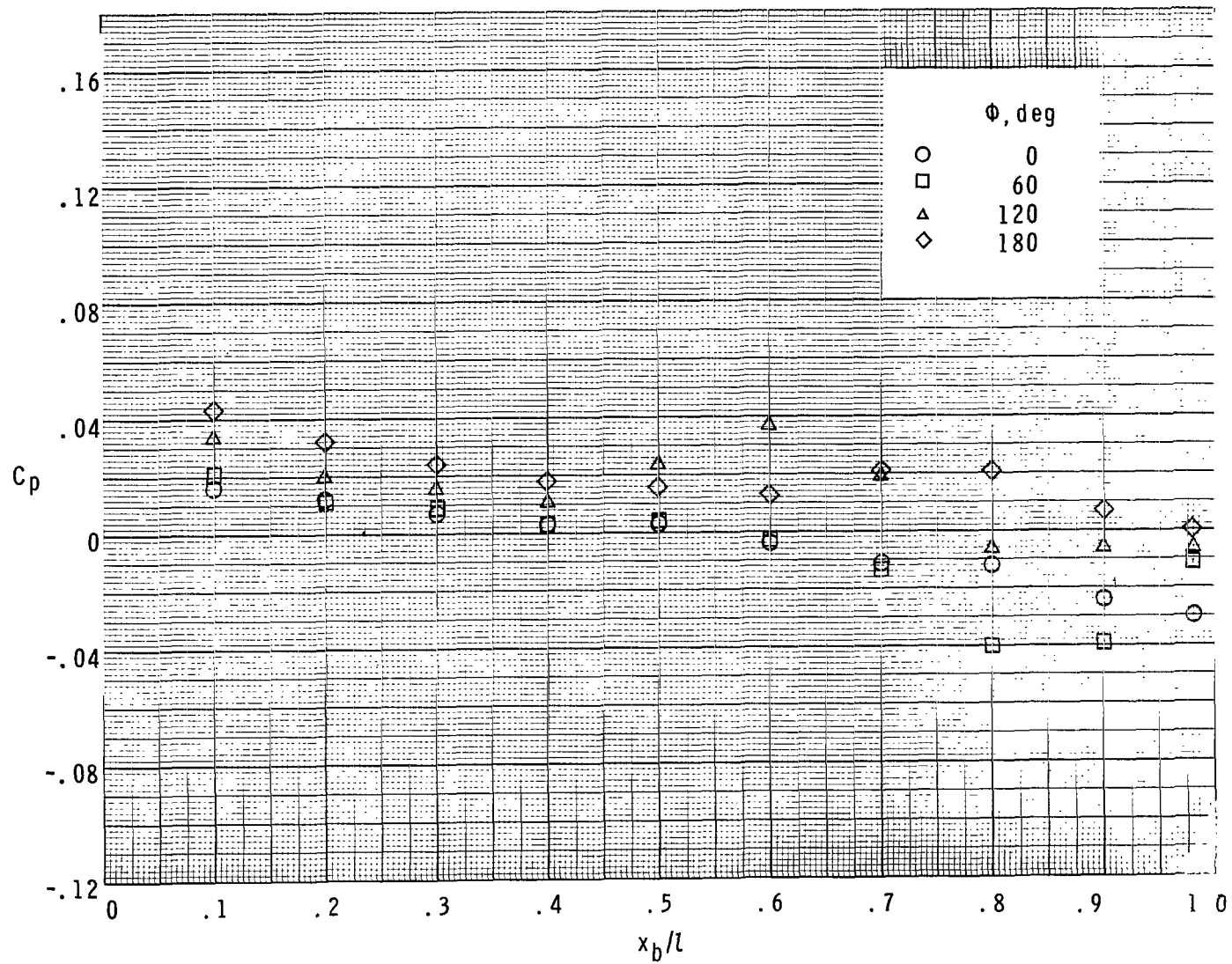
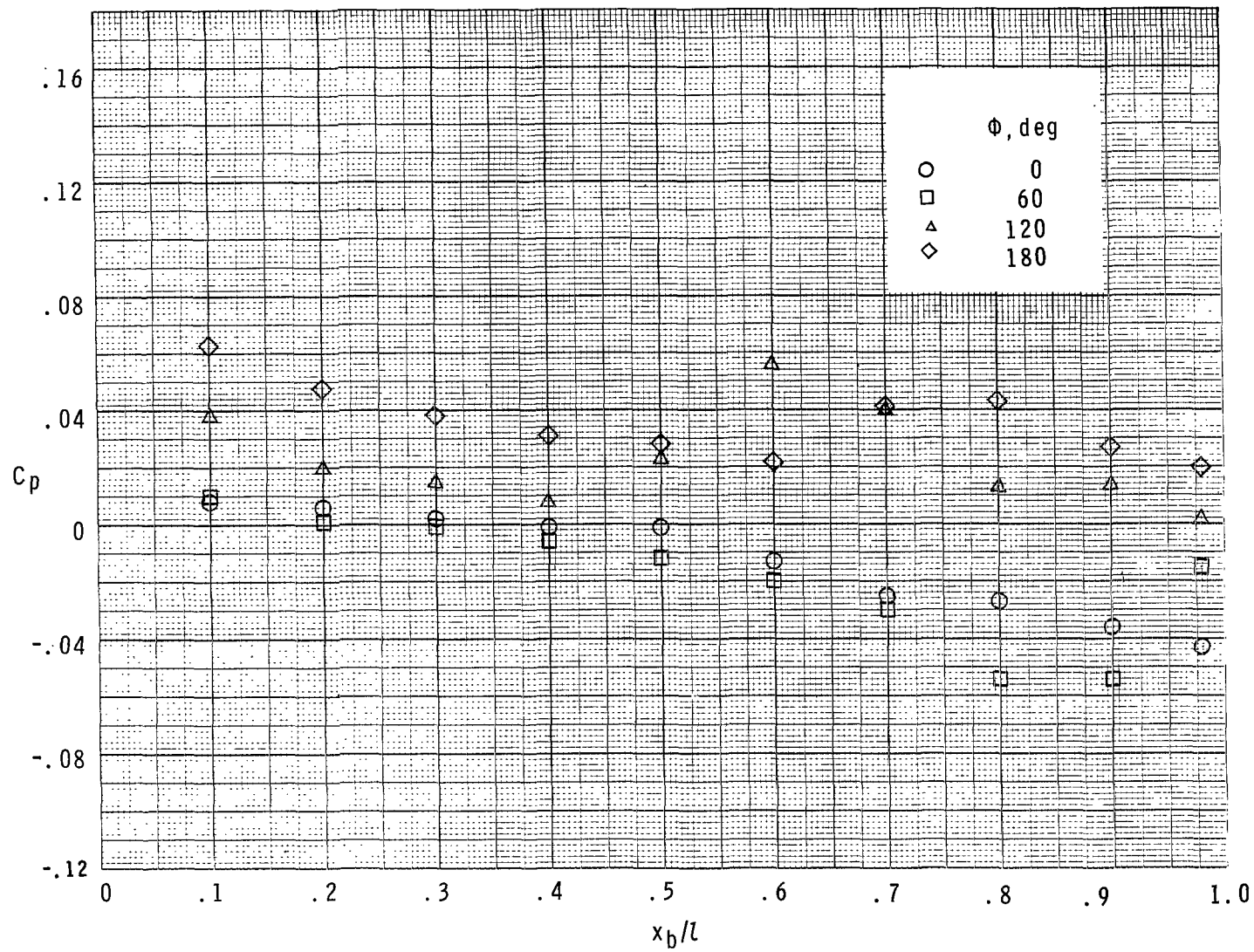


Figure 3.- Experimental pressure coefficients over body; $M = 2.96$.



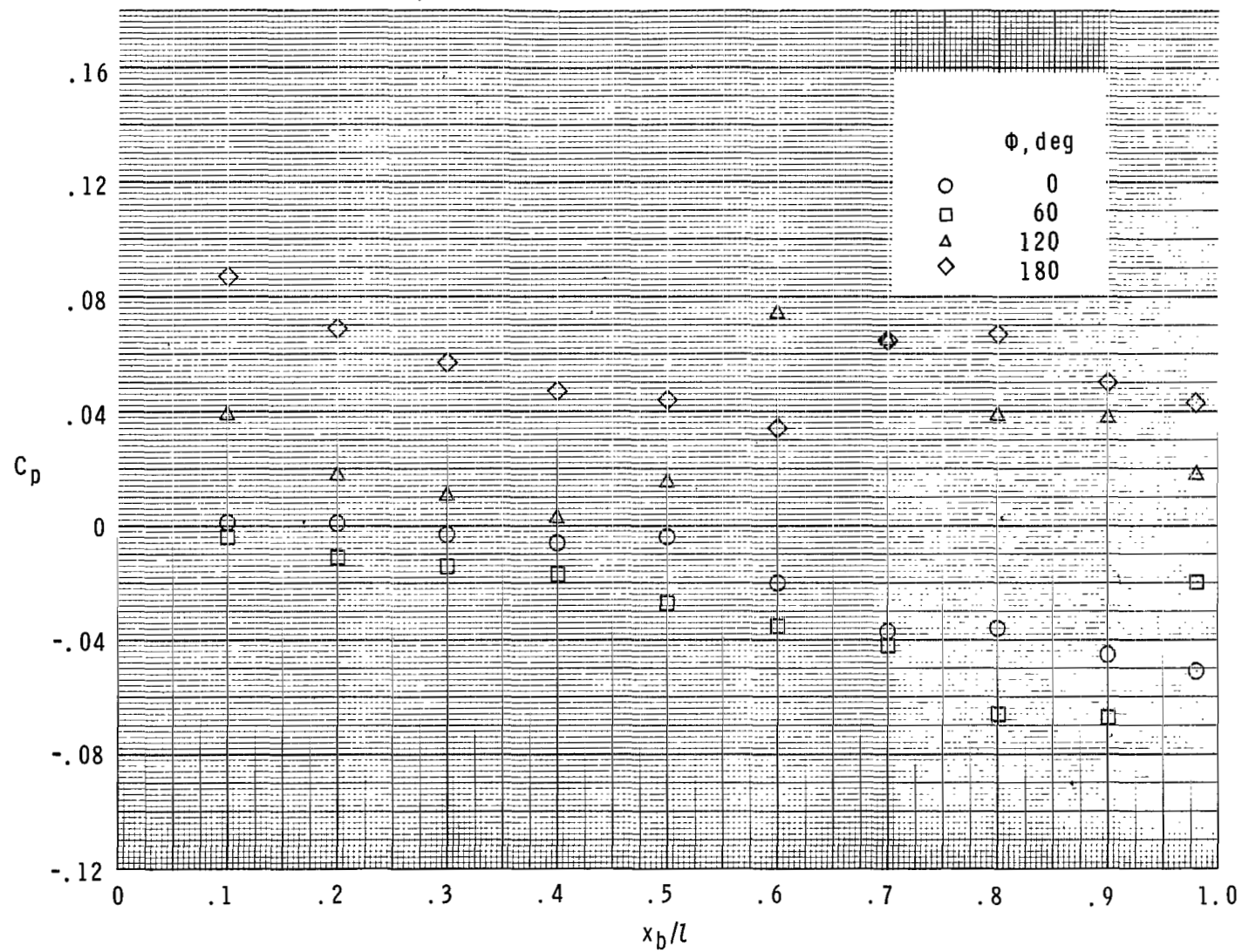
(b) $\alpha = 2.2^\circ$.

Figure 3.- Continued.



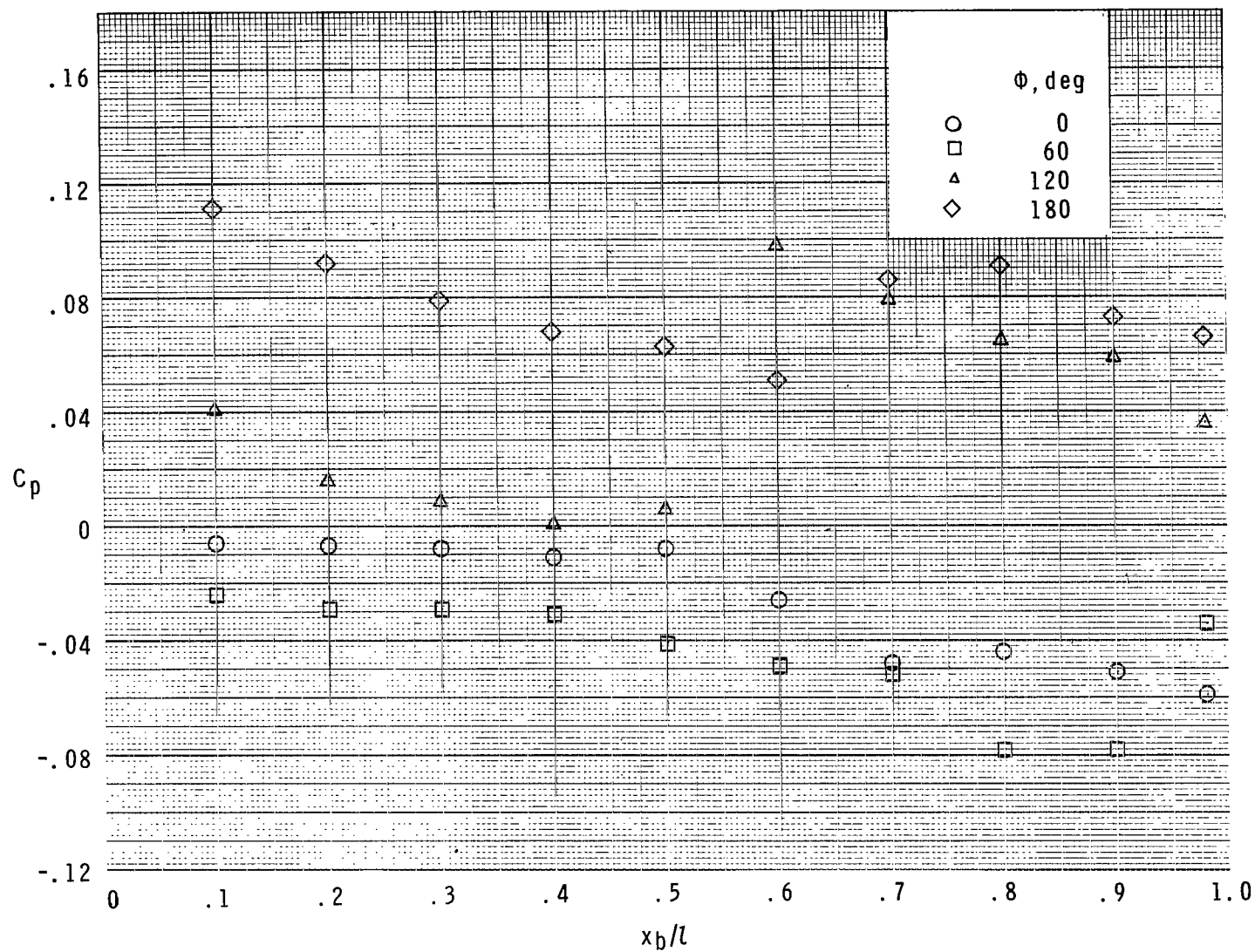
(c) $\alpha = 4.4^\circ$.

Figure 3.- Continued.



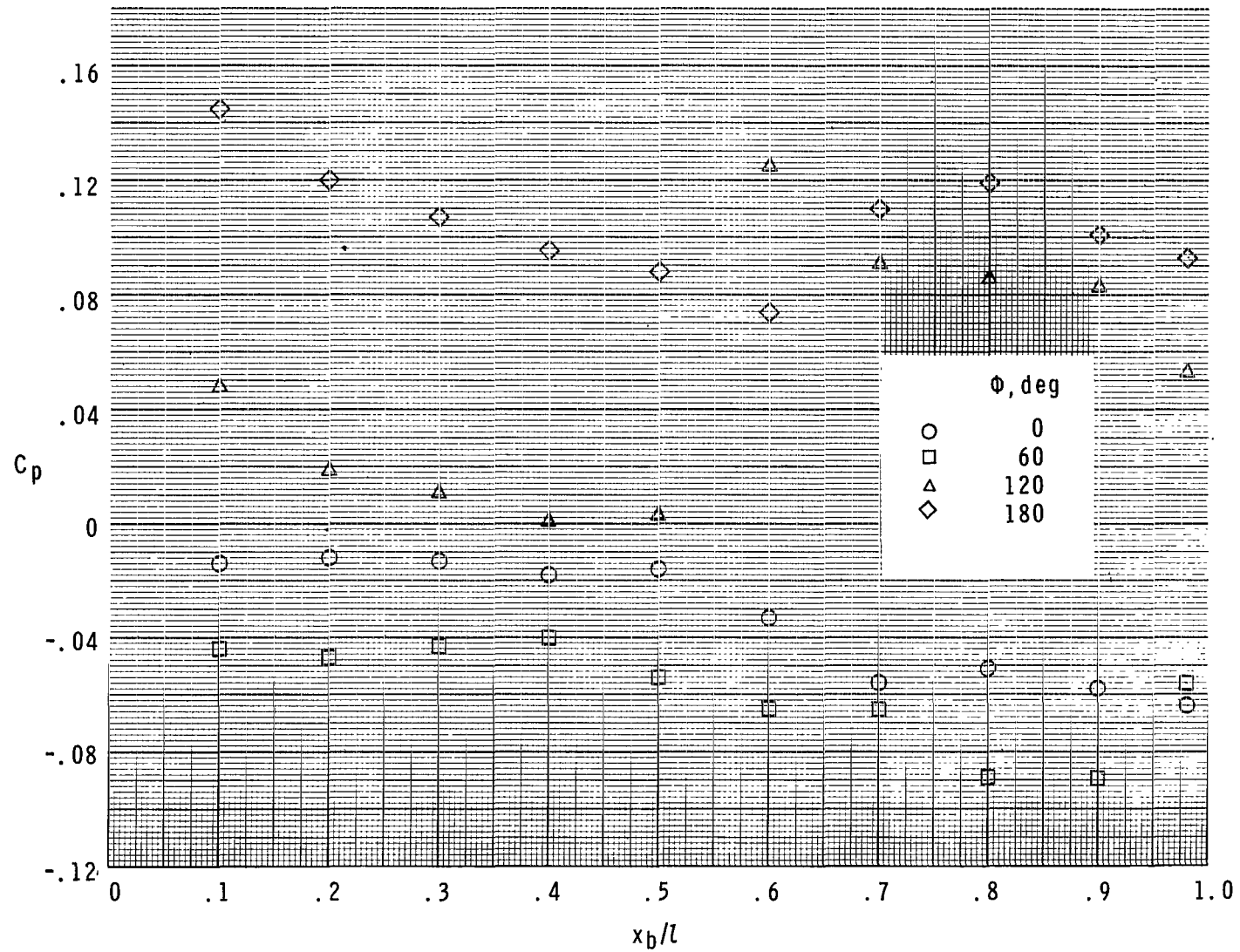
(d) $\alpha = 6.5^\circ$.

Figure 3.- Continued.



(e) $\alpha = 8.6^\circ$.

Figure 3.- Continued.



(f) $\alpha = 10.7^\circ$.

Figure 3.- Concluded.

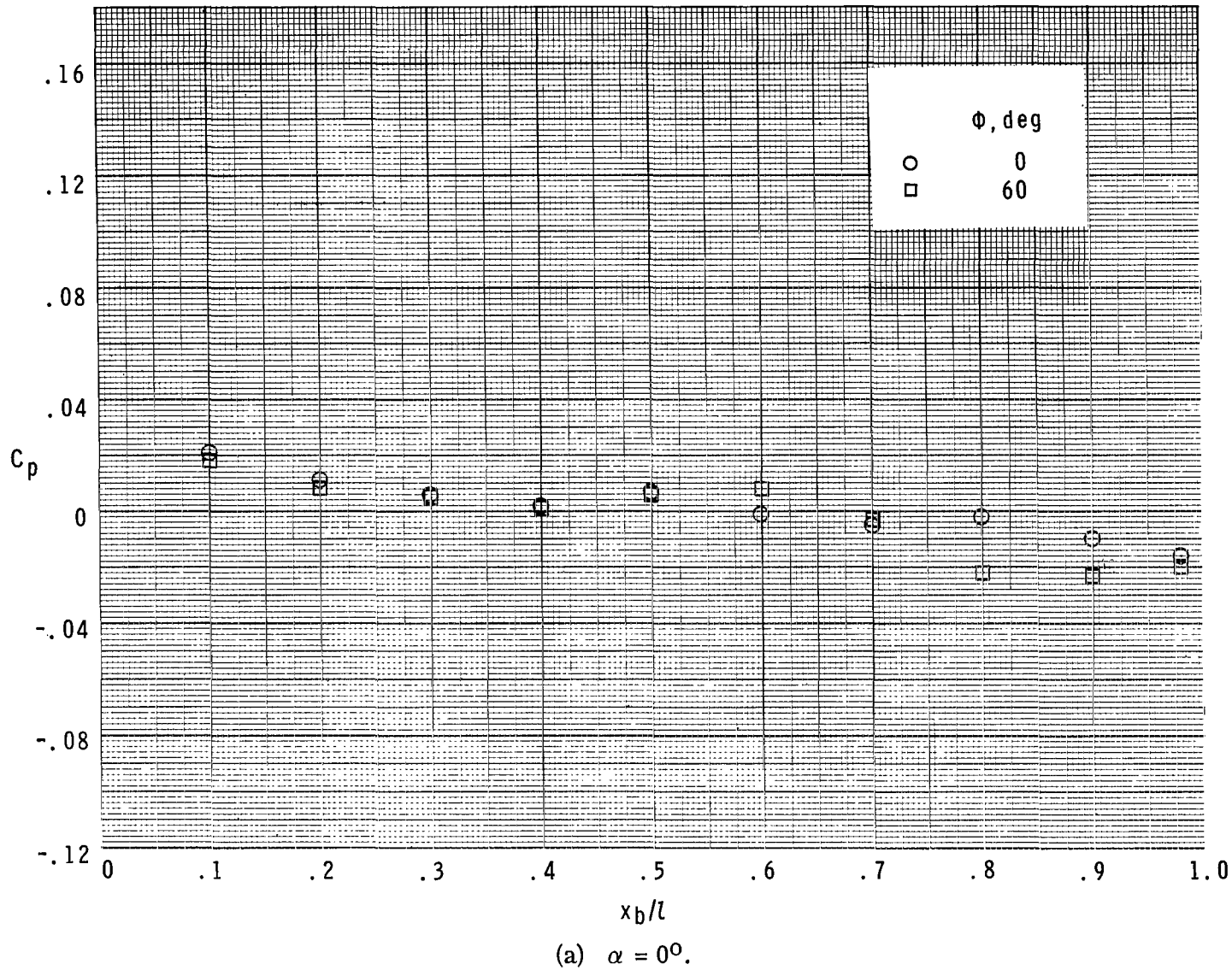
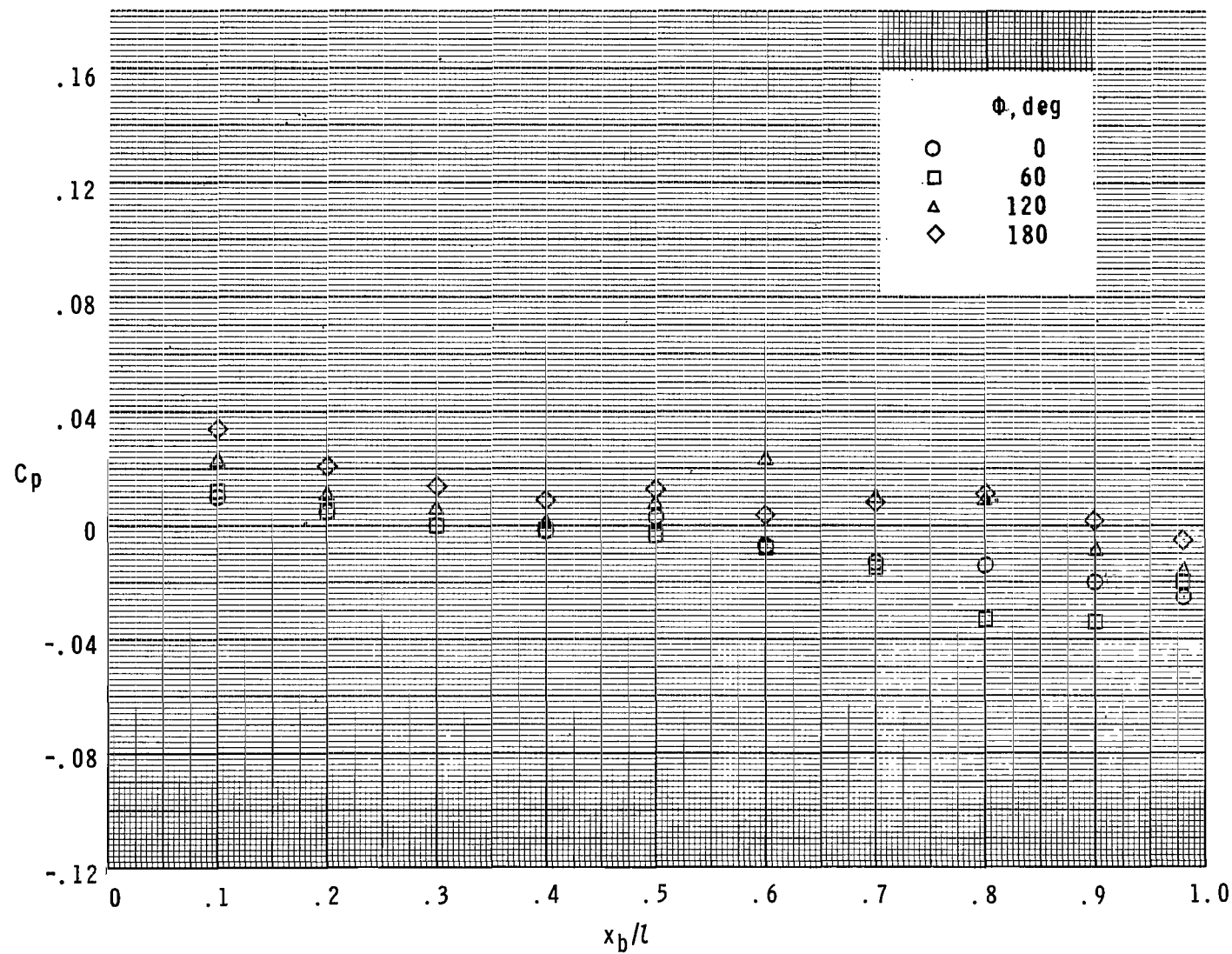
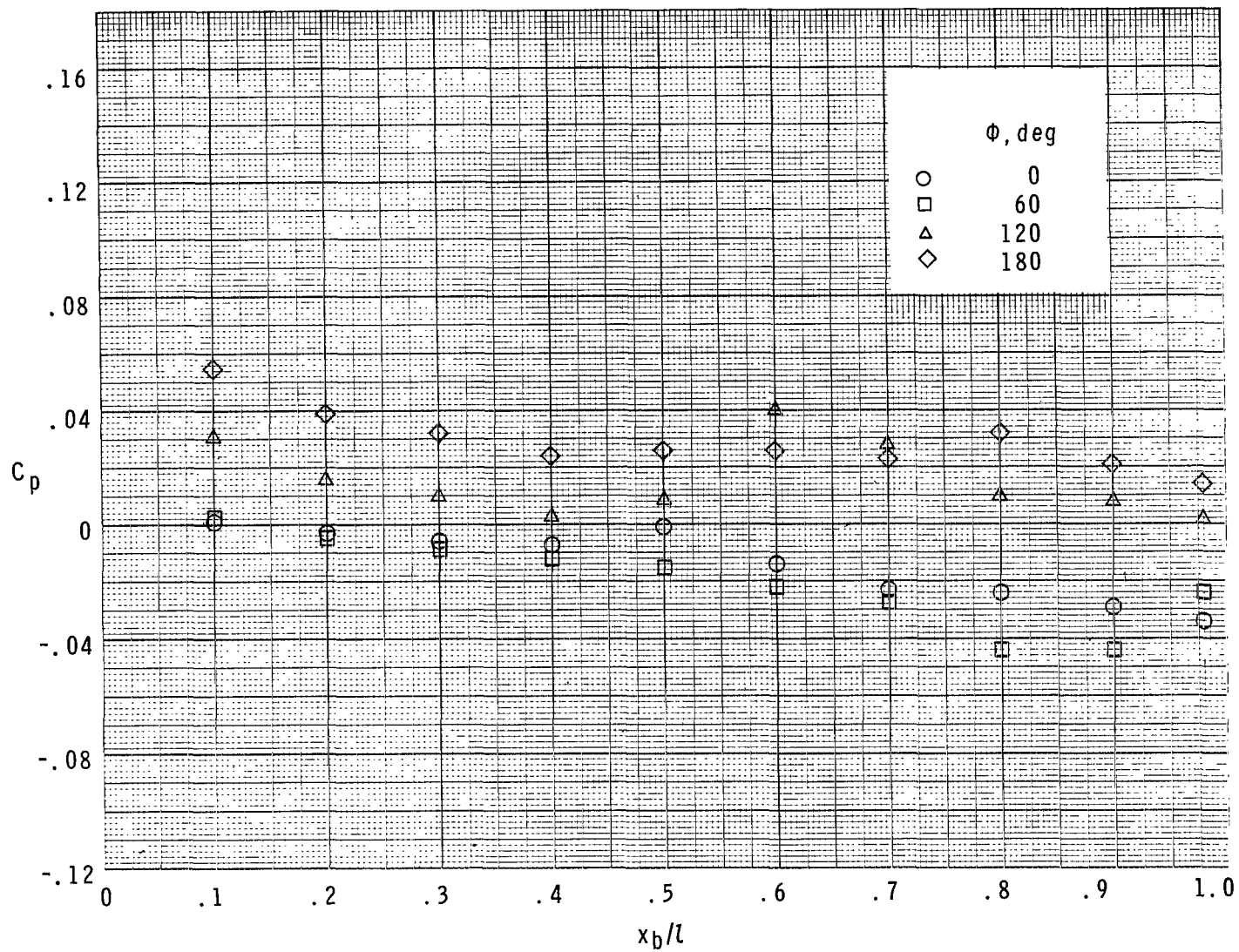


Figure 4.- Experimental pressure coefficients over body; $M = 3.95$.



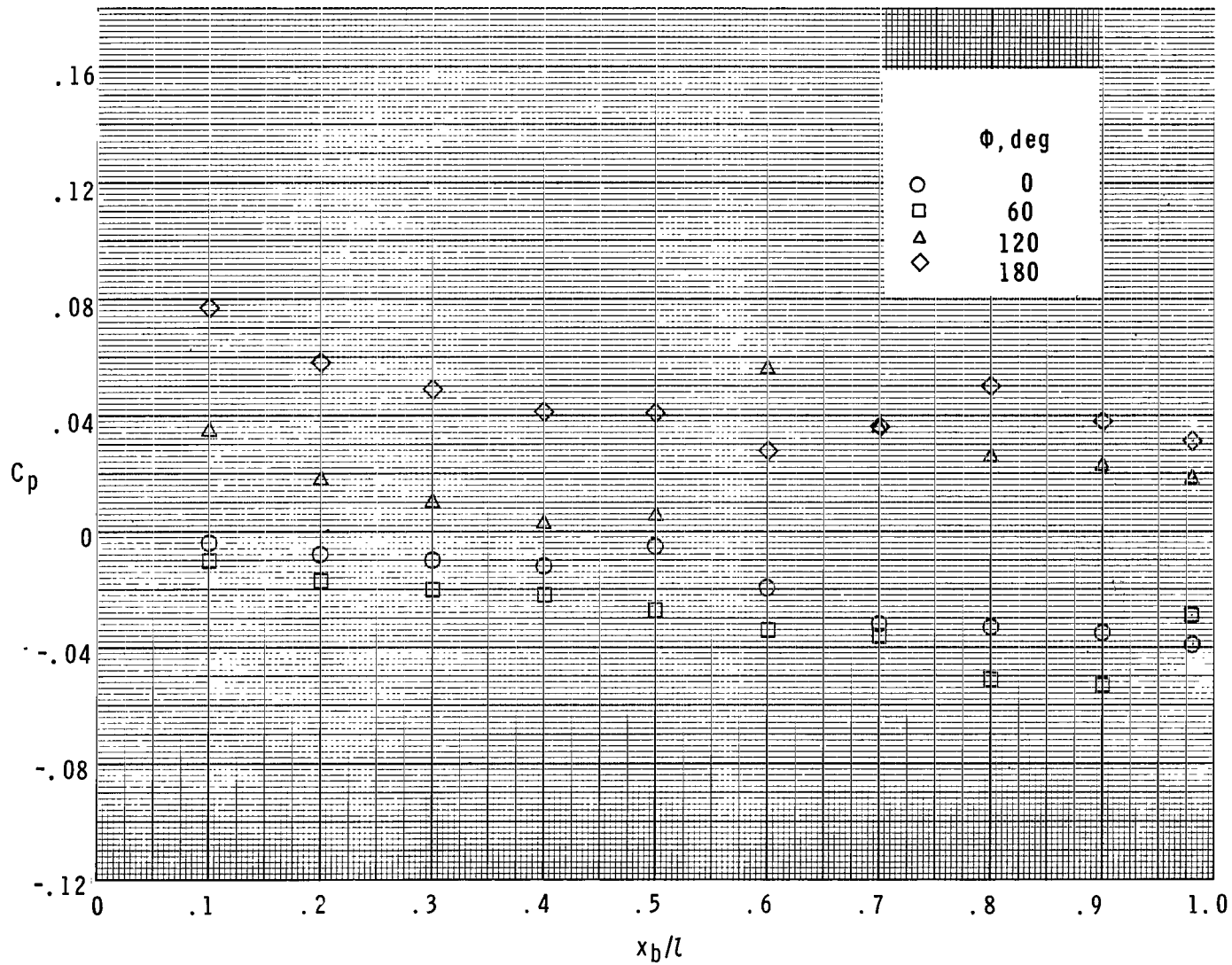
(b) $\alpha = 2.1^\circ$.

Figure 4.- Continued.



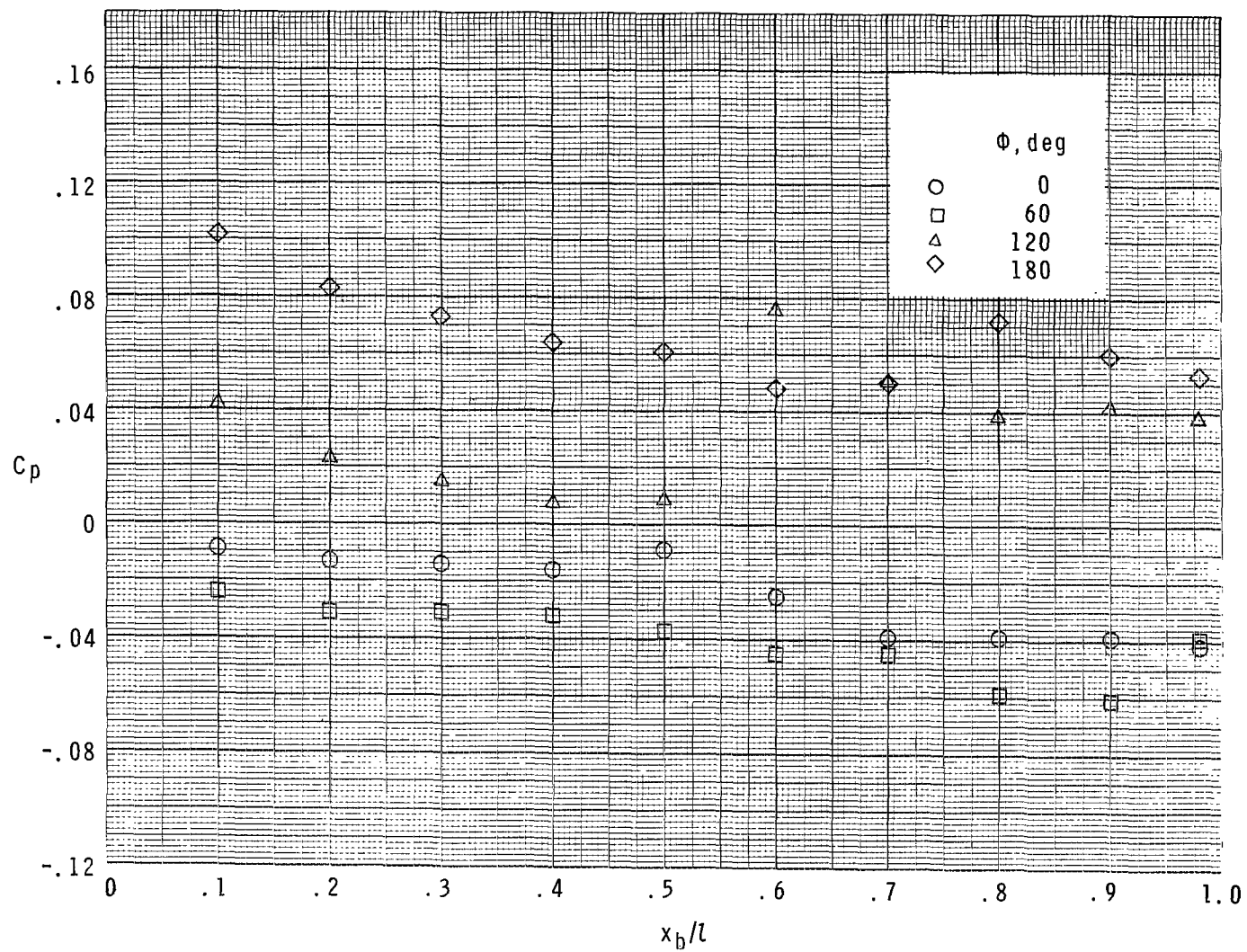
(c) $\alpha = 4.3^\circ$.

Figure 4.- Continued.



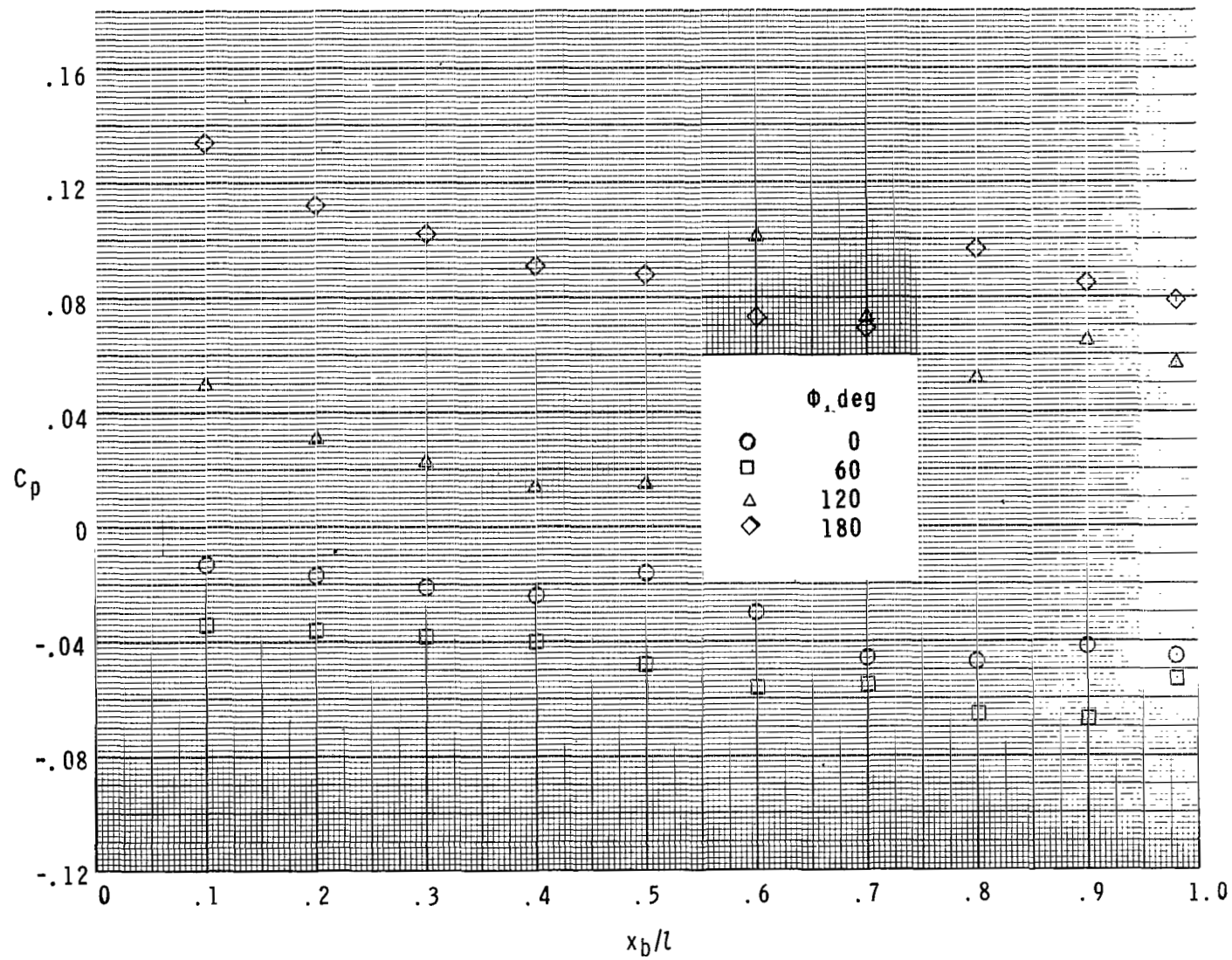
(d) $\alpha = 6.4^\circ$.

Figure 4.- Continued.



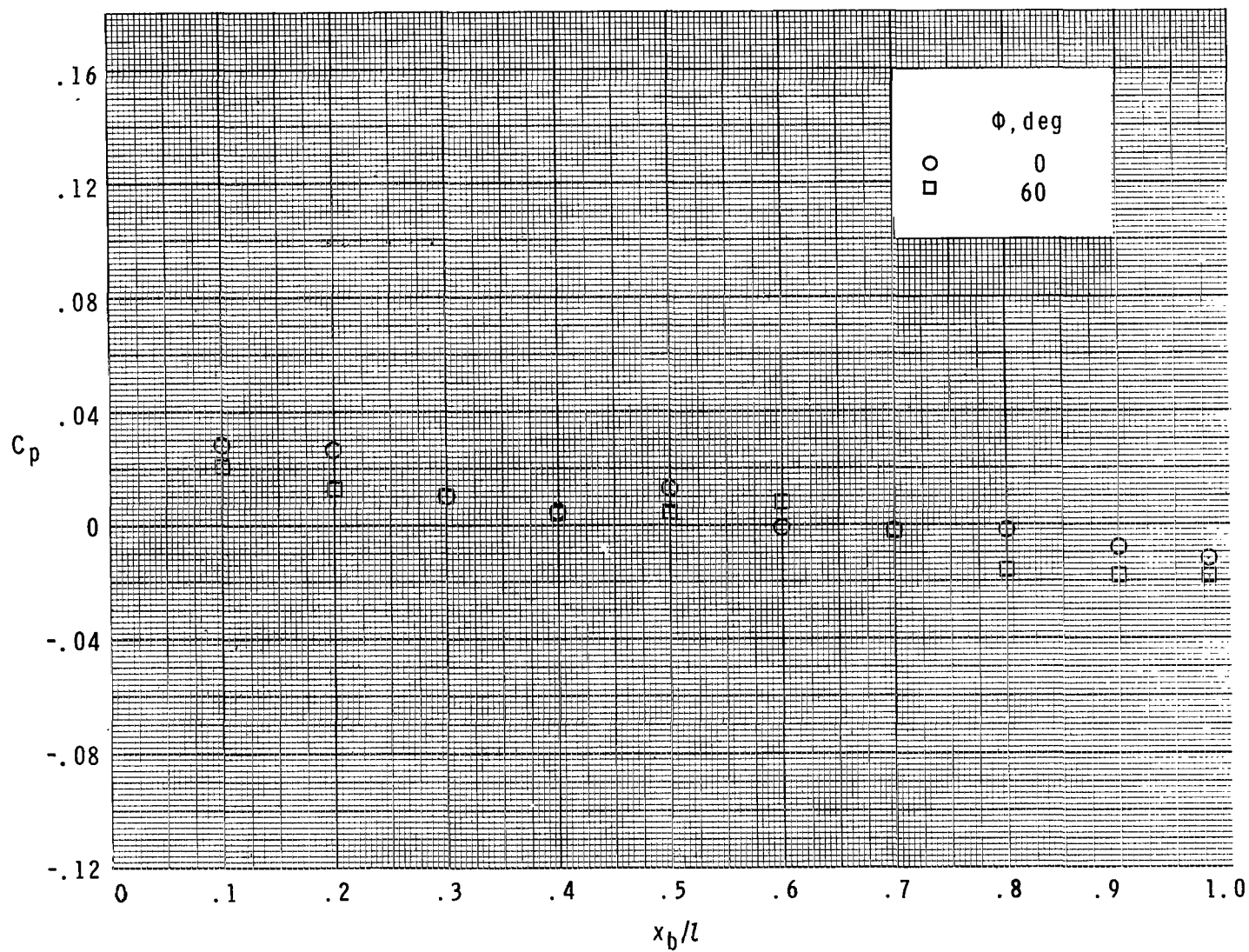
(e) $\alpha = 8.5^\circ$.

Figure 4.- Continued.



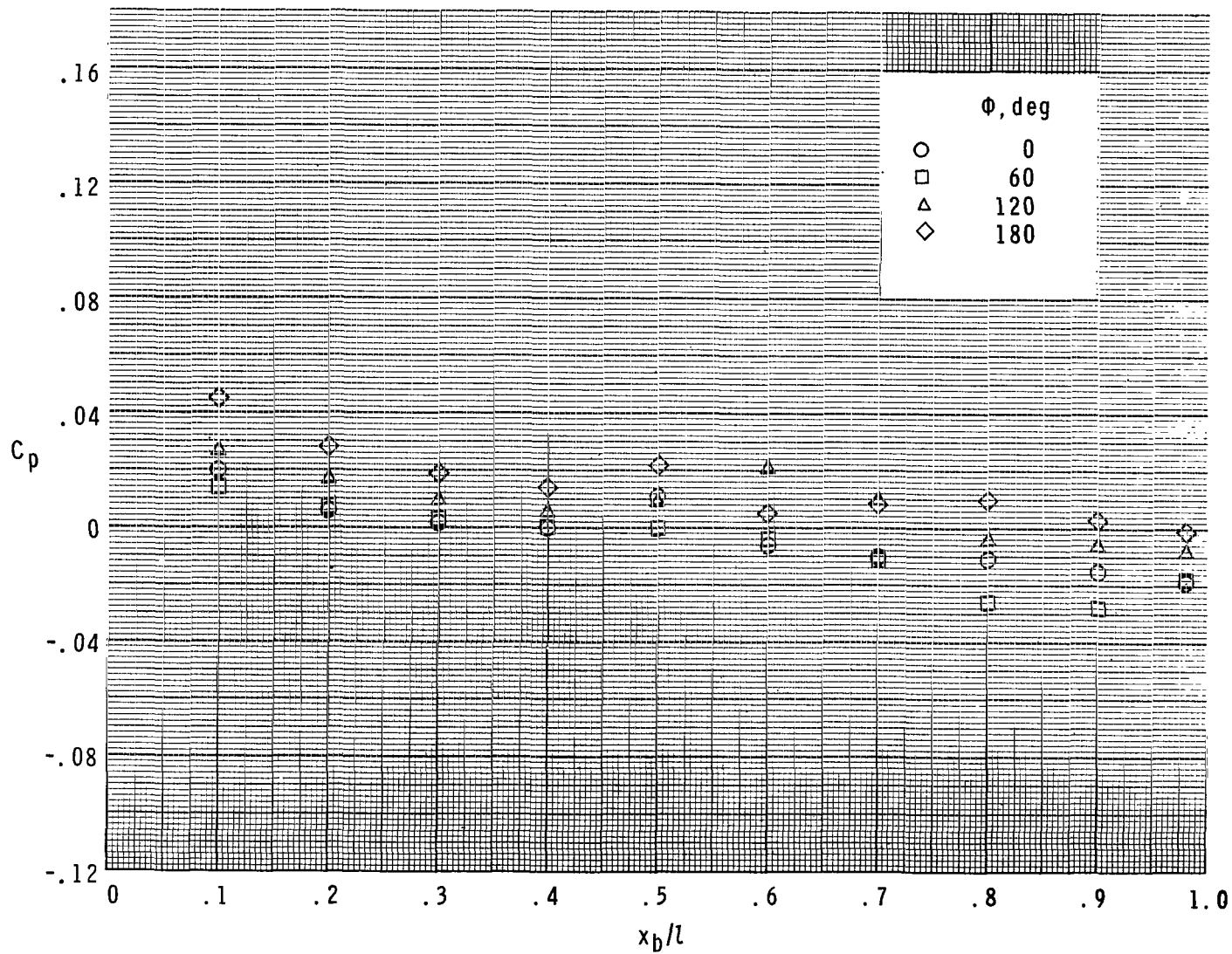
(f) $\alpha = 10.6^\circ$.

Figure 4.- Concluded.



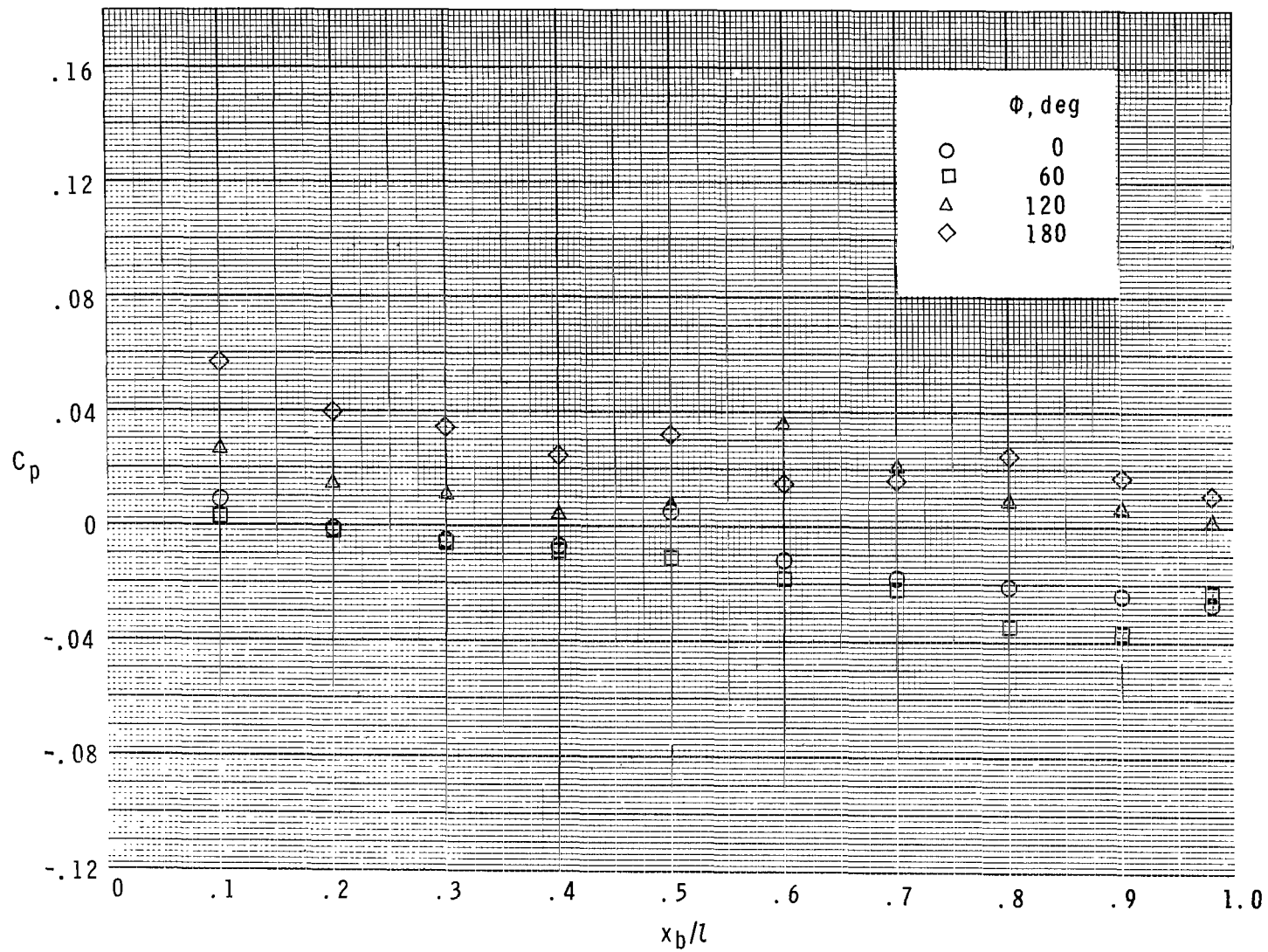
(a) $\alpha = 0^\circ$.

Figure 5.- Experimental pressure coefficients over body; $M = 4.63$.



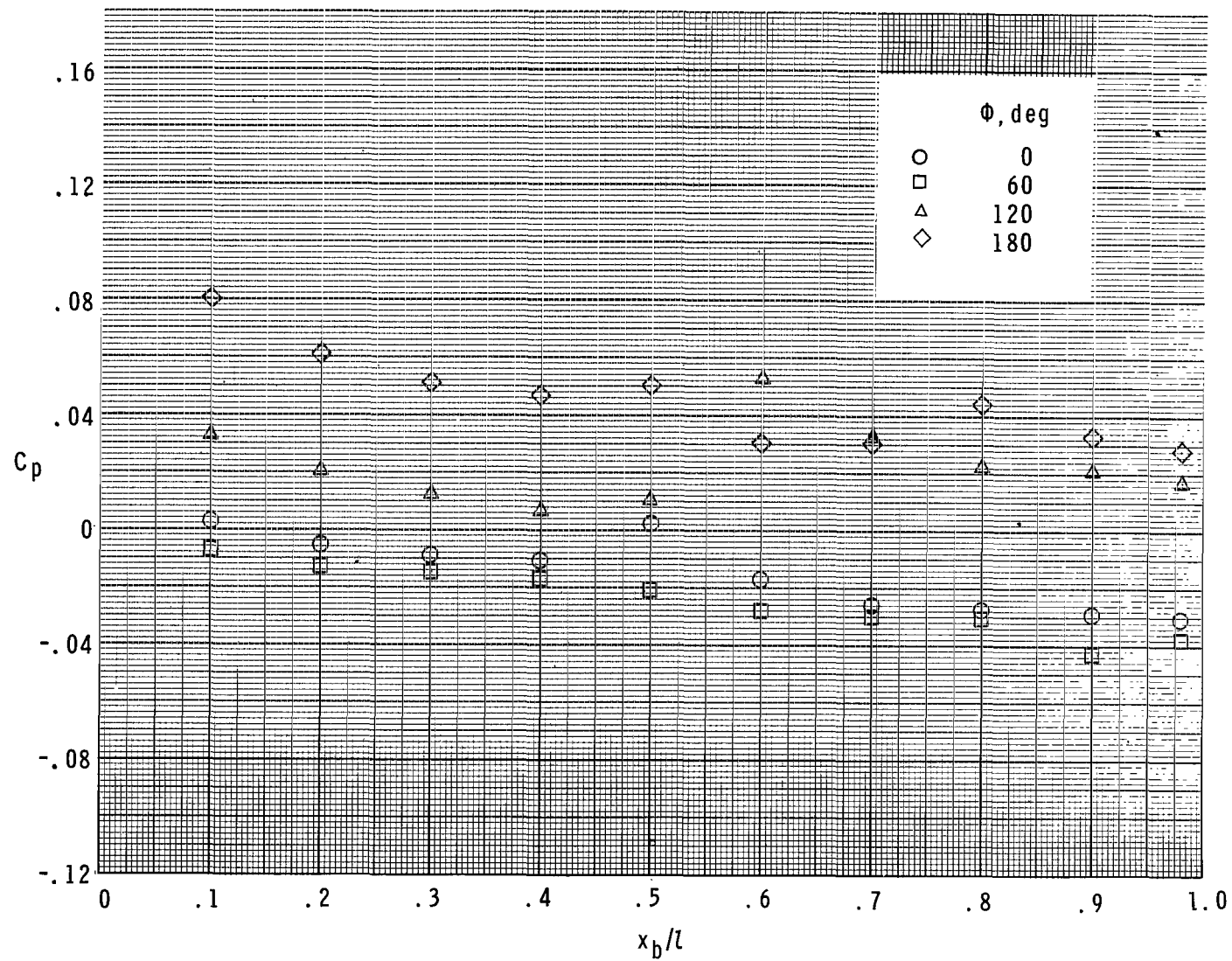
(b) $\alpha = 2.0^\circ$.

Figure 5.- Continued.



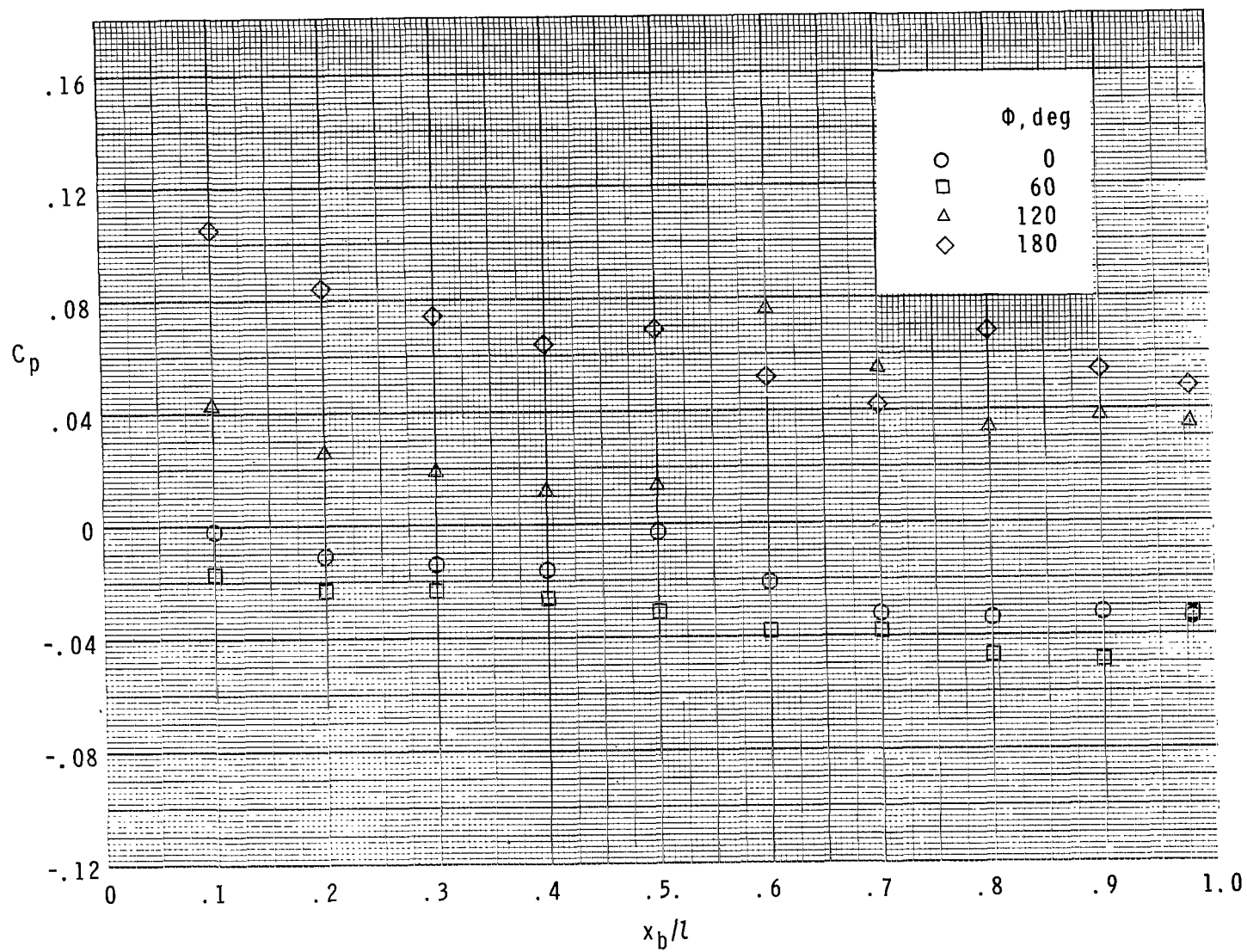
(c) $\alpha = 4.2^\circ$.

Figure 5.- Continued.



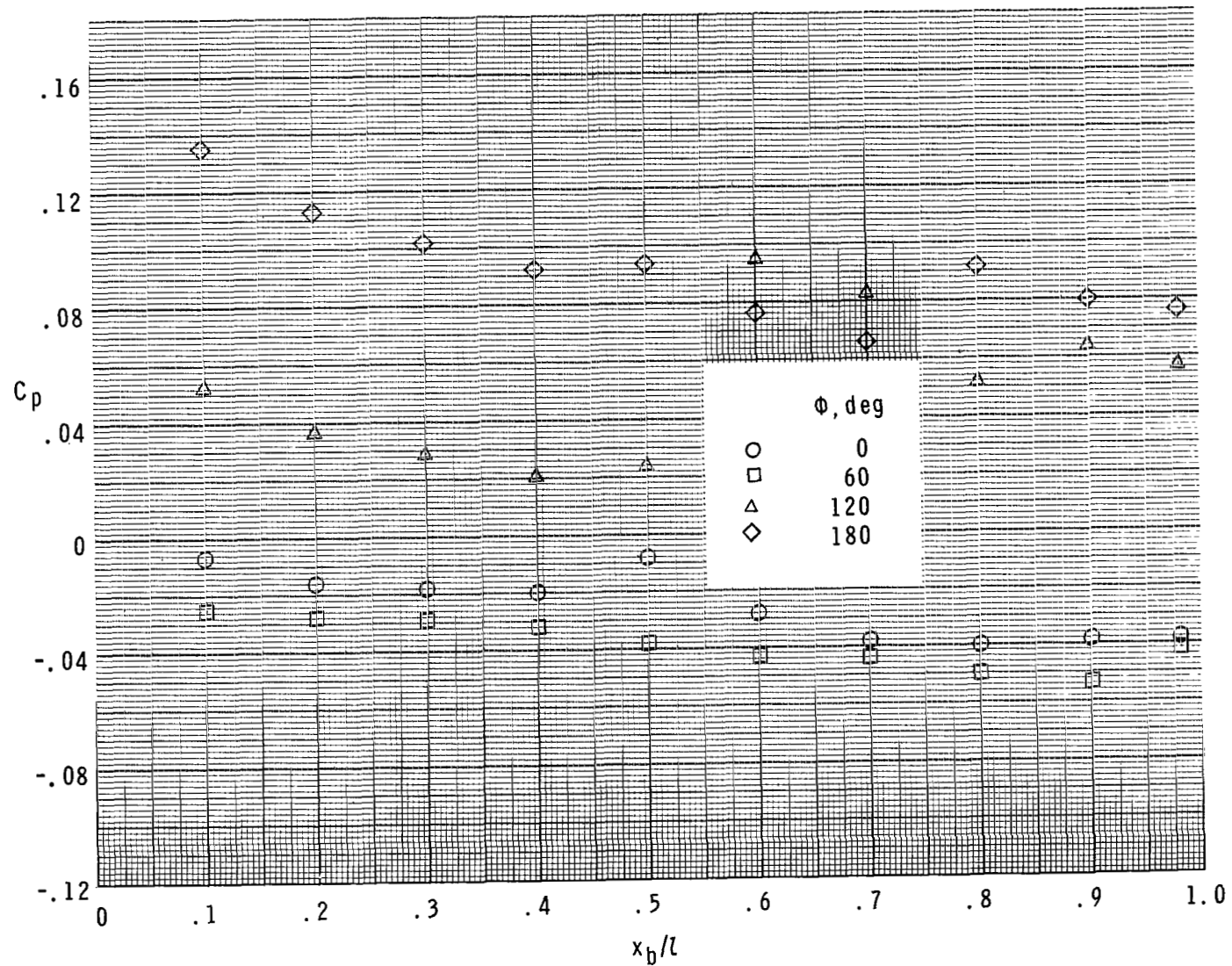
(d) $\alpha = 6.2^\circ$.

Figure 5.- Continued.



(e) $\alpha = 8.3^\circ$.

Figure 5.- Continued.



(f) $\alpha = 10.4^\circ$.

Figure 5.- Concluded.

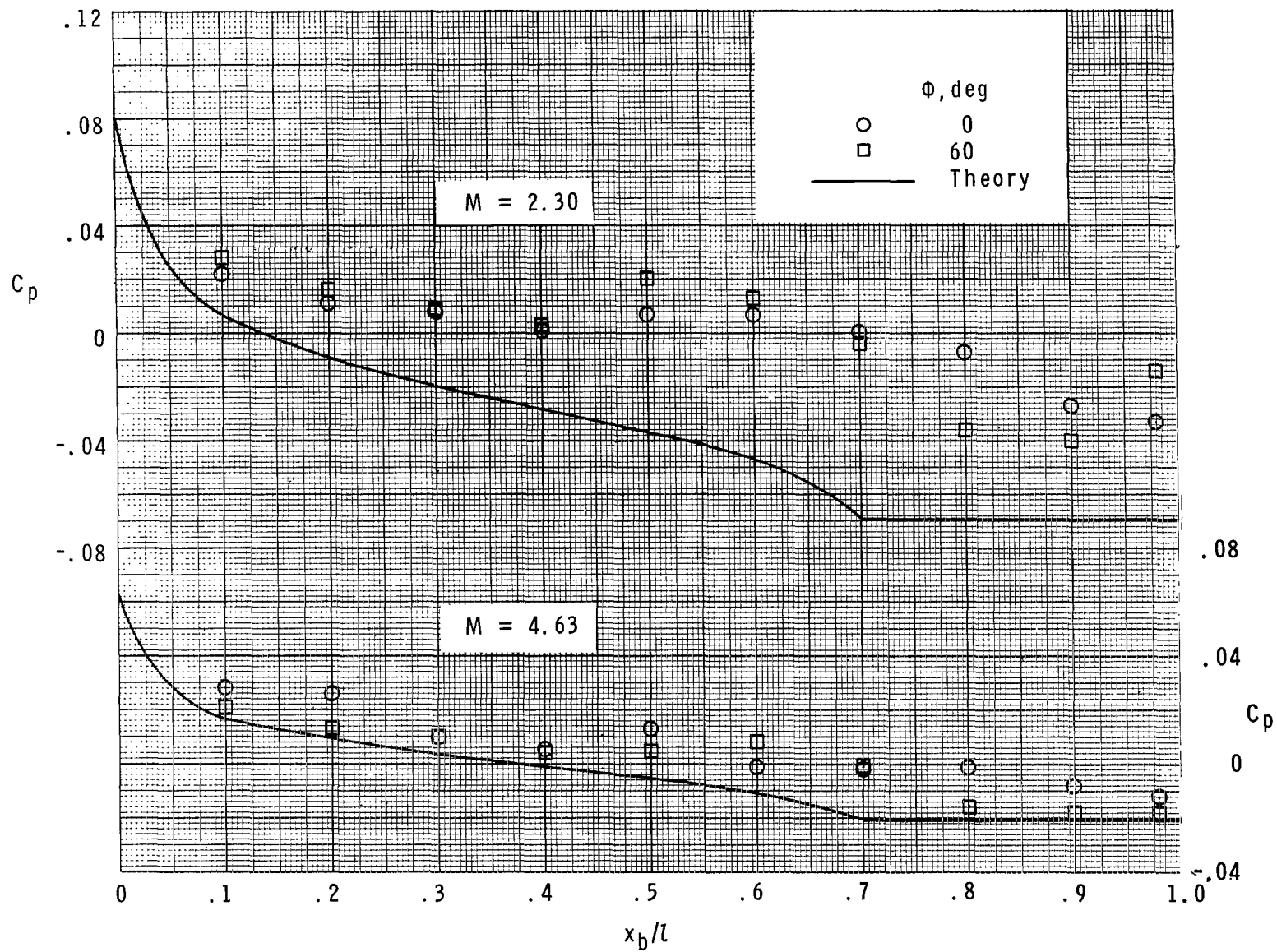


Figure 6.- Comparison of body experimental data with conical-shock-expansion method; $\alpha = 0^\circ$.

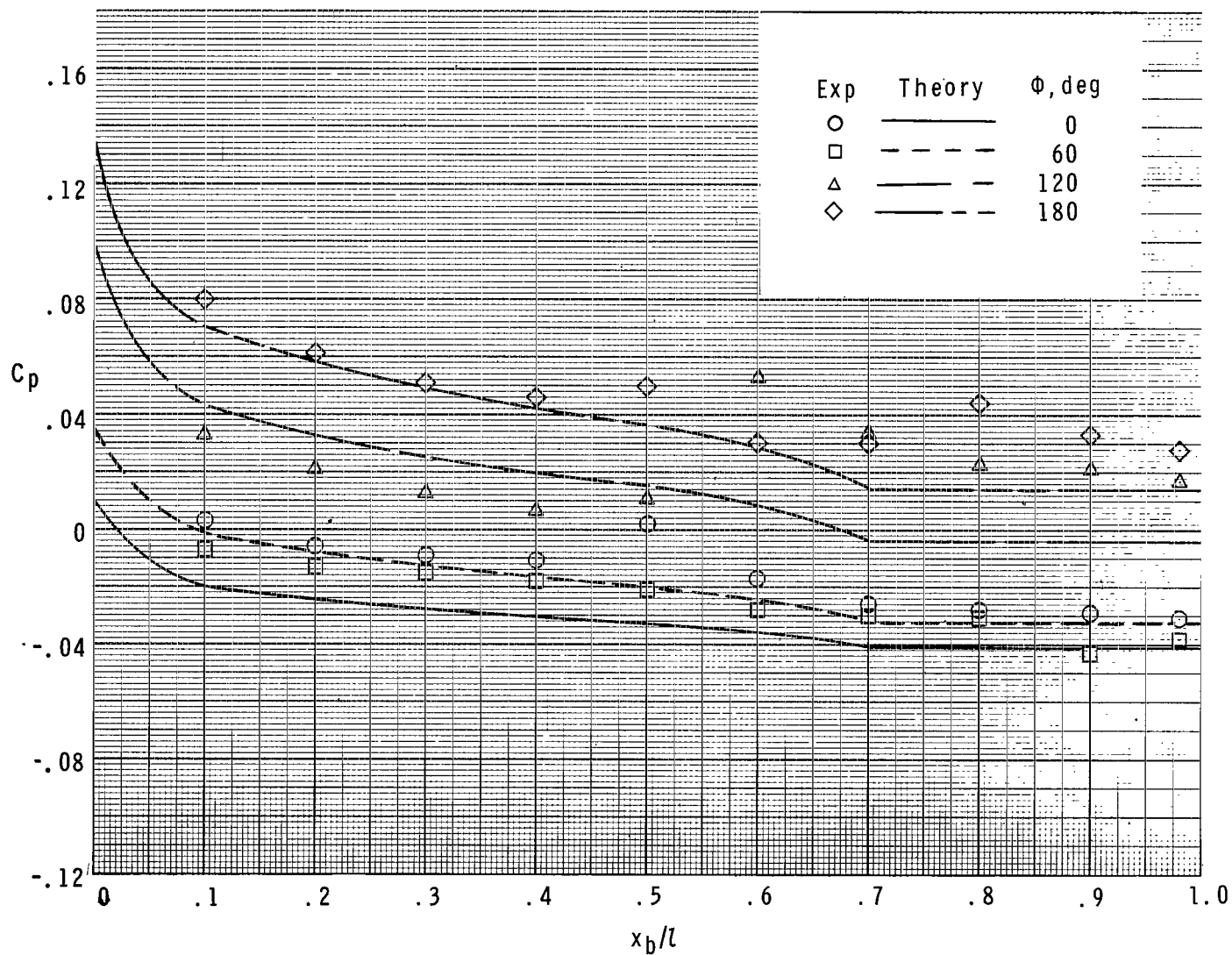
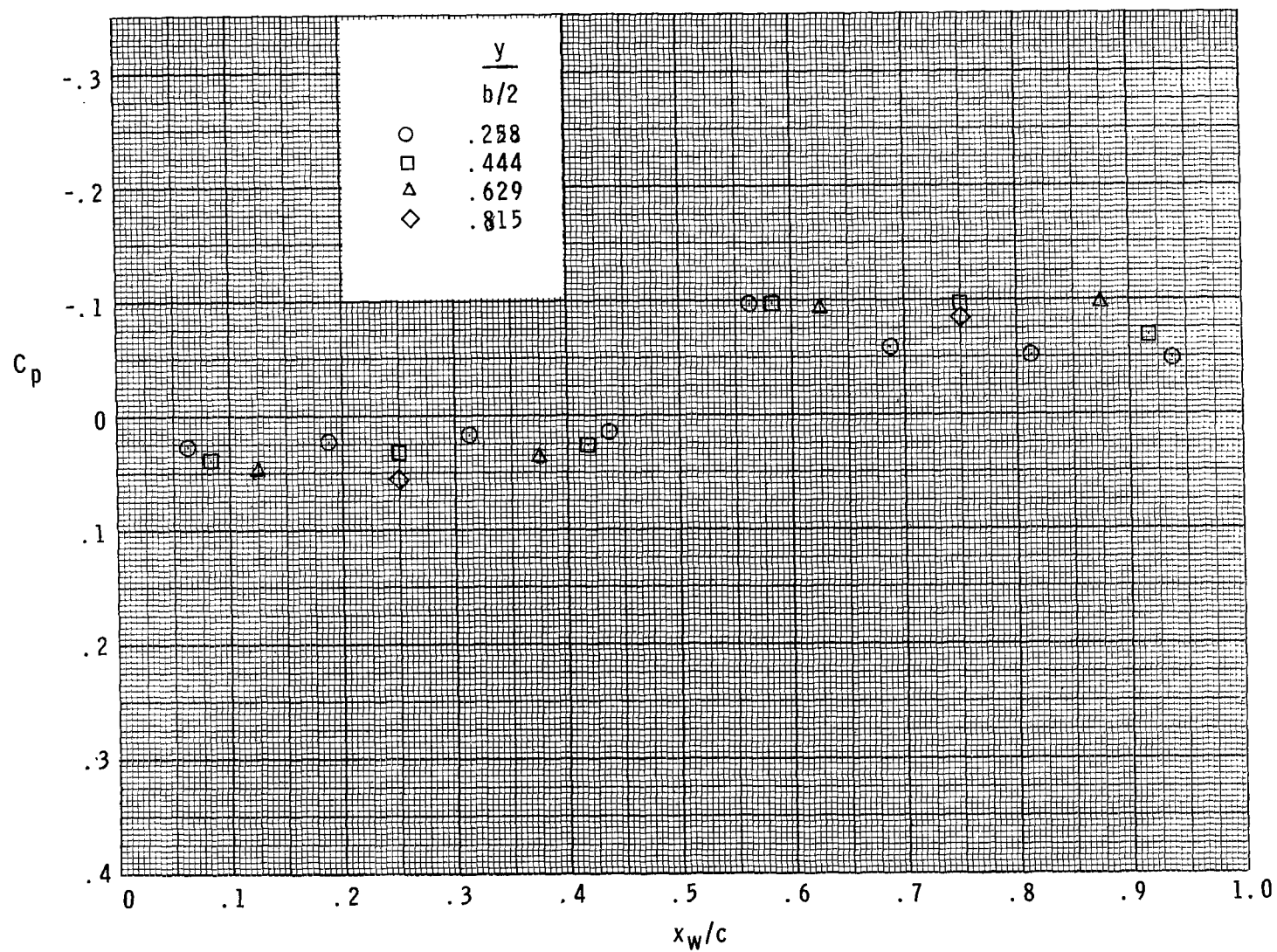
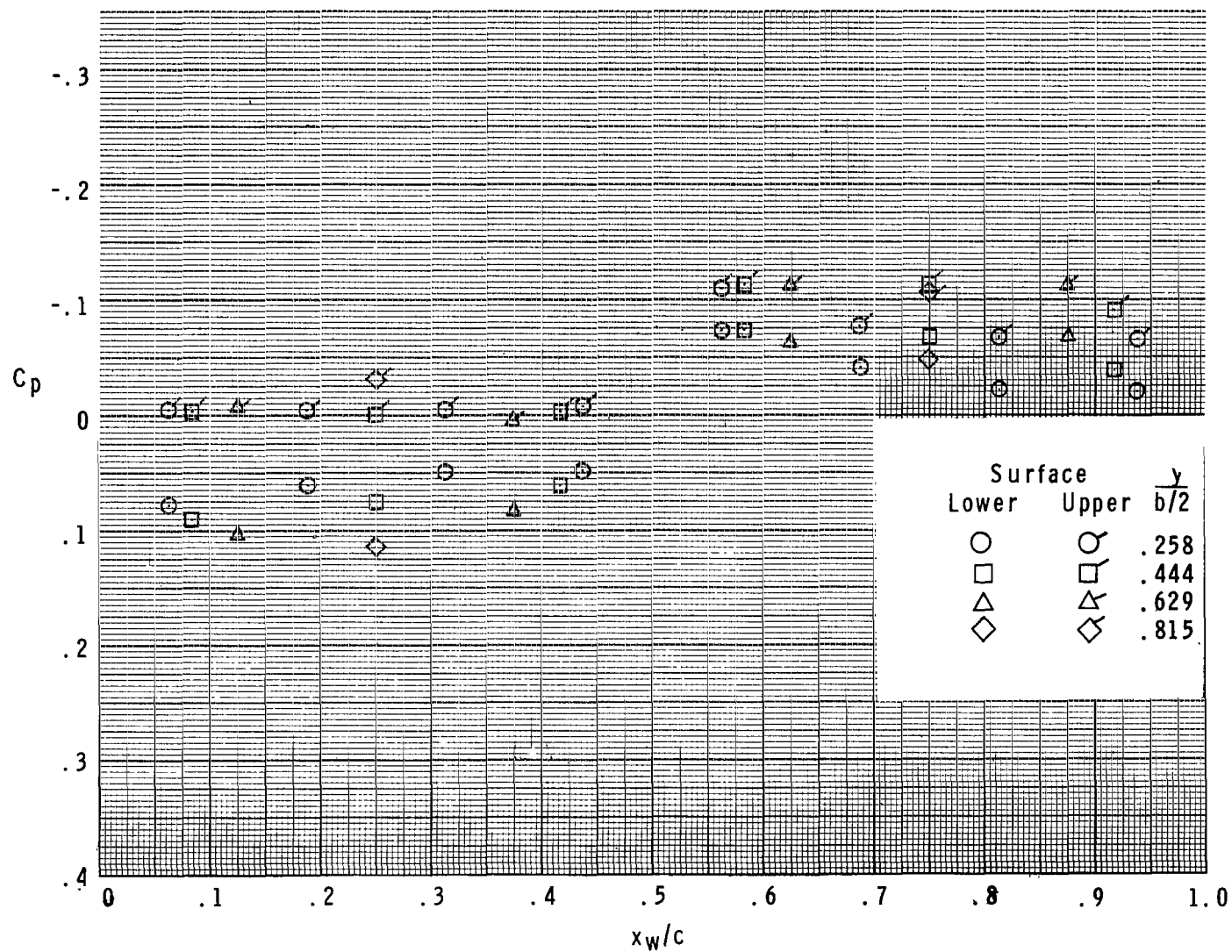


Figure 7.- Comparison of body experimental data with conical-shock-expansion method; $\alpha = 6.2^\circ$; $M = 4.63$.



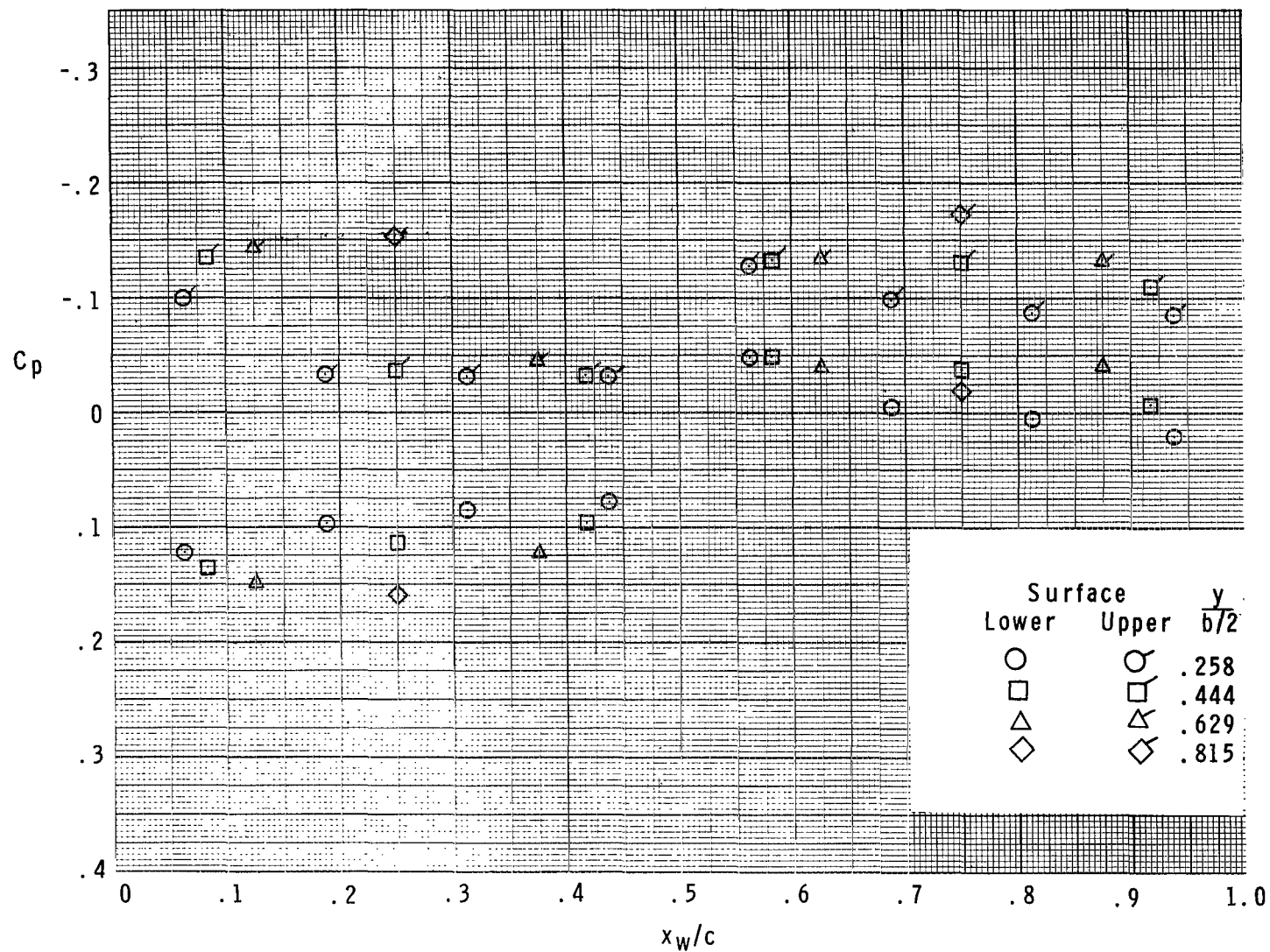
(a) $\alpha = 0^\circ$.

Figure 8.- Experimental pressure coefficients over wing; $M = 2.30$.



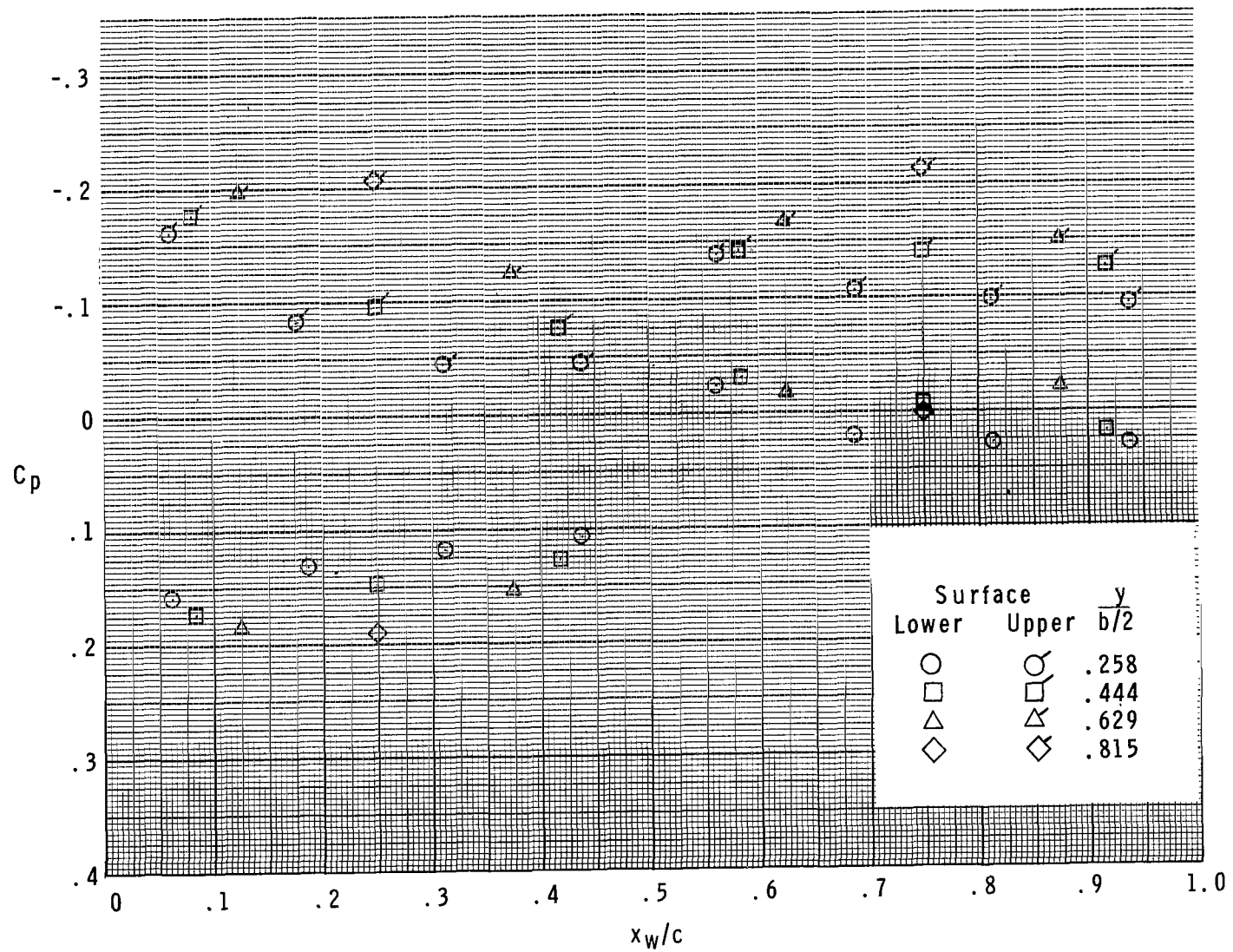
(b) $\alpha = 2.2^\circ$.

Figure 8.- Continued.



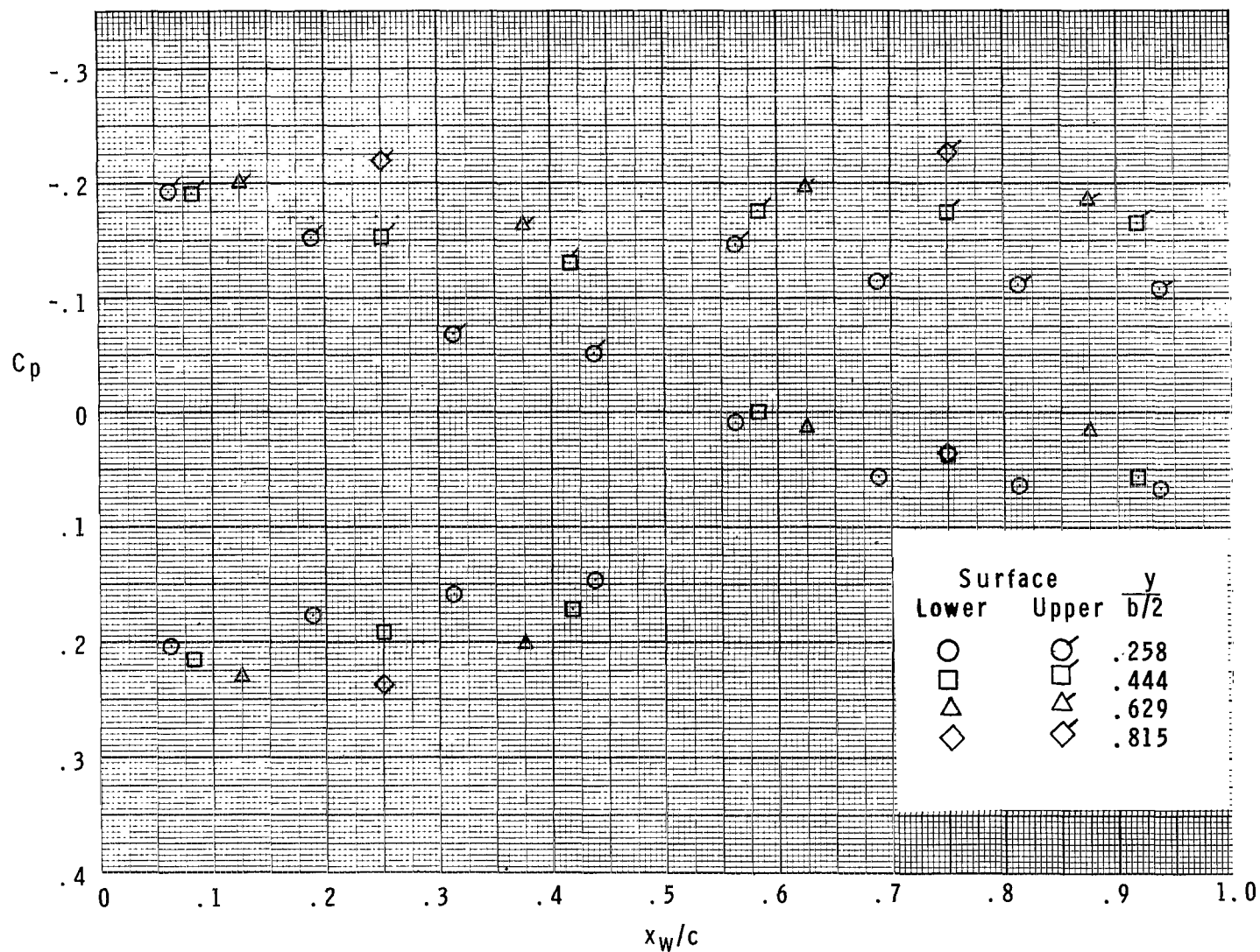
(c) $\alpha = 4.5^\circ$.

Figure 8.- Continued.



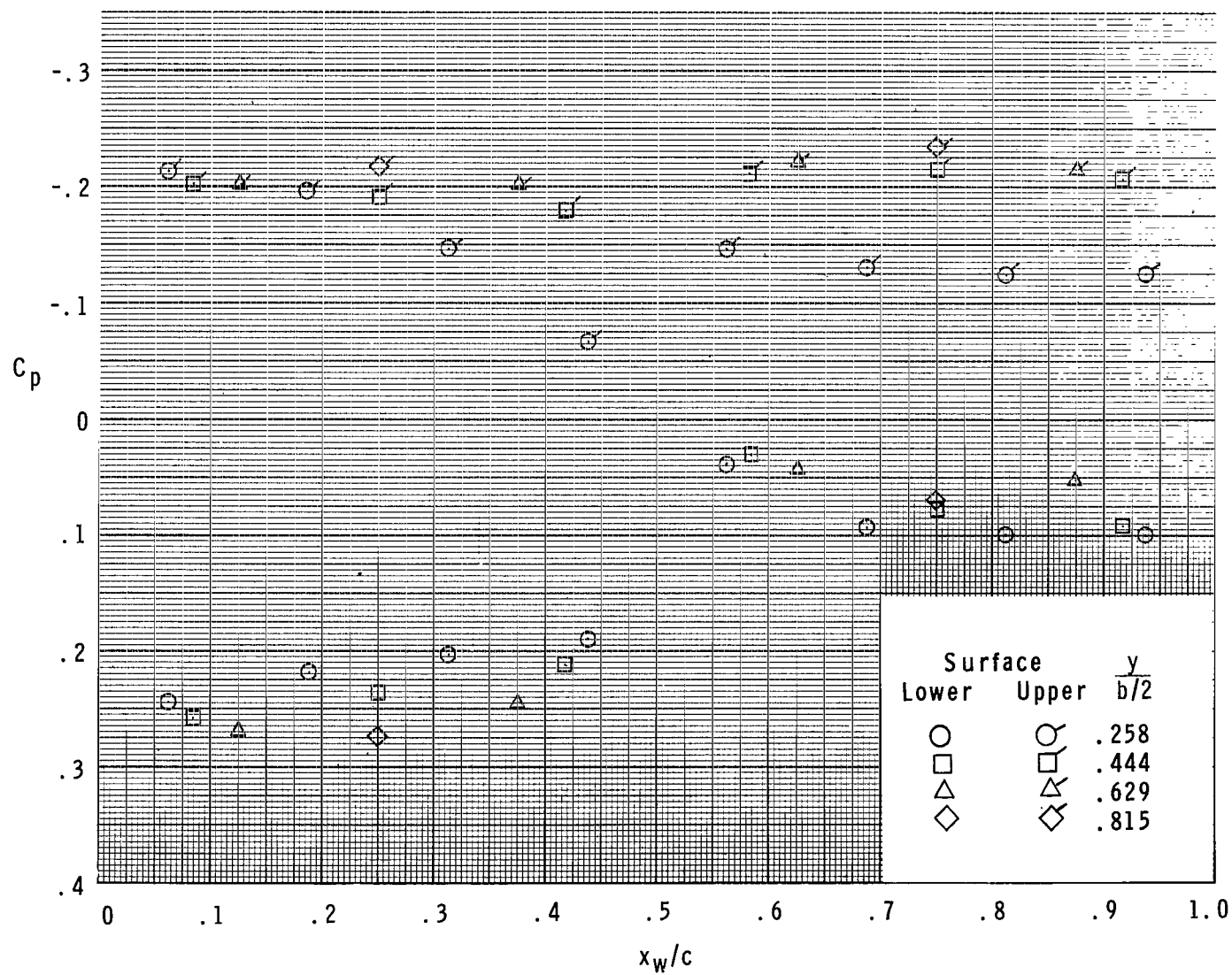
(d) $\alpha = 6.5^\circ$.

Figure 8.- Continued.



(e) $\alpha = 8.8^\circ$.

Figure 8.- Continued.



(f) $\alpha = 11.1^\circ$.

Figure 8.- Concluded.

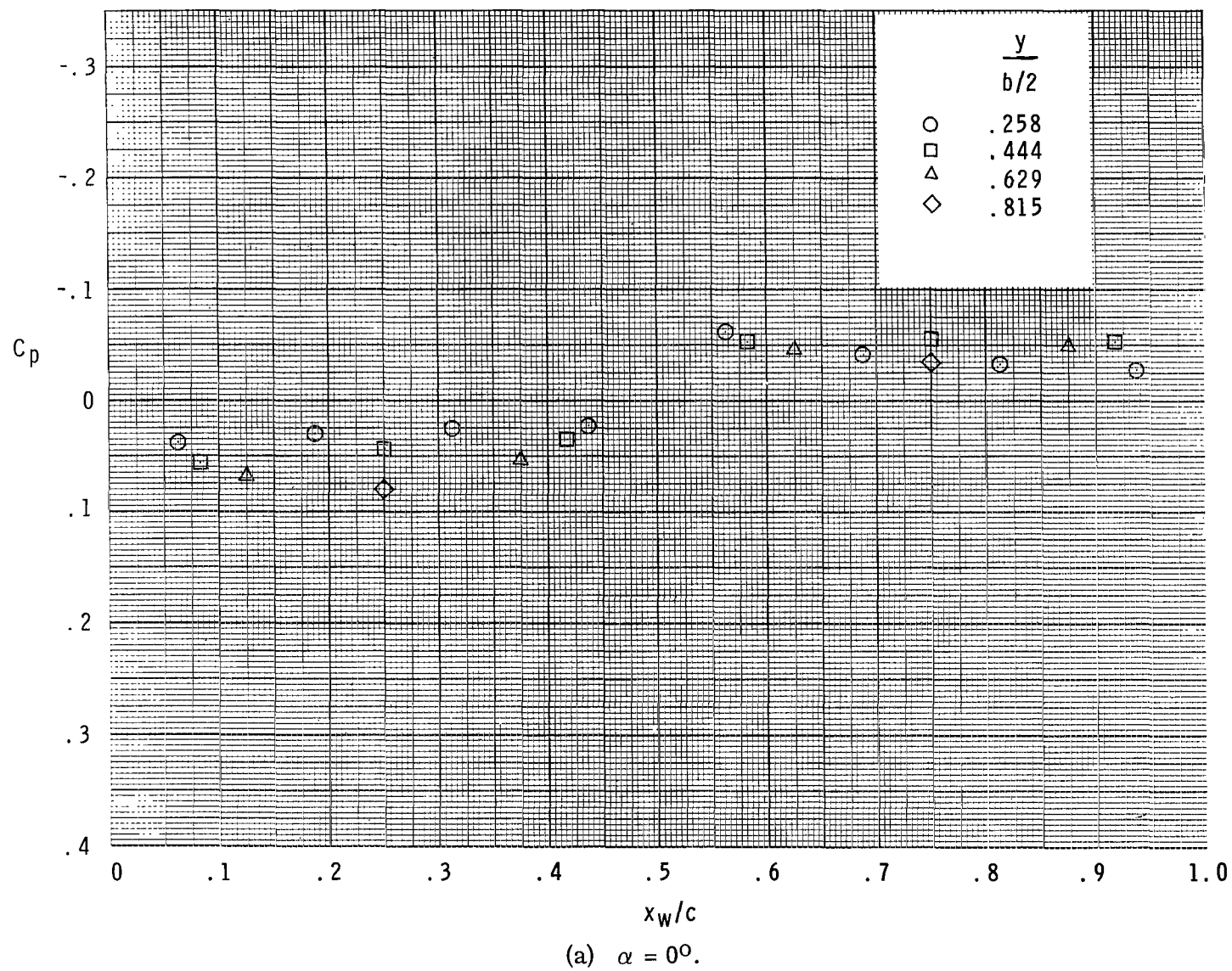


Figure 9.- Experimental pressure coefficients over wing; $M = 2.96$.

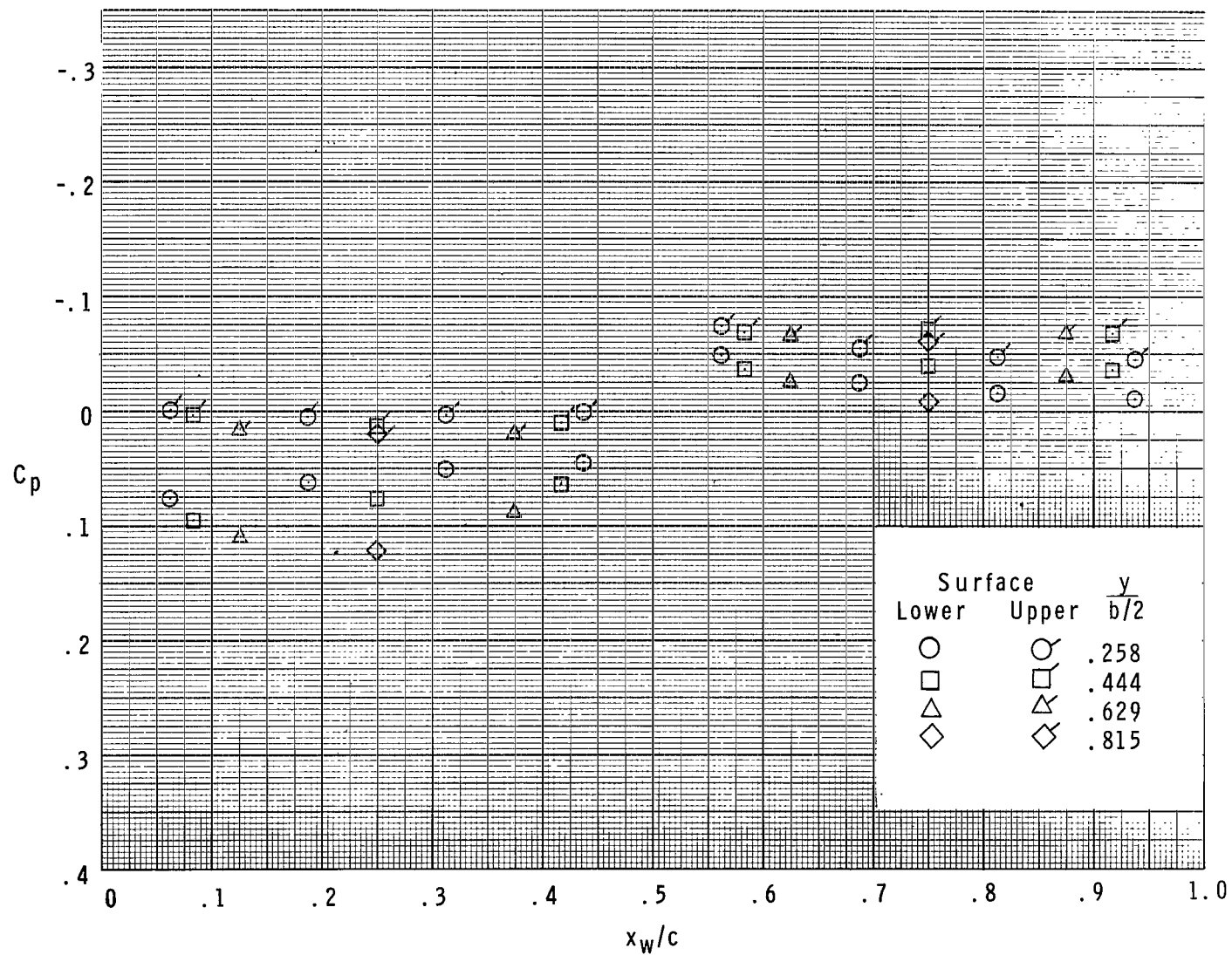
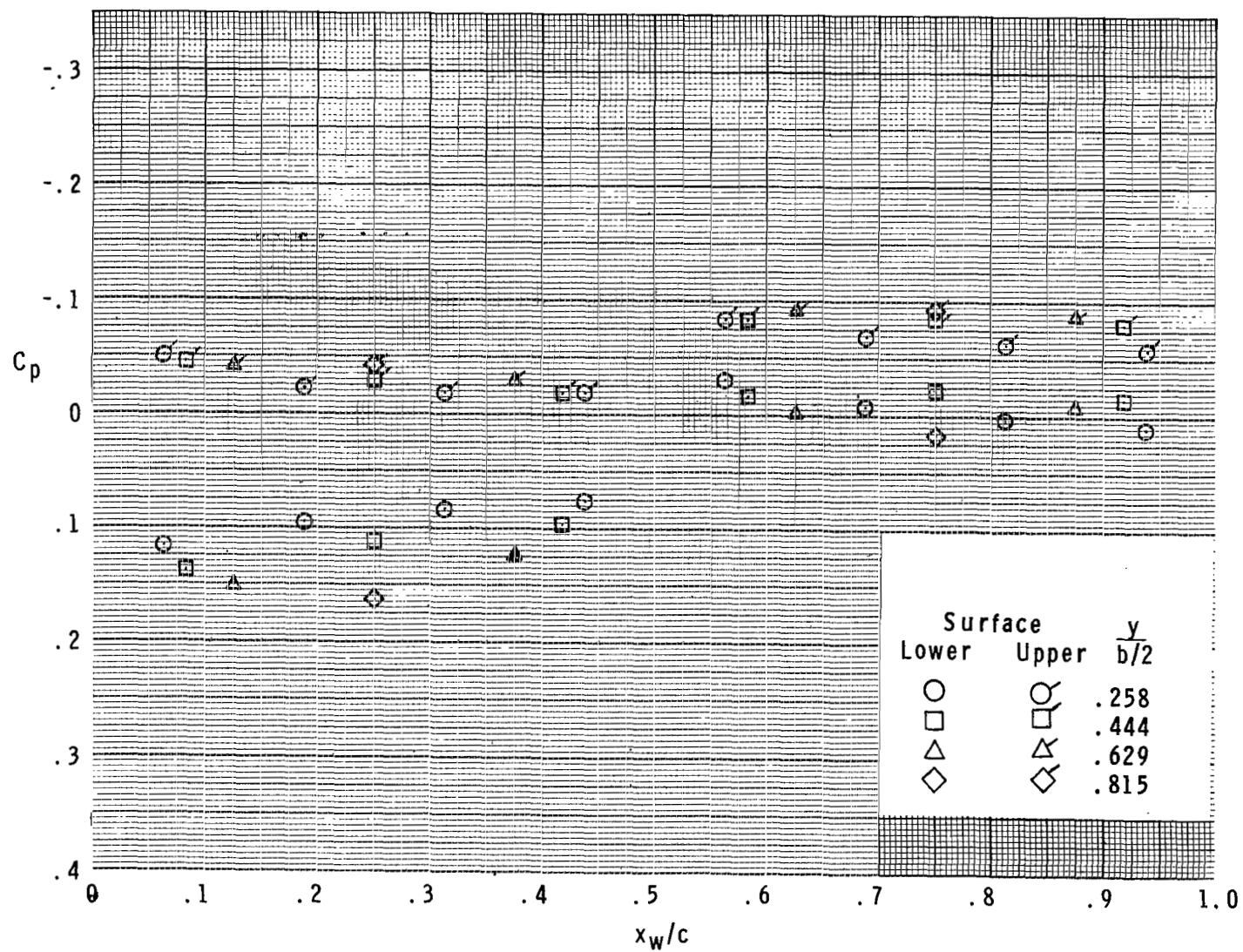
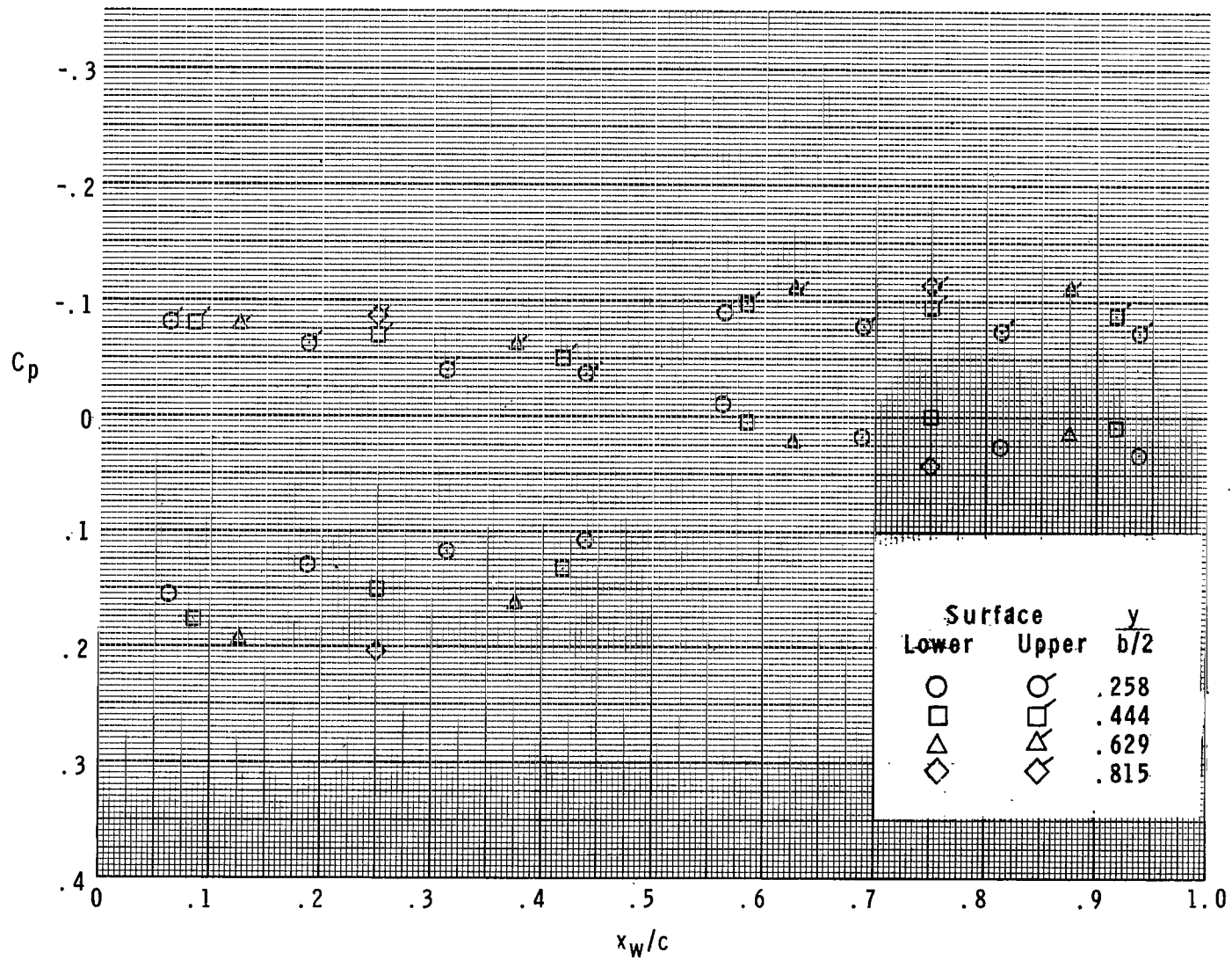


Figure 9.- Continued.



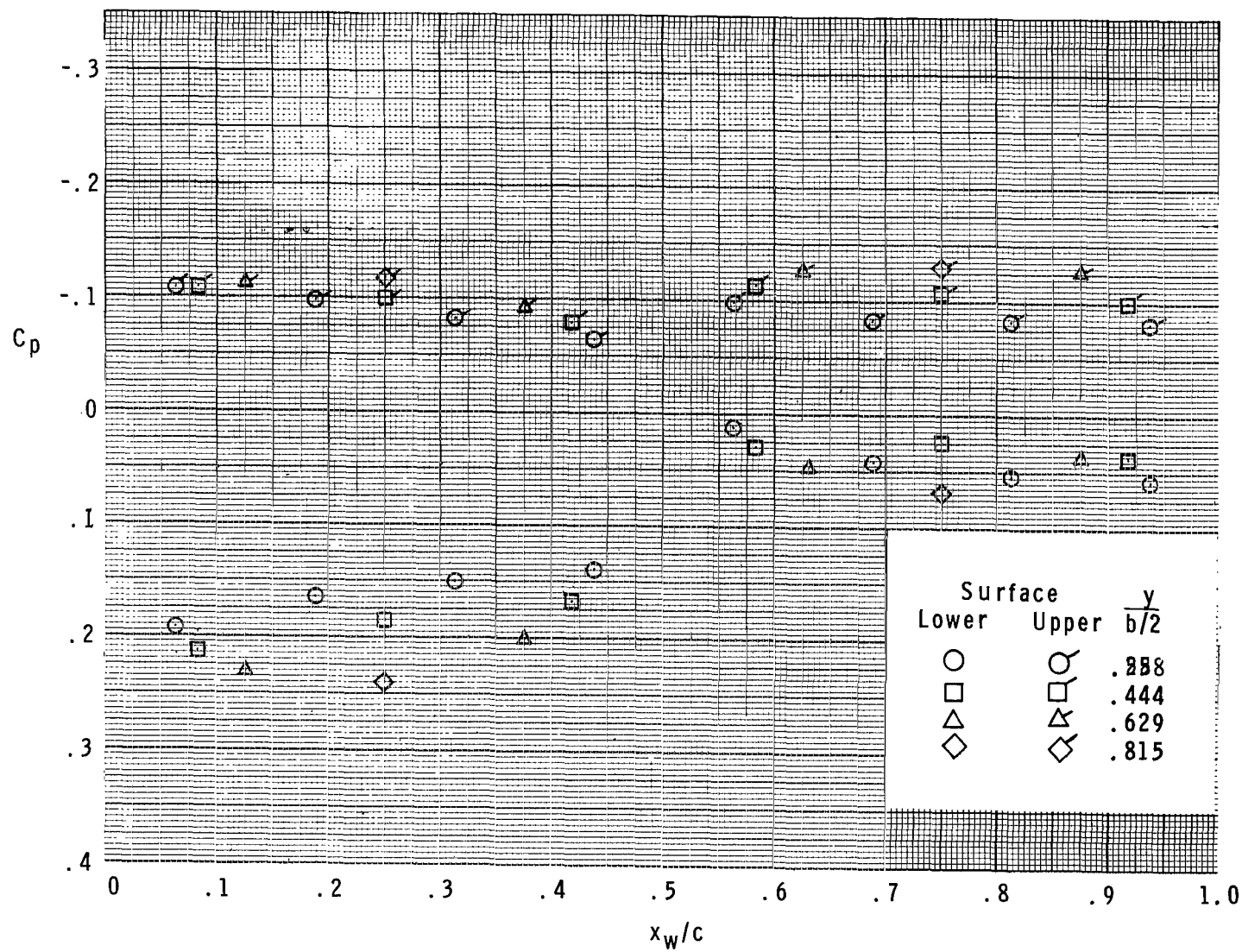
(c) $\alpha = 4.4^\circ$.

Figure 9.- Continued.



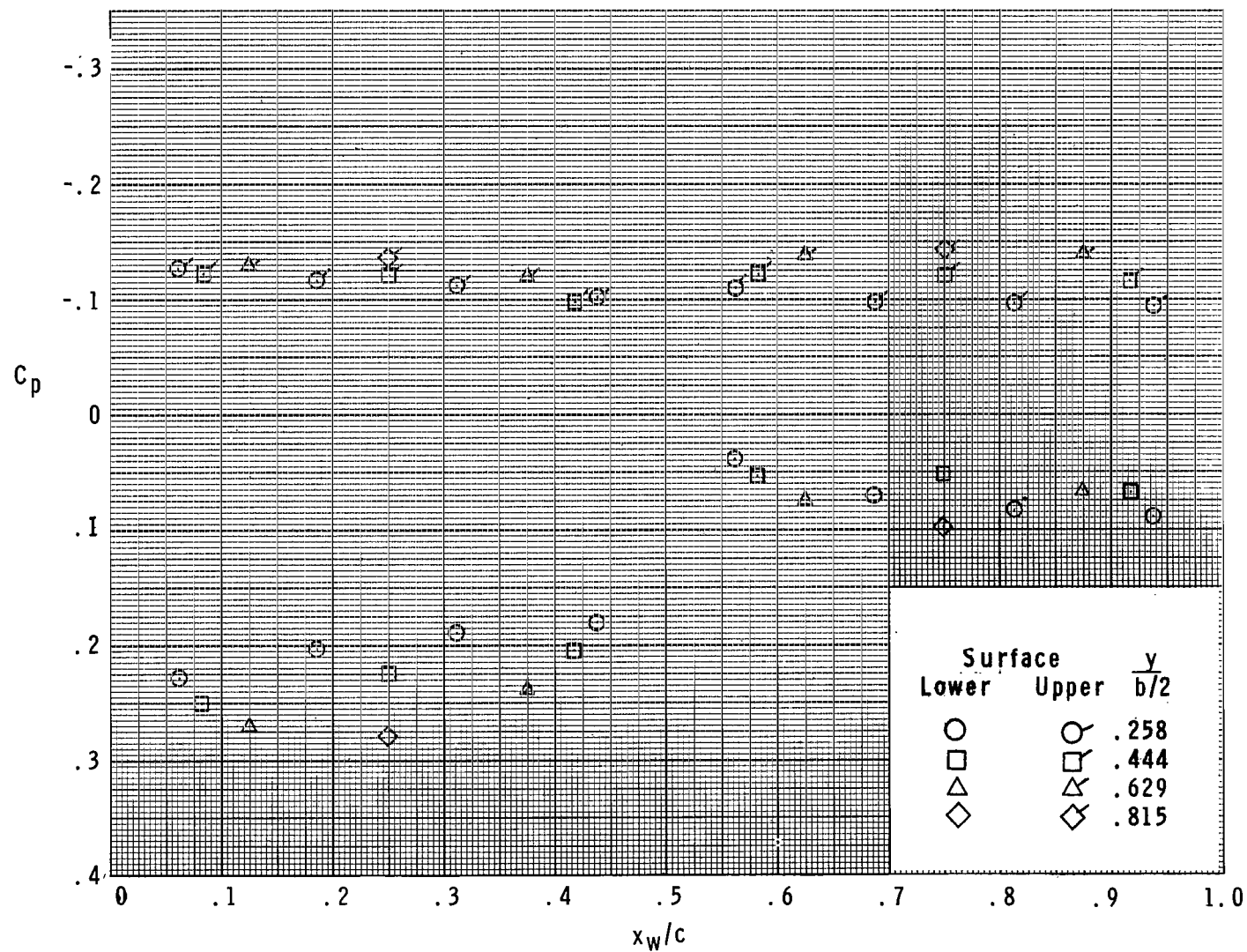
(d) $\alpha = 6.5^\circ$.

Figure 9.- Continued.



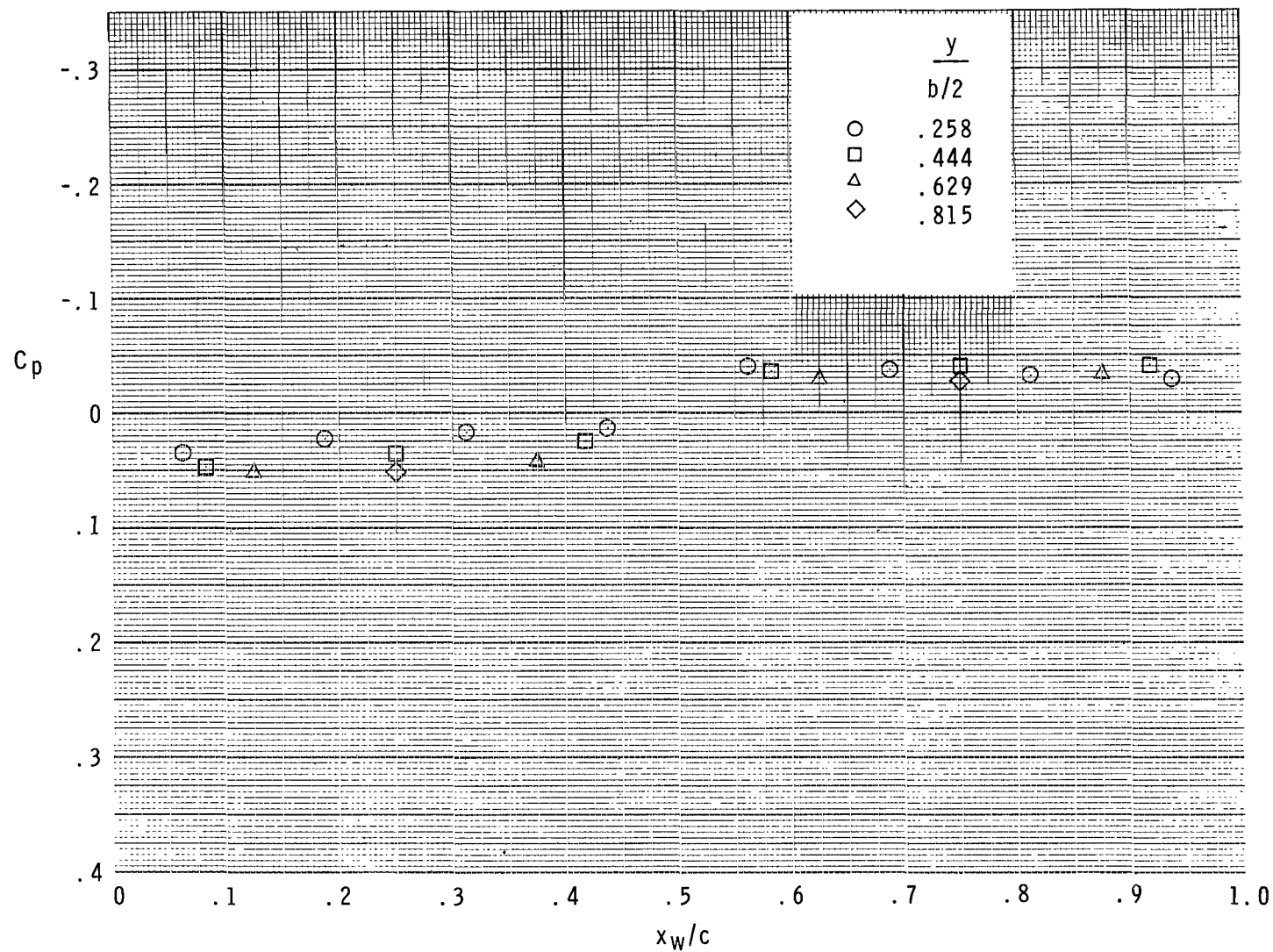
(e) $\alpha = 8.6^\circ$.

Figure 9.- Continued.



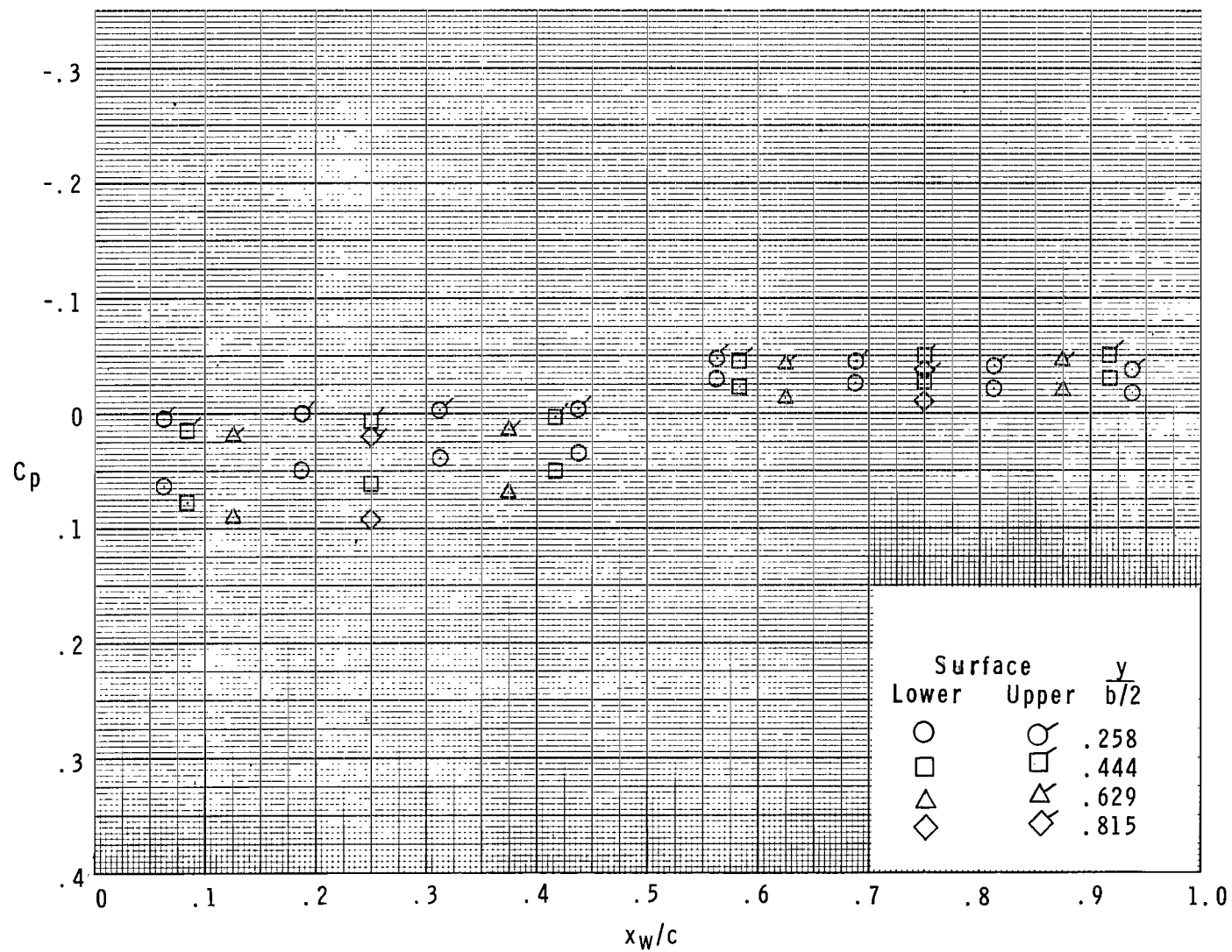
(f) $\alpha = 10.7^\circ$.

Figure 9.- Concluded.



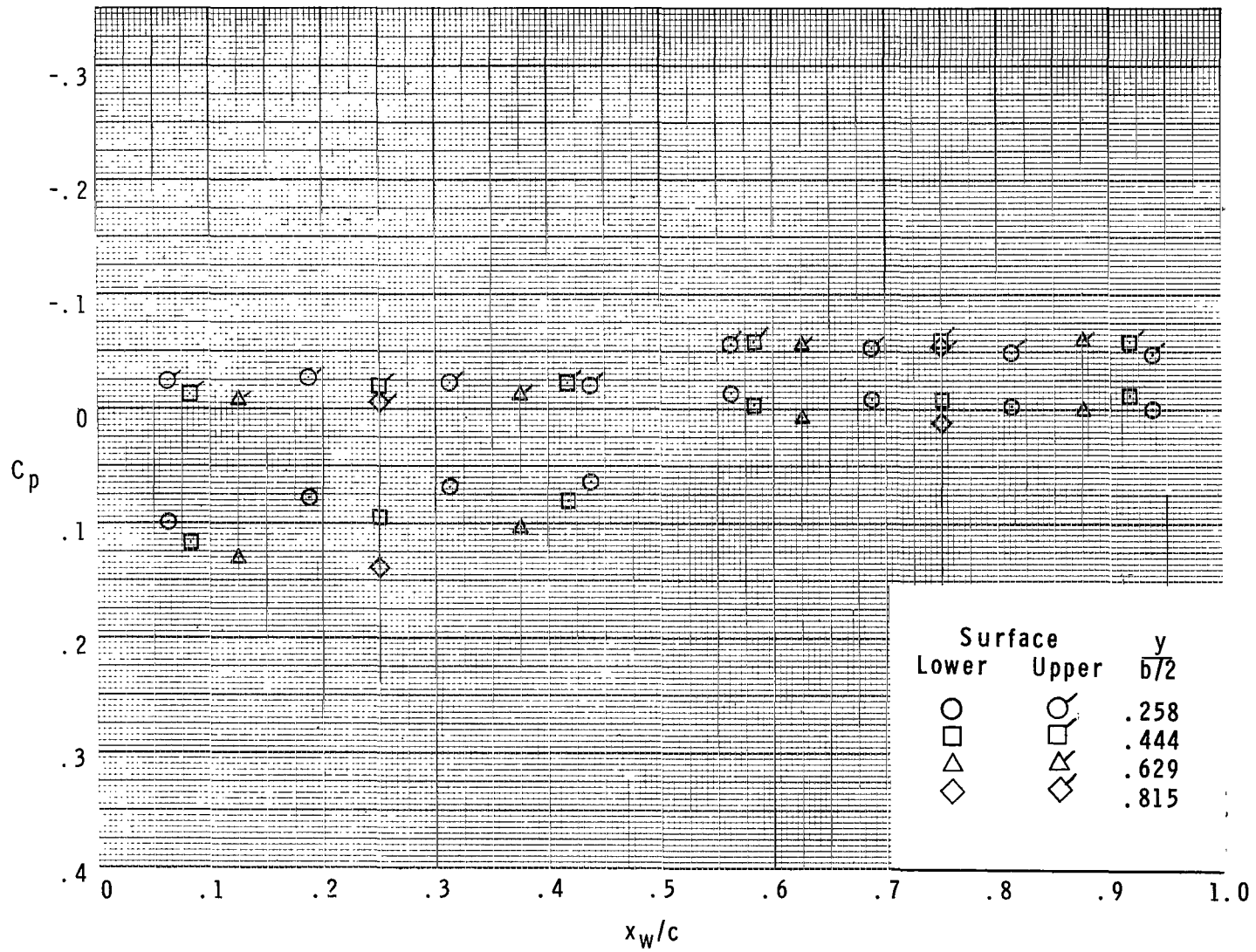
(a) $\alpha = 0^\circ$.

Figure 10.- Experimental pressure coefficients over wing; $M = 3.95$.



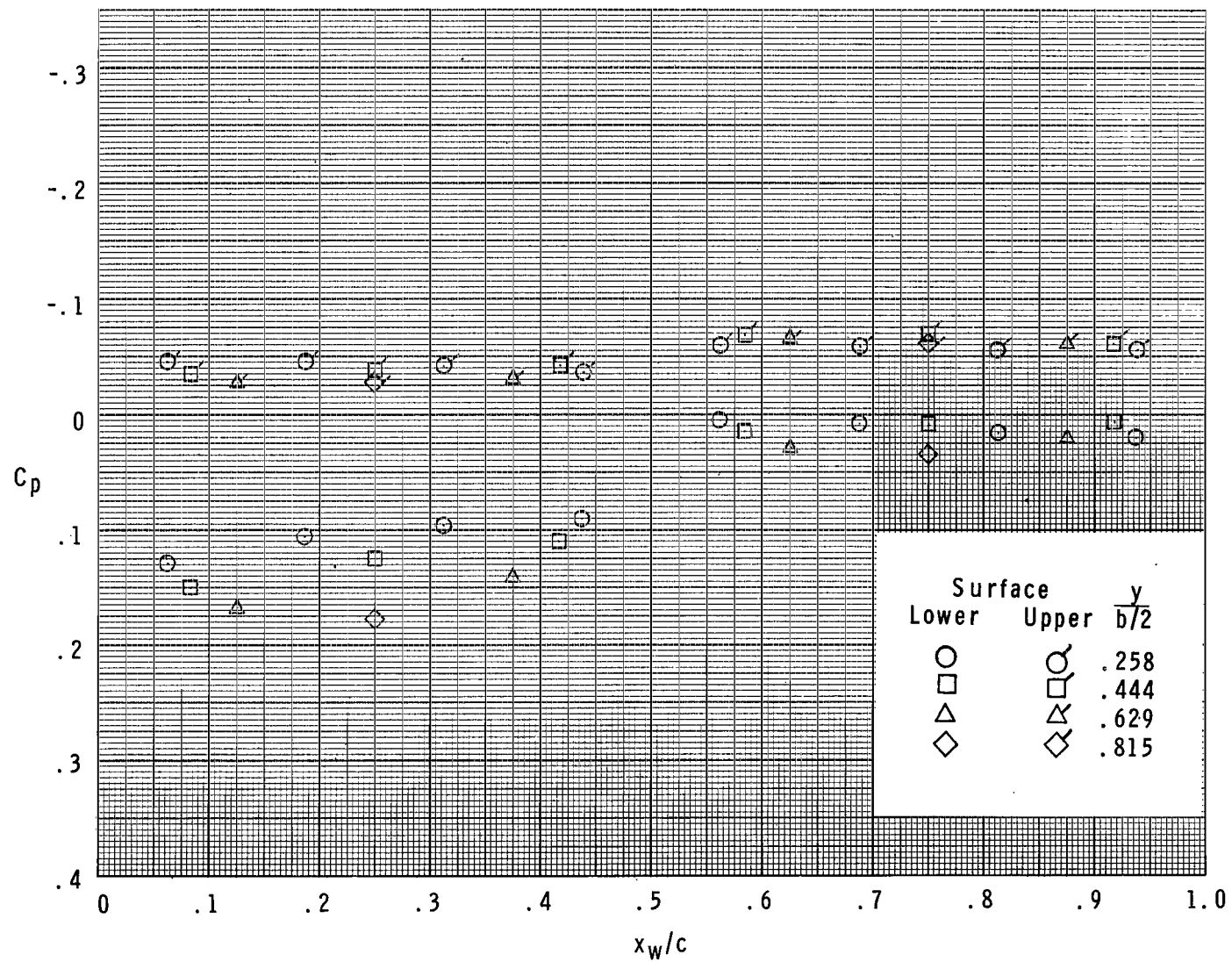
(b) $\alpha = 2.1^\circ$.

Figure 10.- Continued.



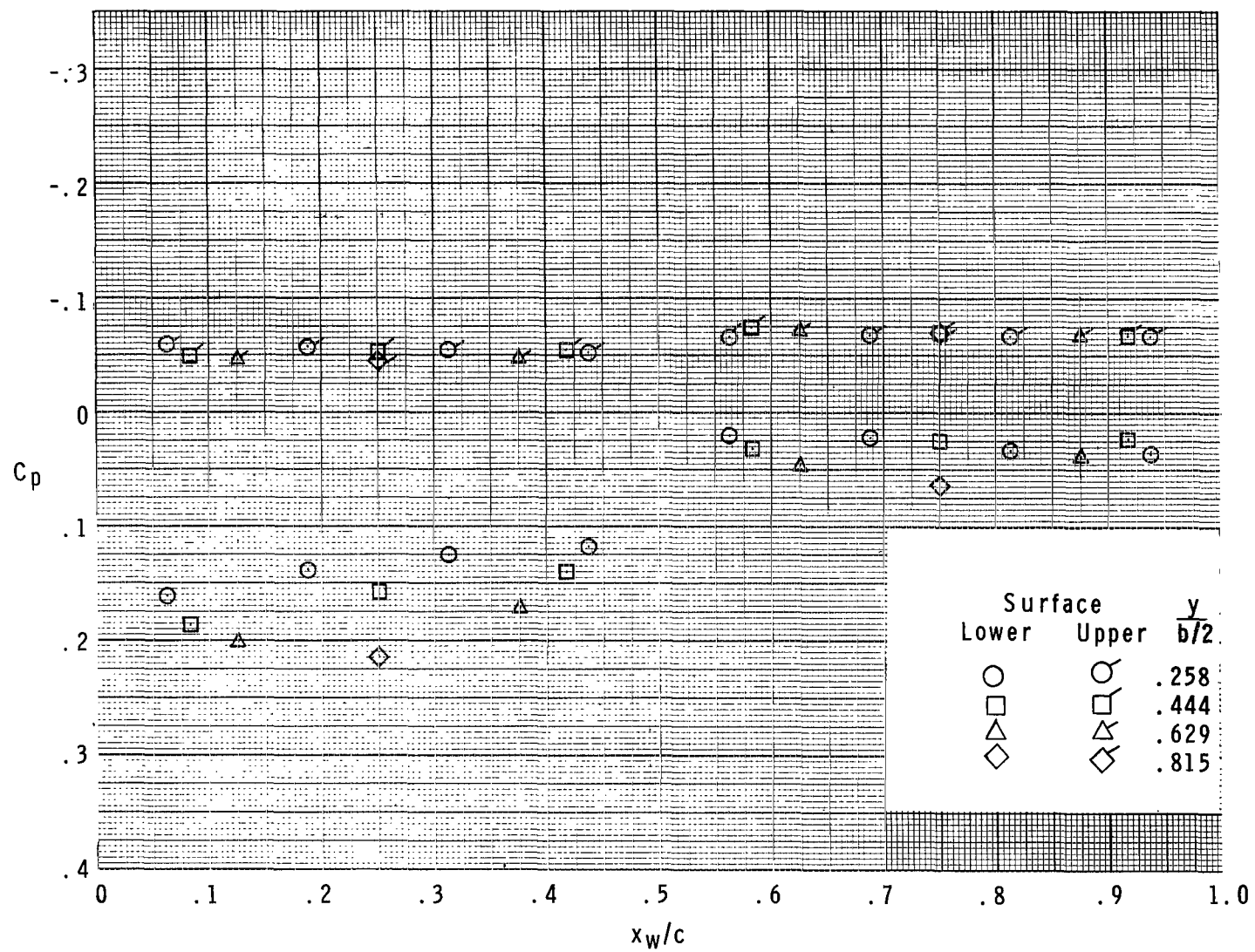
(c) $\alpha = 4.3^\circ$.

Figure 10.- Continued.



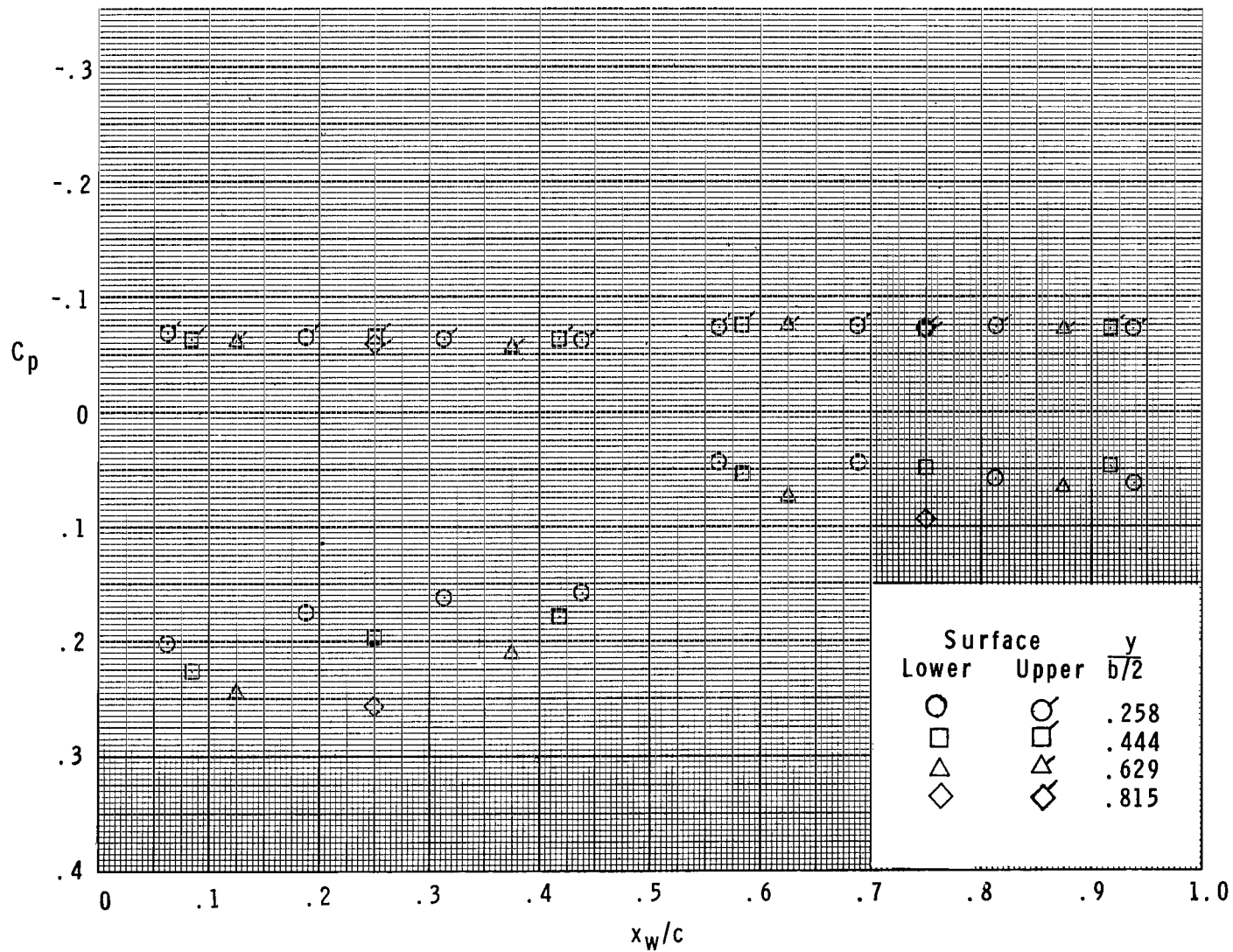
(d) $\alpha = 6.4^\circ$.

Figure 10.- Continued.



(e) $\alpha = 8.5^\circ$.

Figure 10.- Continued.



(f) $\alpha = 10.6^\circ$.

Figure 10.- Concluded.

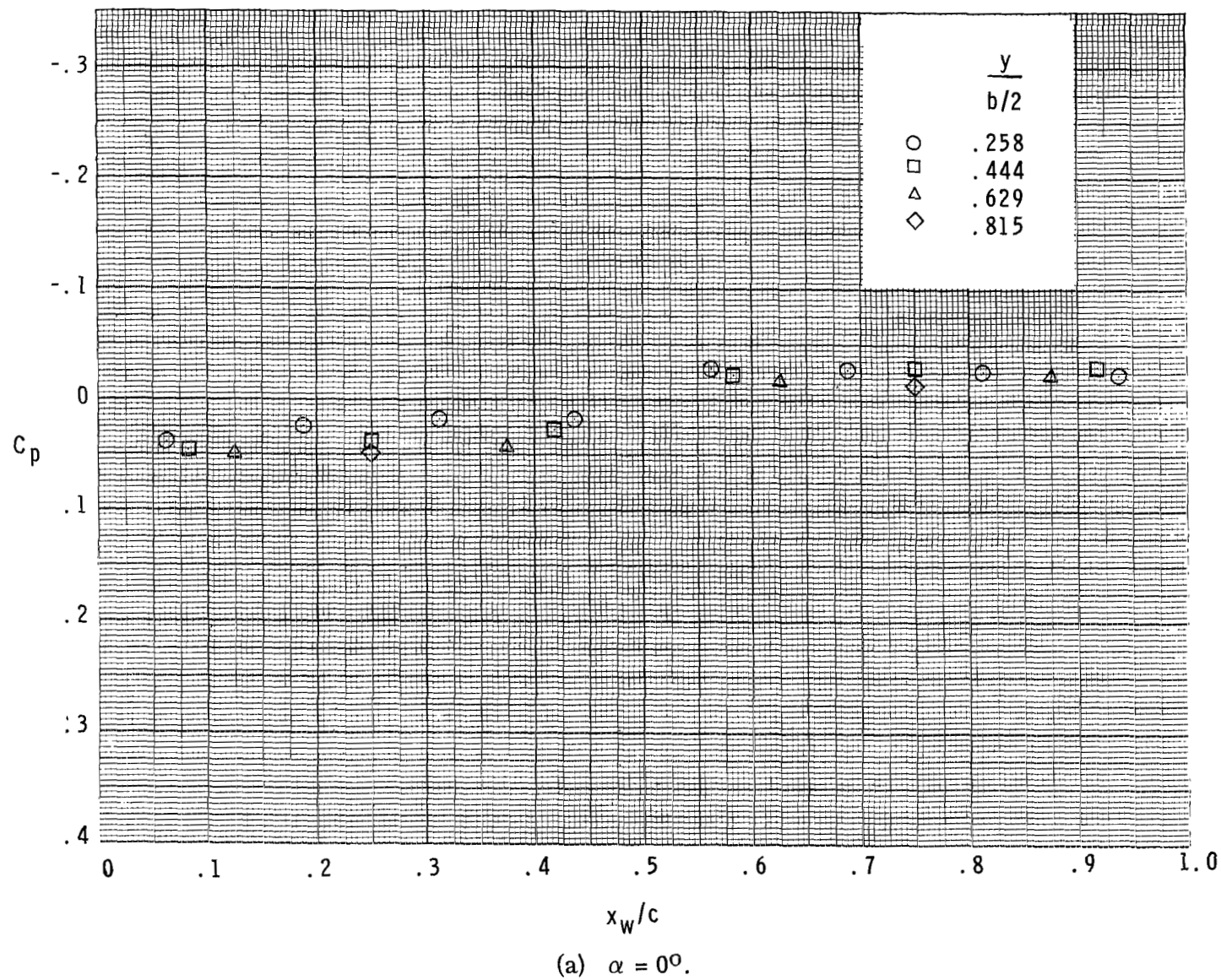
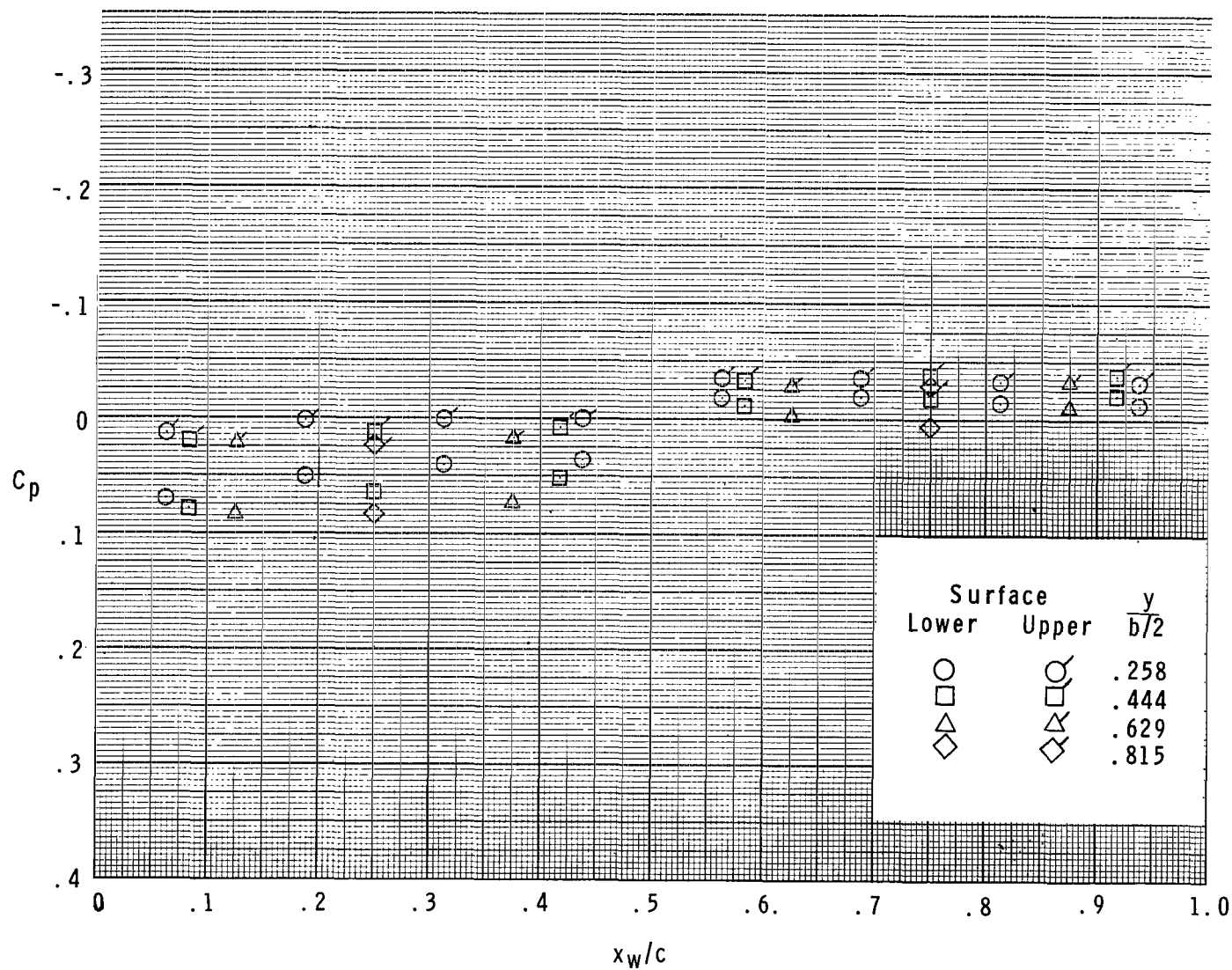
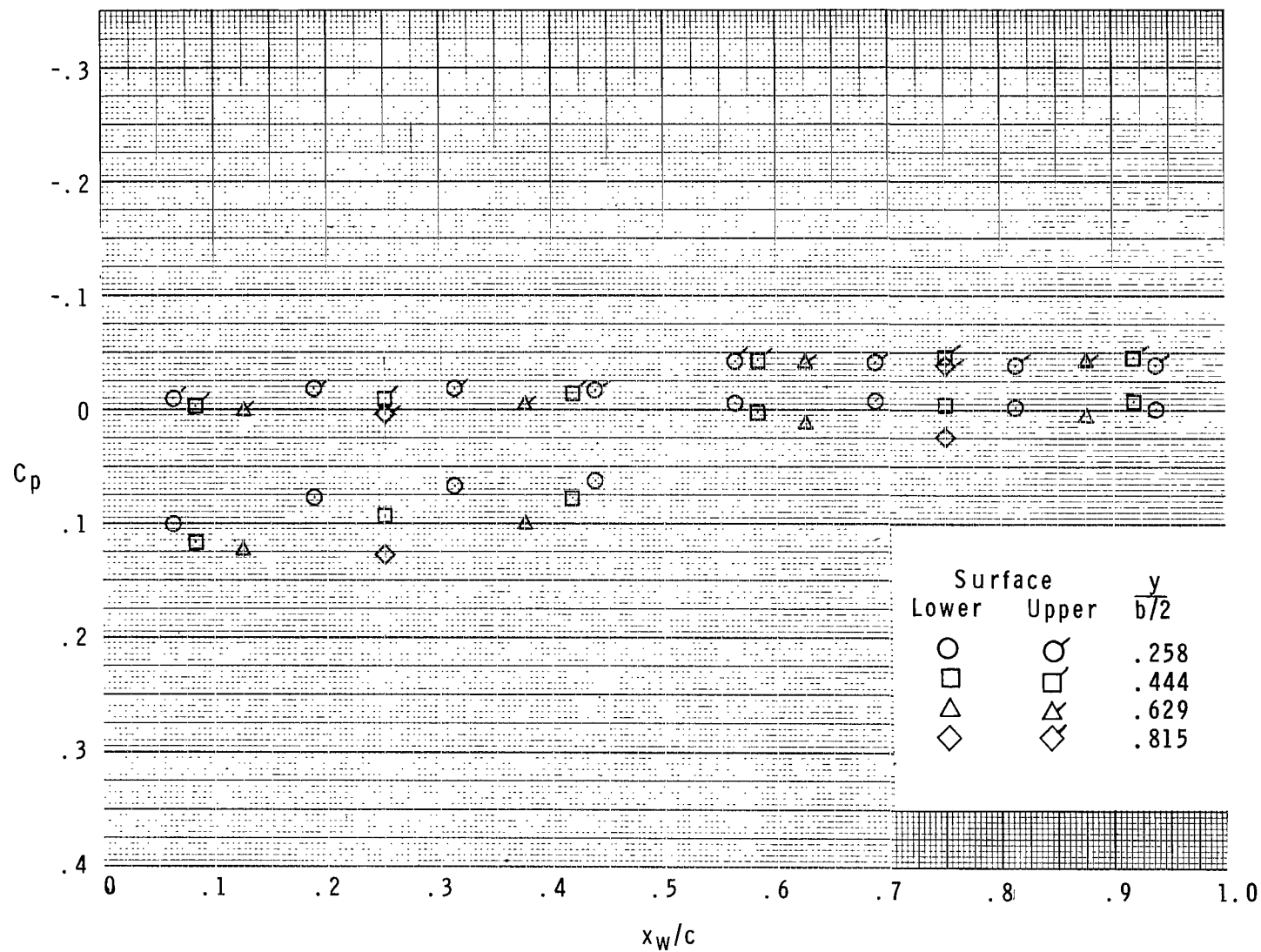


Figure 11.- Experimental pressure coefficients over wing; $M = 4.63$.



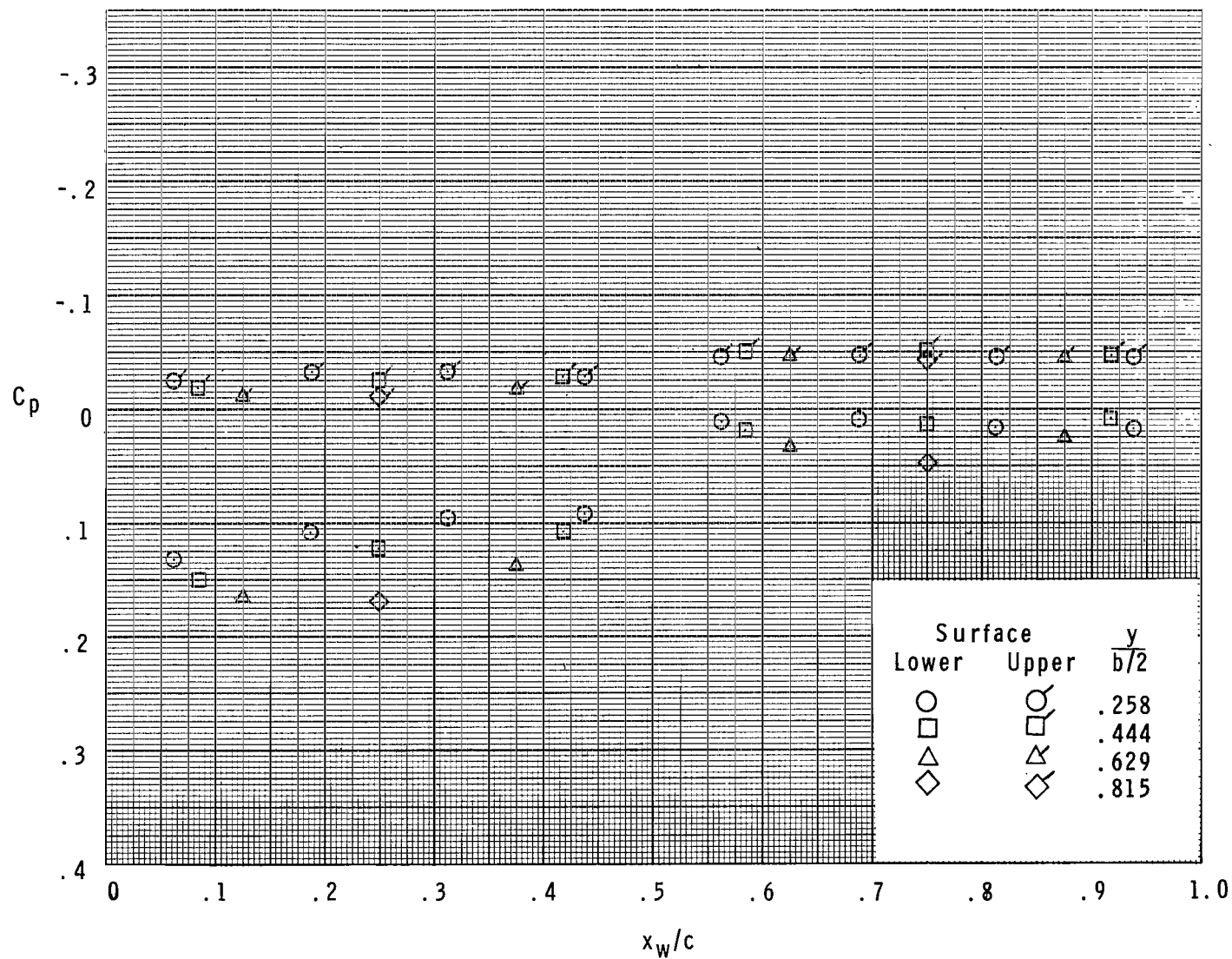
(b) $\alpha = 2.0^\circ$.

Figure 11.- Continued.



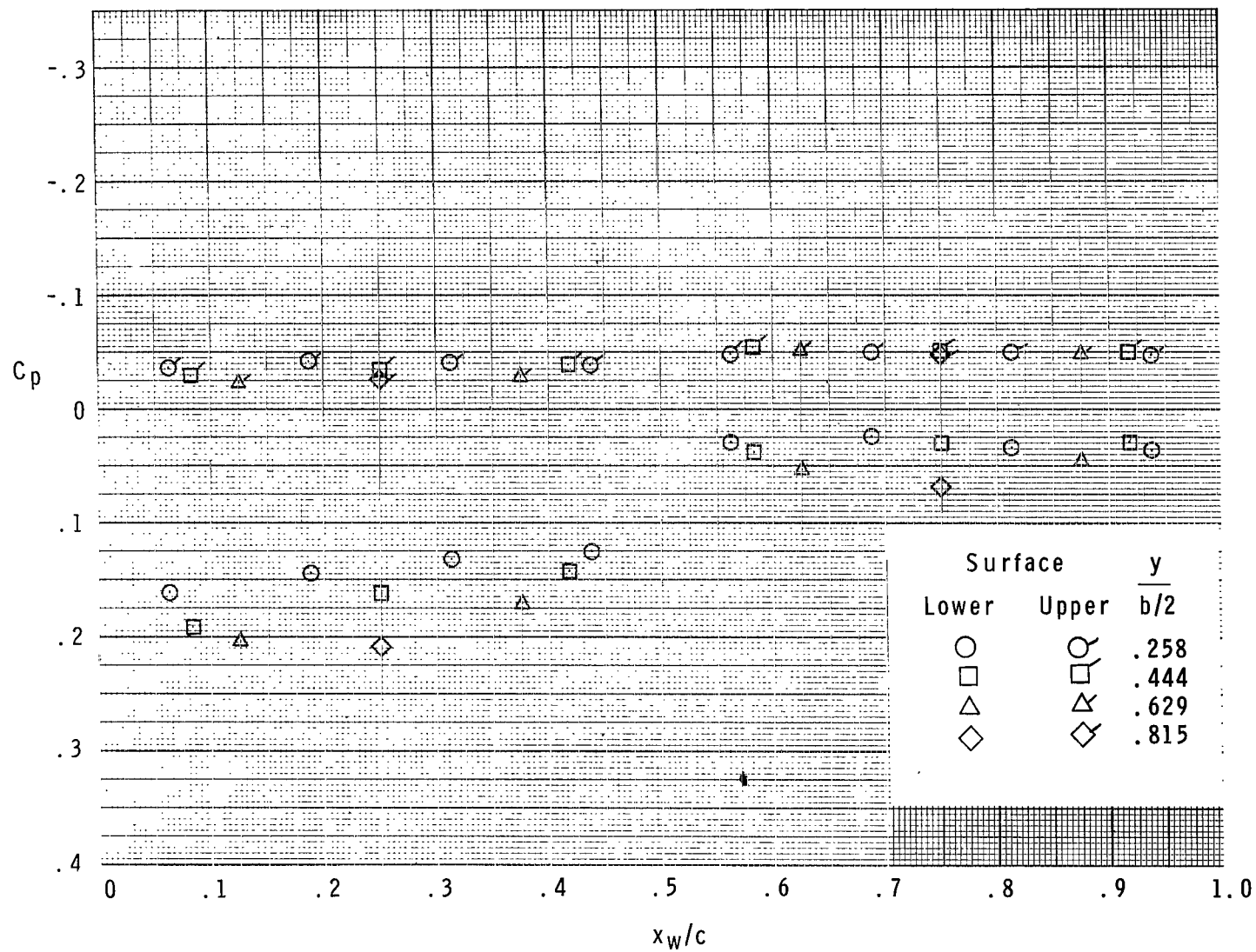
(c) $\alpha = 4.2^\circ$.

Figure 11.- Continued.



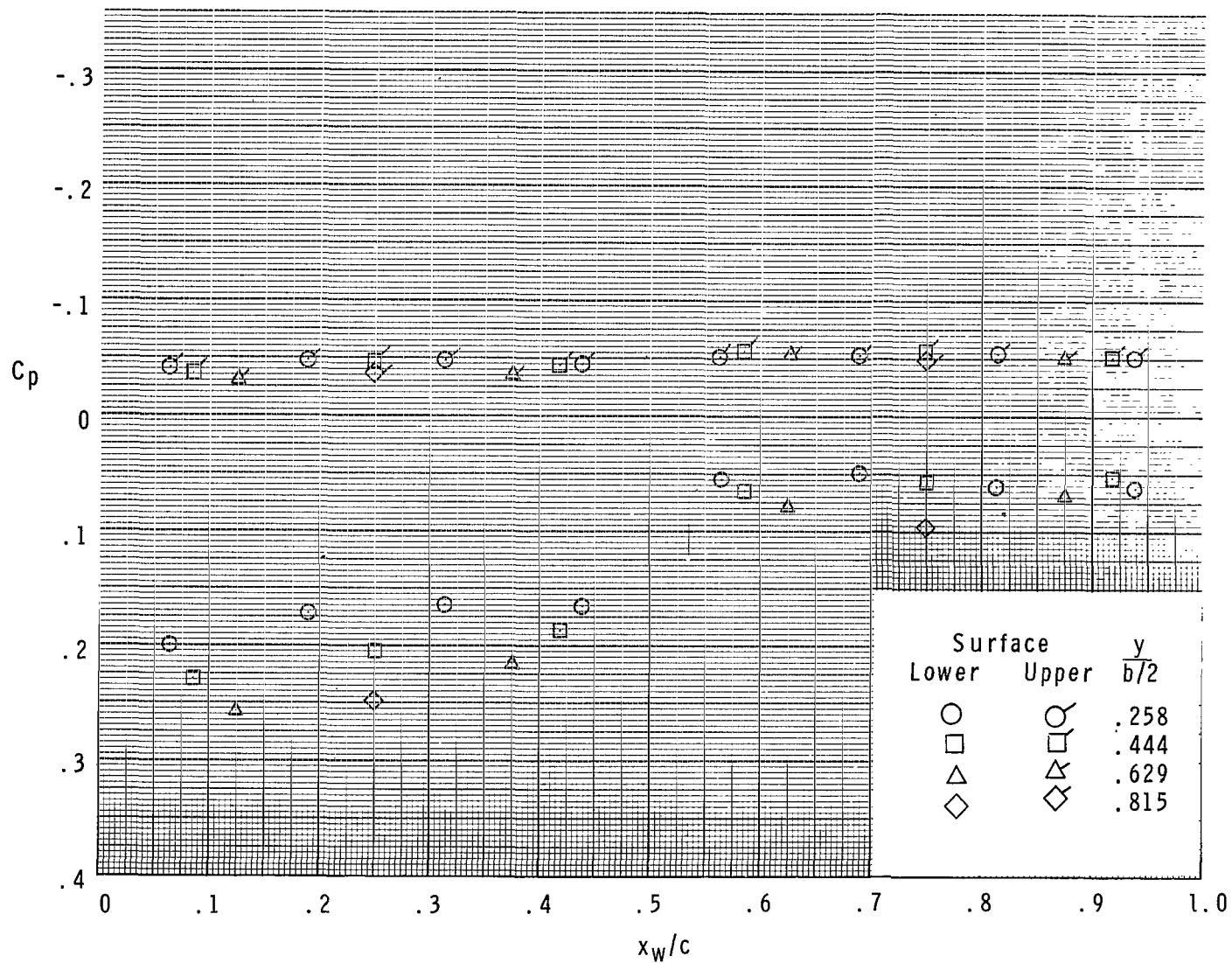
(d) $\alpha = 6.2^\circ$.

Figure 11.- Continued.



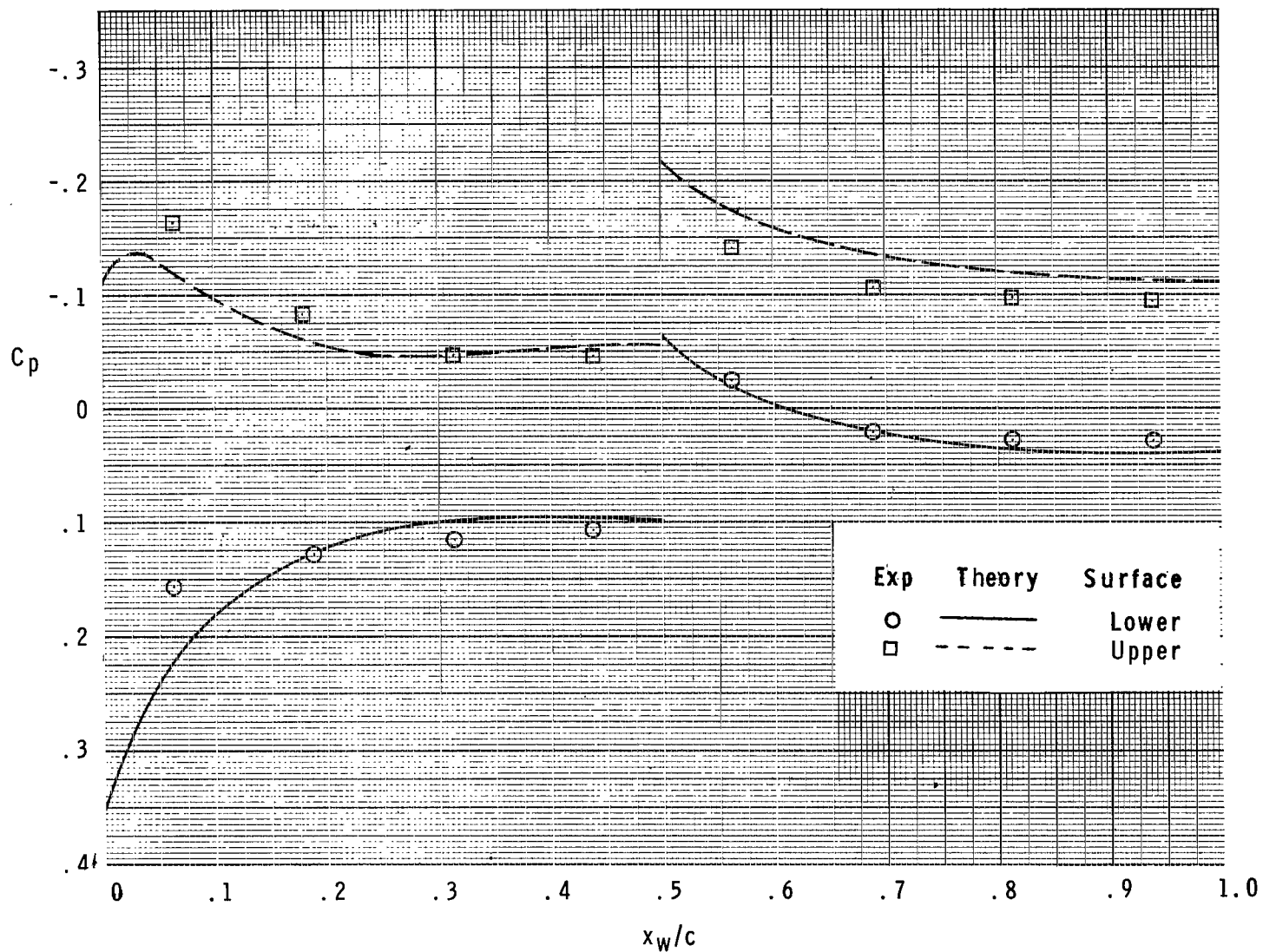
(e) $\alpha = 8.3^\circ$.

Figure 11.- Continued.



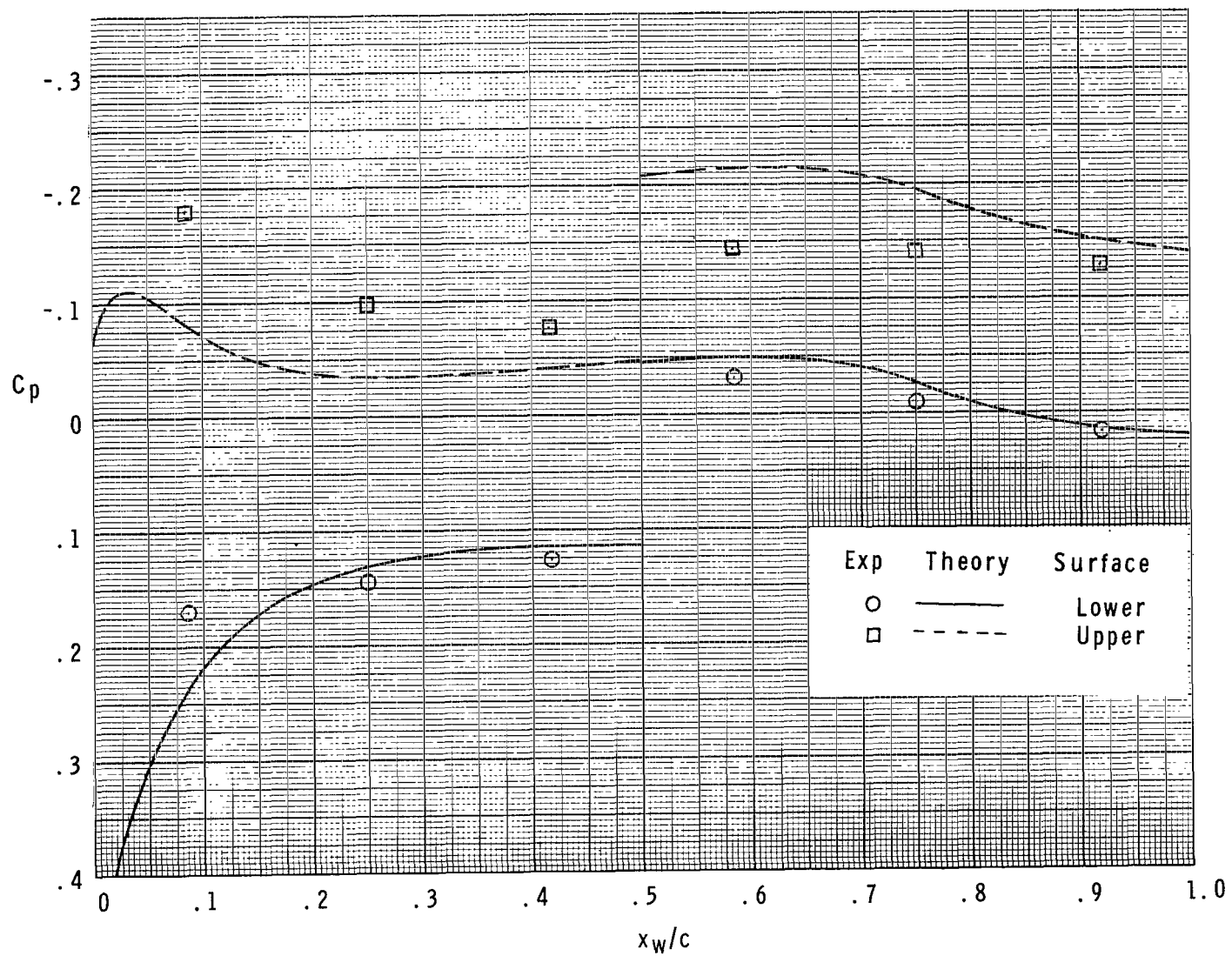
(f) $\alpha = 10.4^\circ$.

Figure 11.- Concluded.



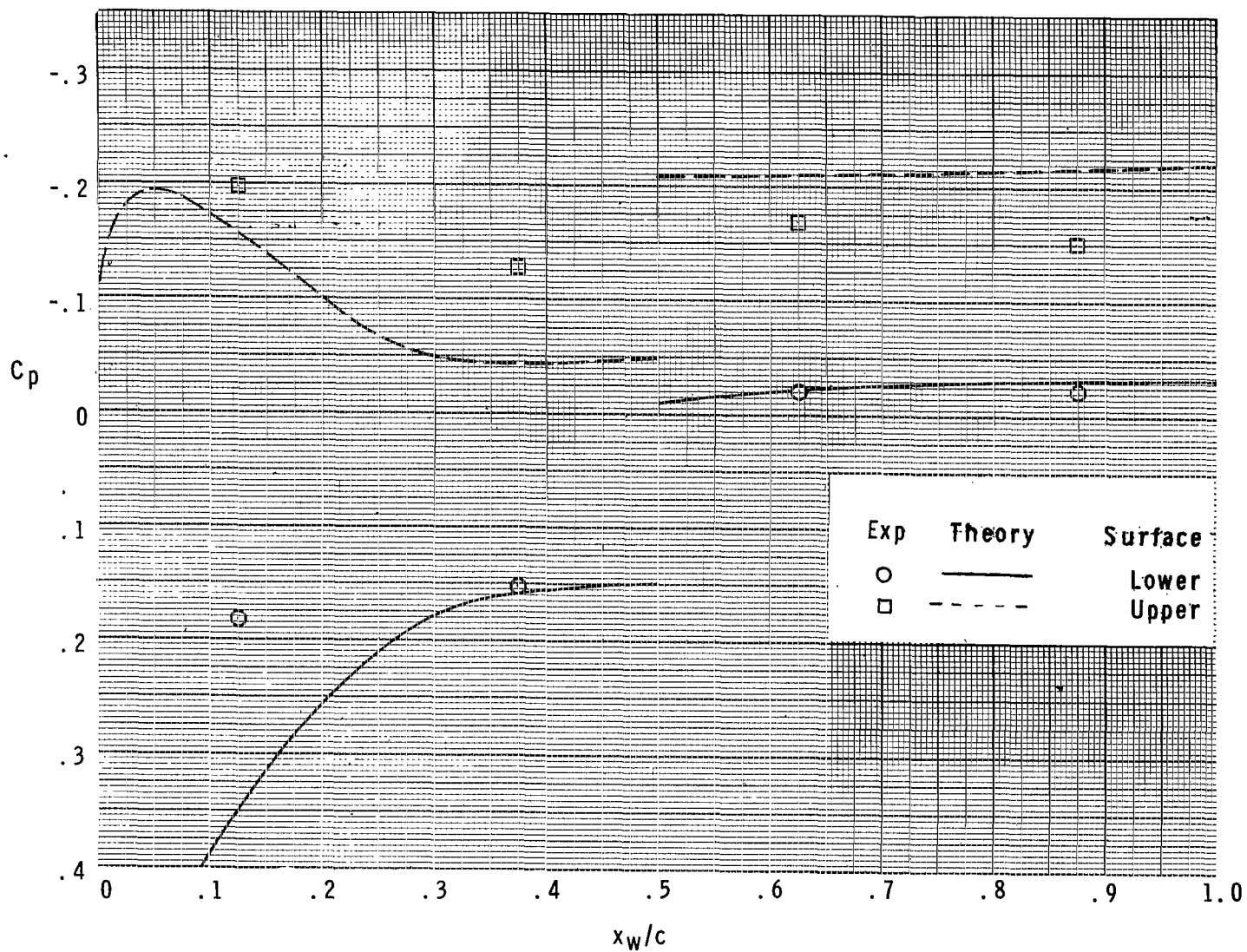
(a) $\frac{y}{b/2} = 0.258$.

Figure 12.- Comparison of wing experimental data with linear-theory method; $\alpha = 6.7^\circ$; $M = 2.30$.



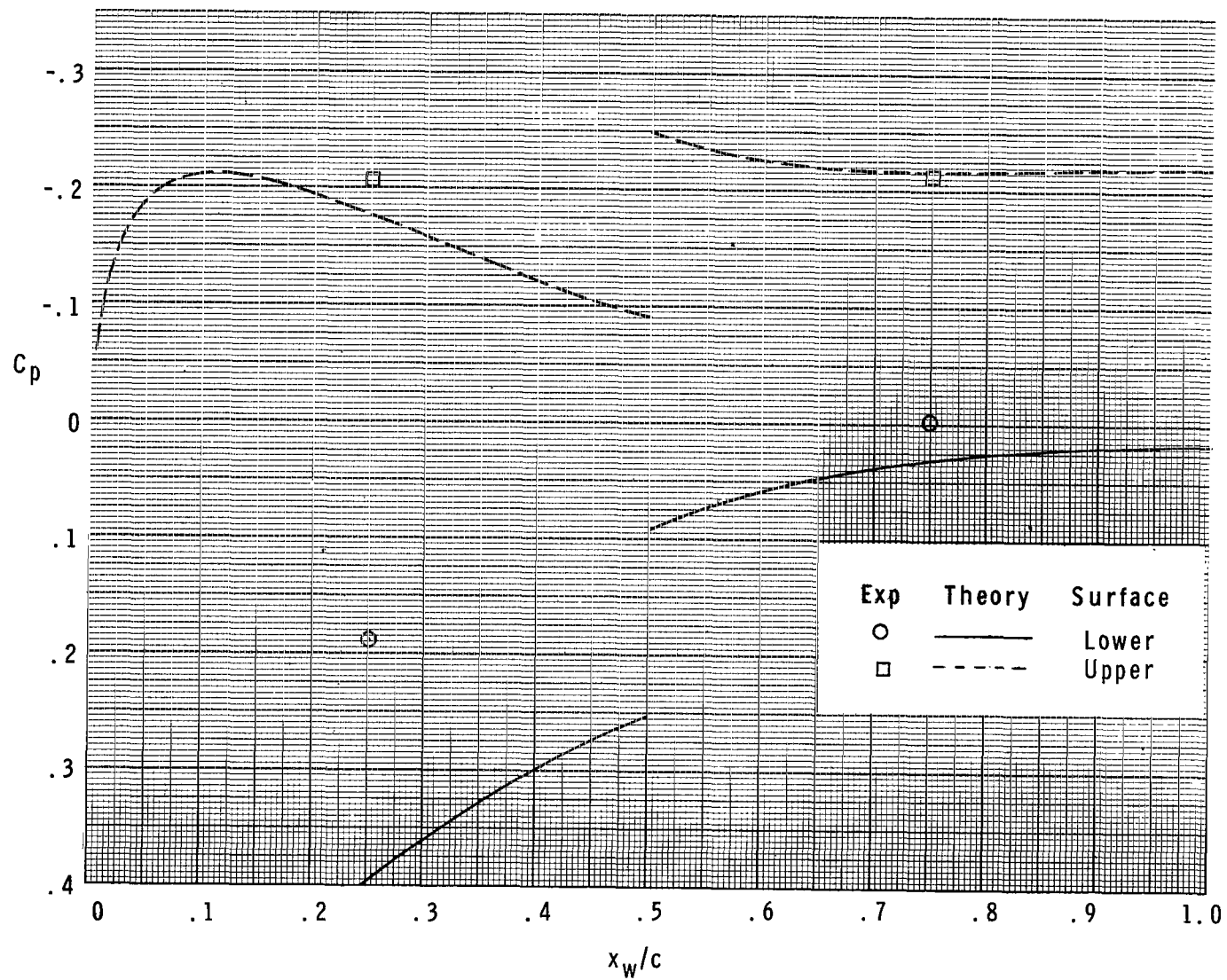
(b) $\frac{y}{b/2} = 0.444$.

Figure 12.- Continued.



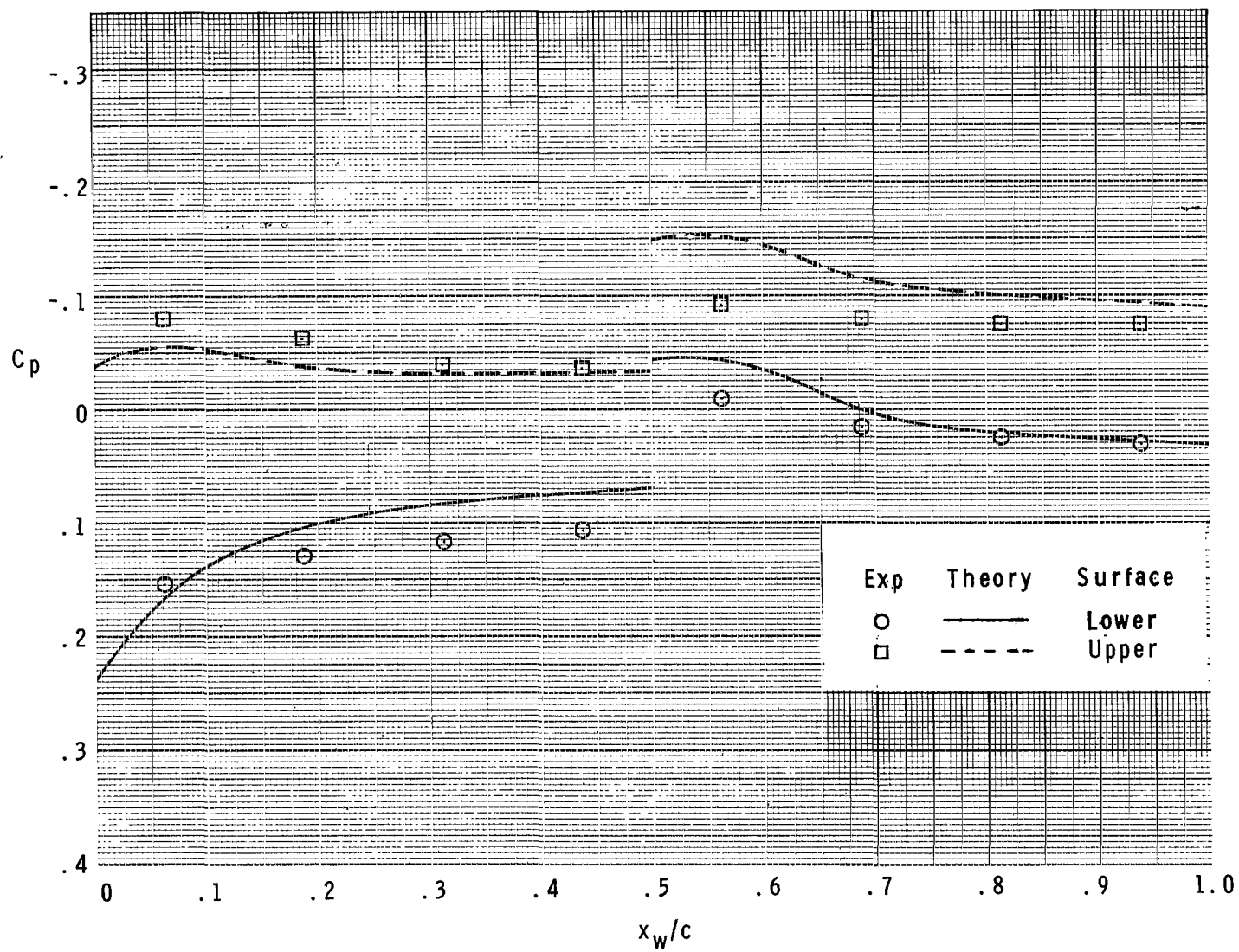
(c) $\frac{y}{b/2} = 0.629$.

Figure 12.- Continued.



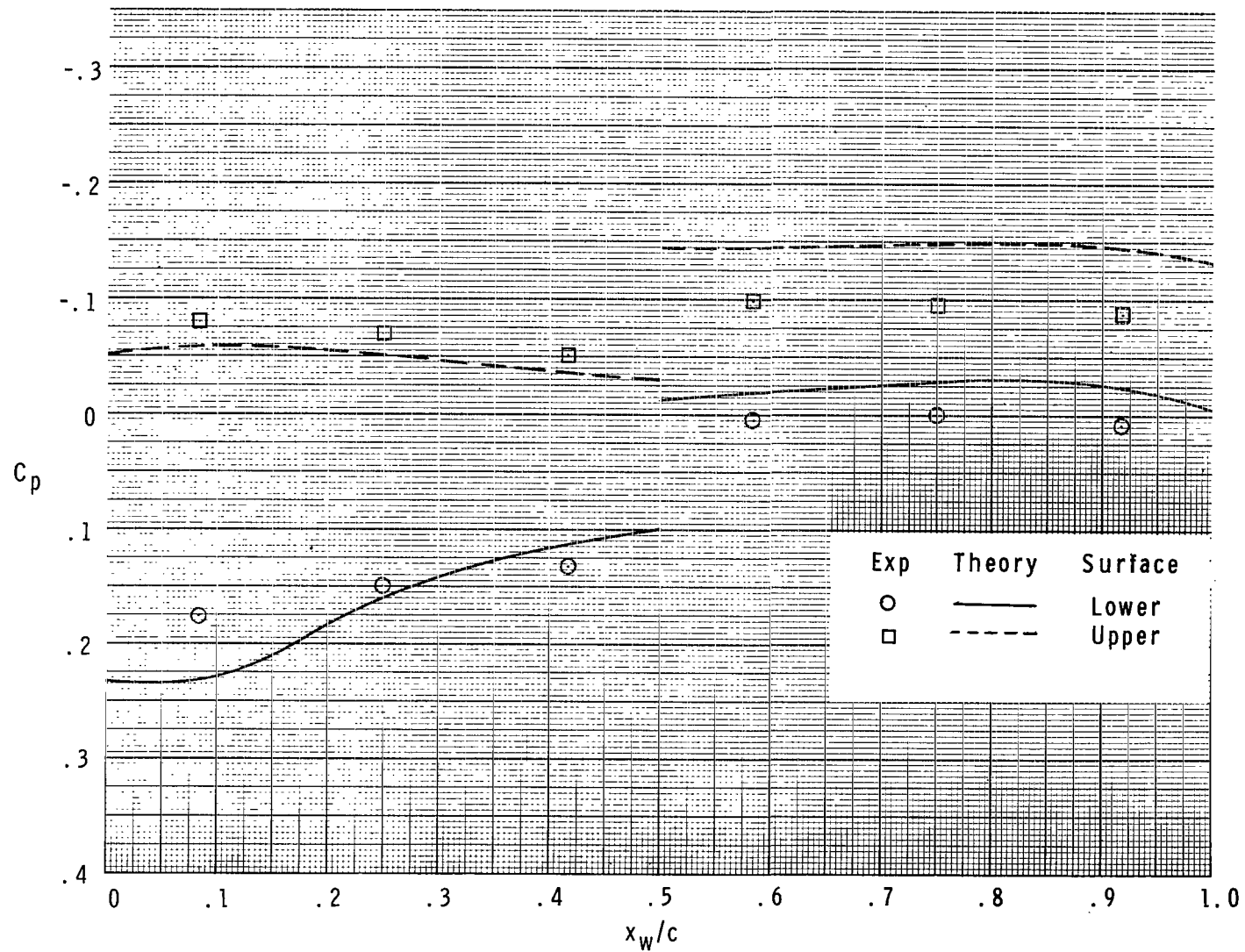
(d) $\frac{y}{b/2} = 0.815.$

Figure 12.- Concluded.



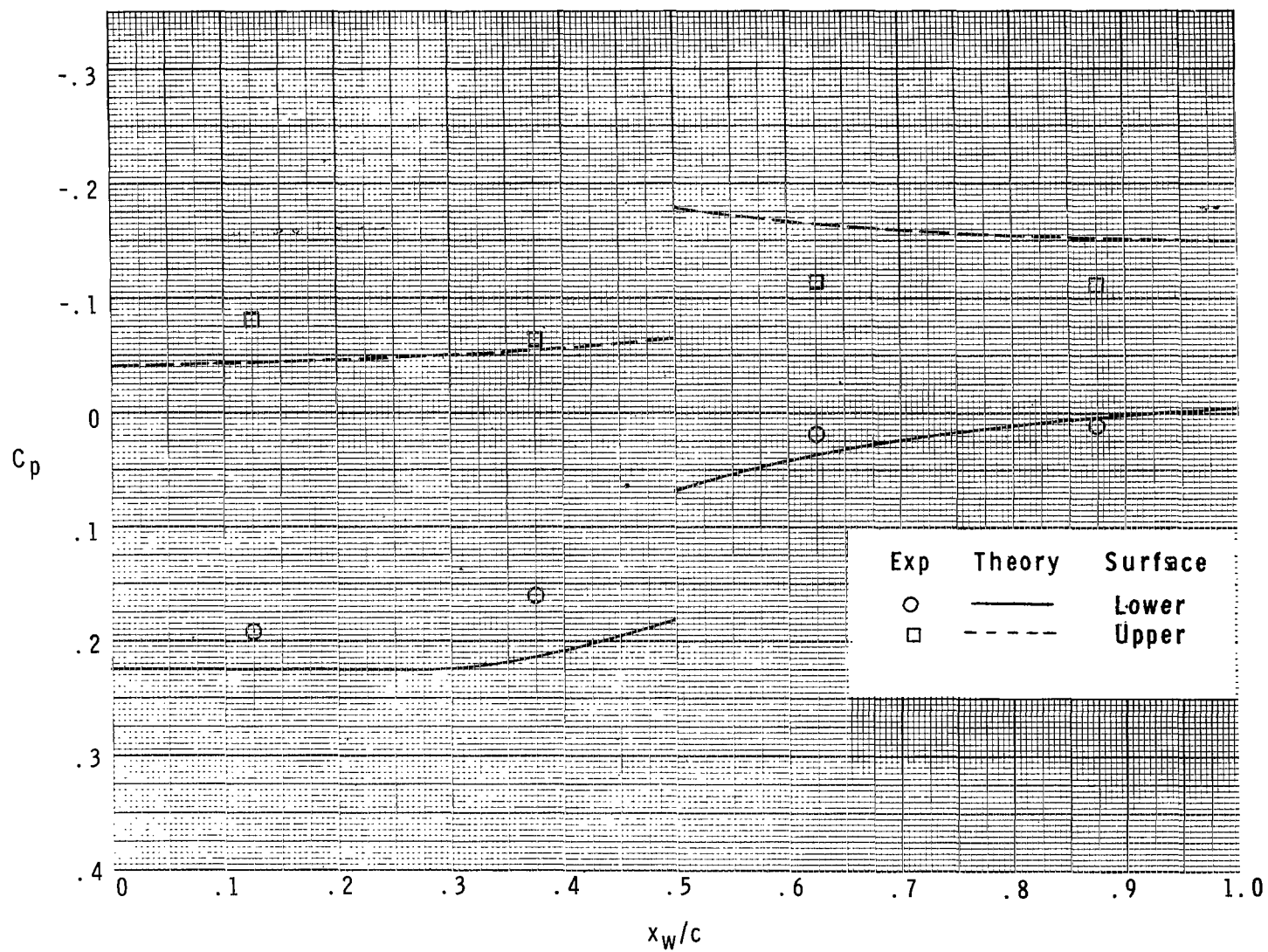
(a) $\frac{y}{b/2} = 0.258$.

Figure 13.- Comparison of wing experimental data with linear-theory method; $\alpha = 6.5^\circ$; $M = 2.96$.



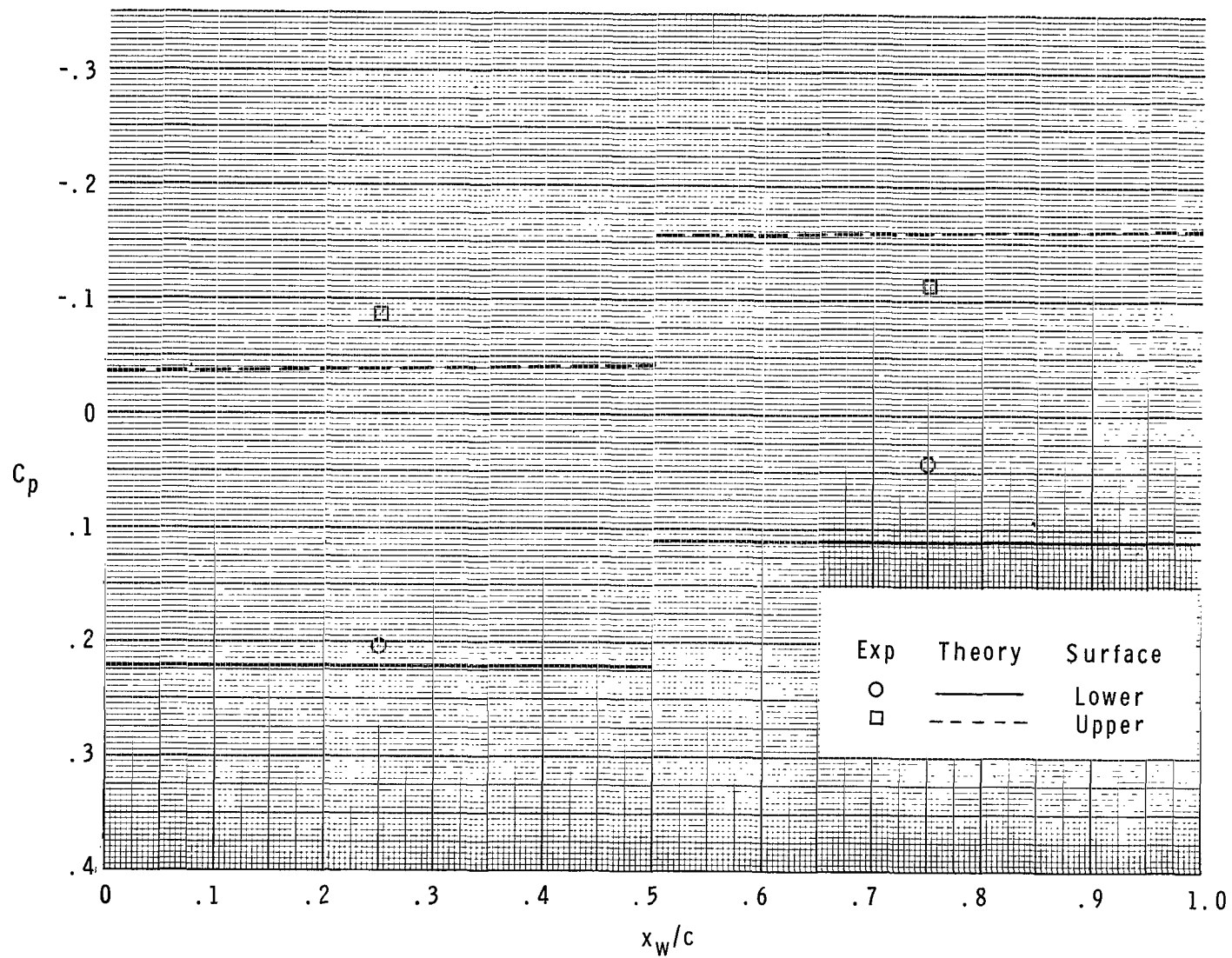
(b) $\frac{y}{b/2} = 0.444.$

Figure 13.- Continued.



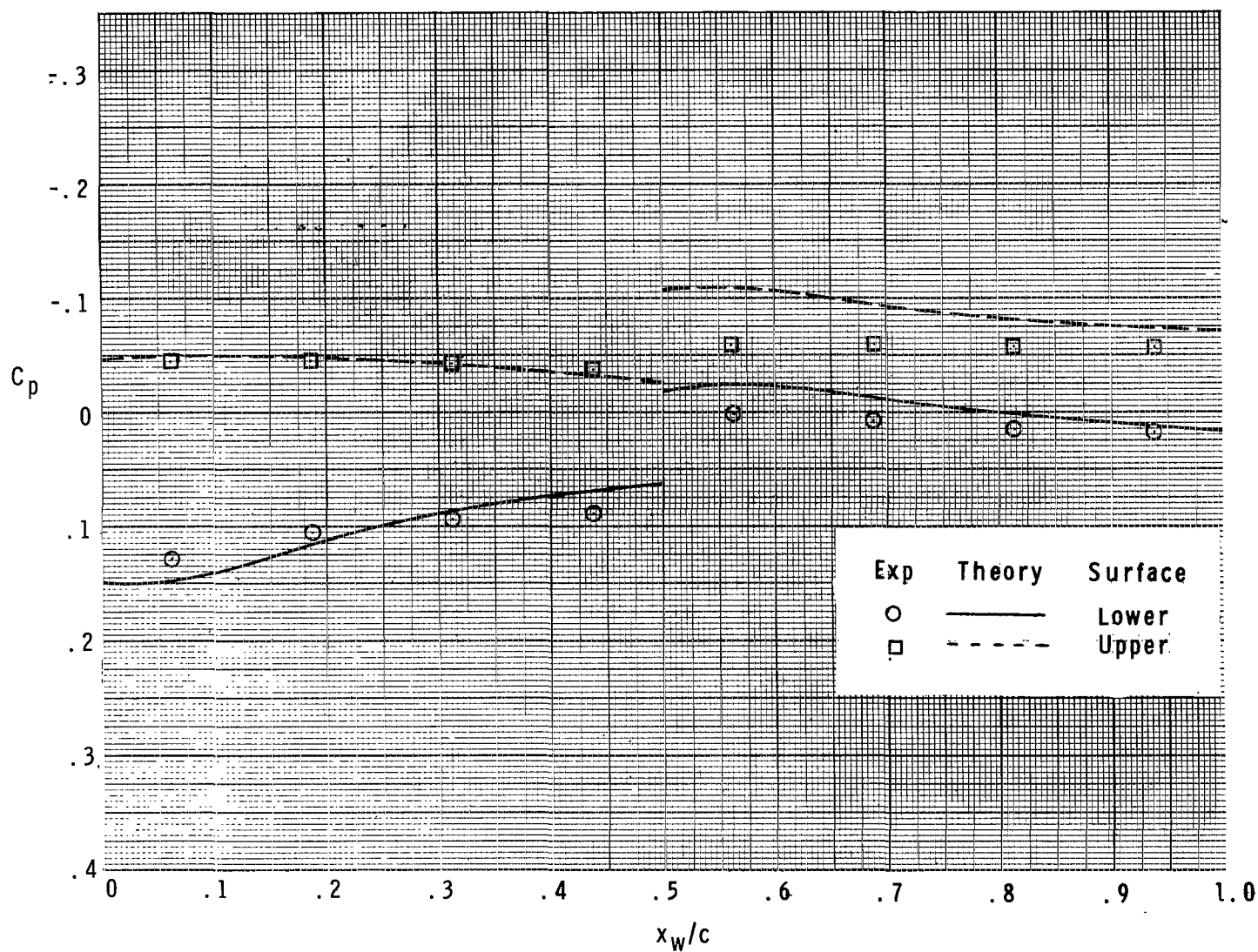
(c) $\frac{y}{b/2} = 0.629$.

Figure 13.- Continued.



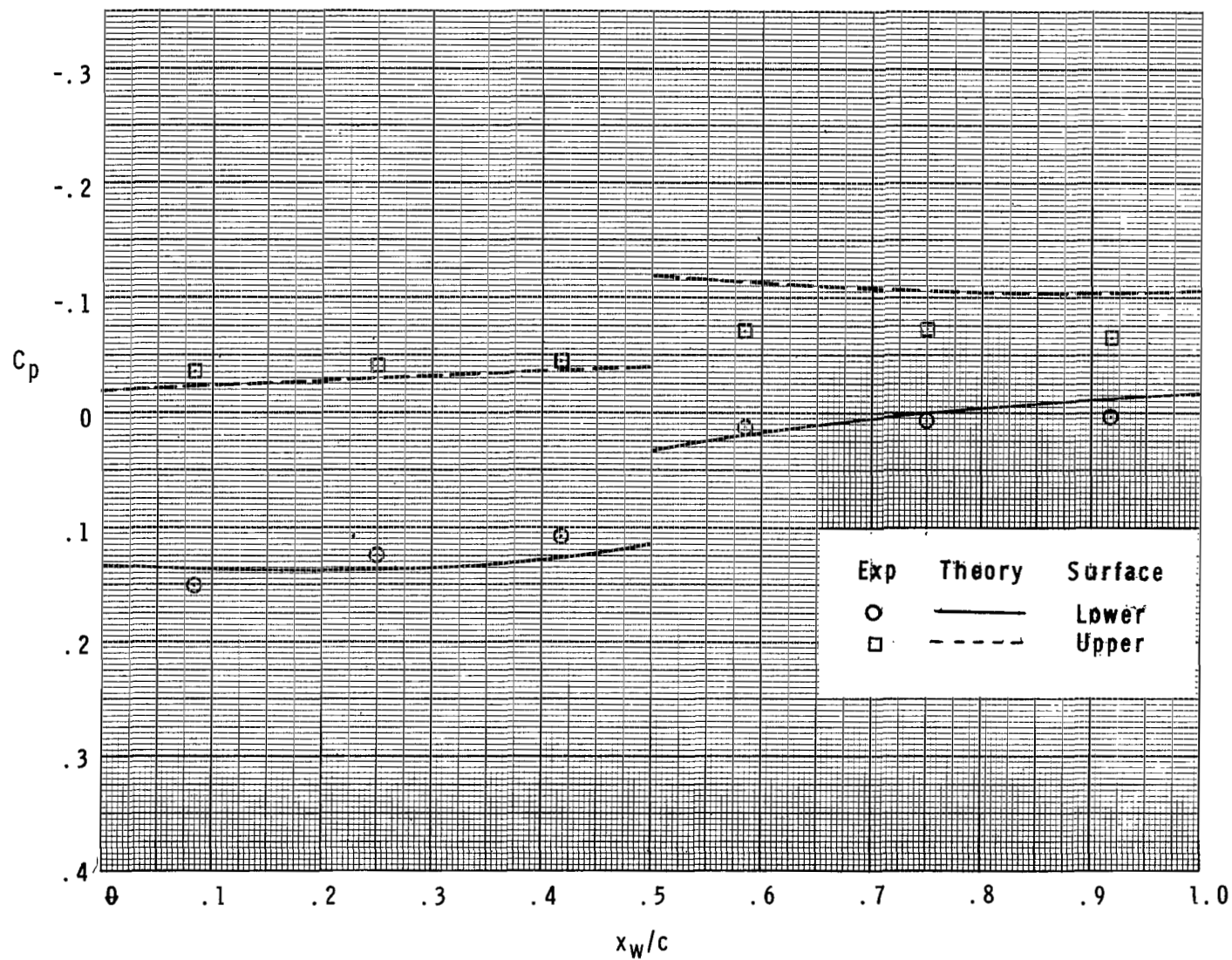
(d) $\frac{y}{b/2} = 0.815$.

Figure 13.- Concluded.



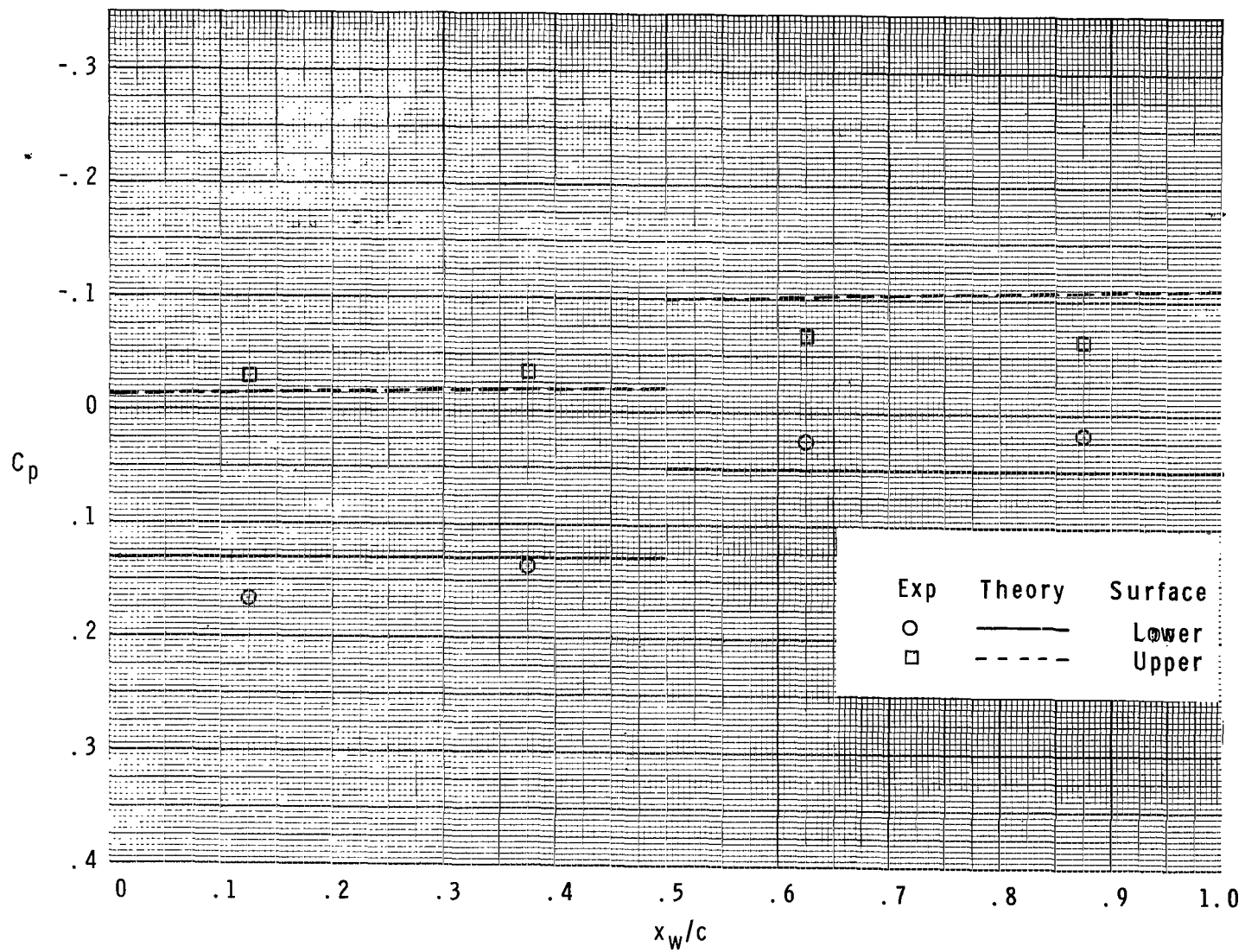
(a) $\frac{y}{b/2} = 0.258$.

Figure 14.- Comparison of wing experimental data with linear-theory method; $\alpha = 6.4^\circ$; $M = 3.95$.



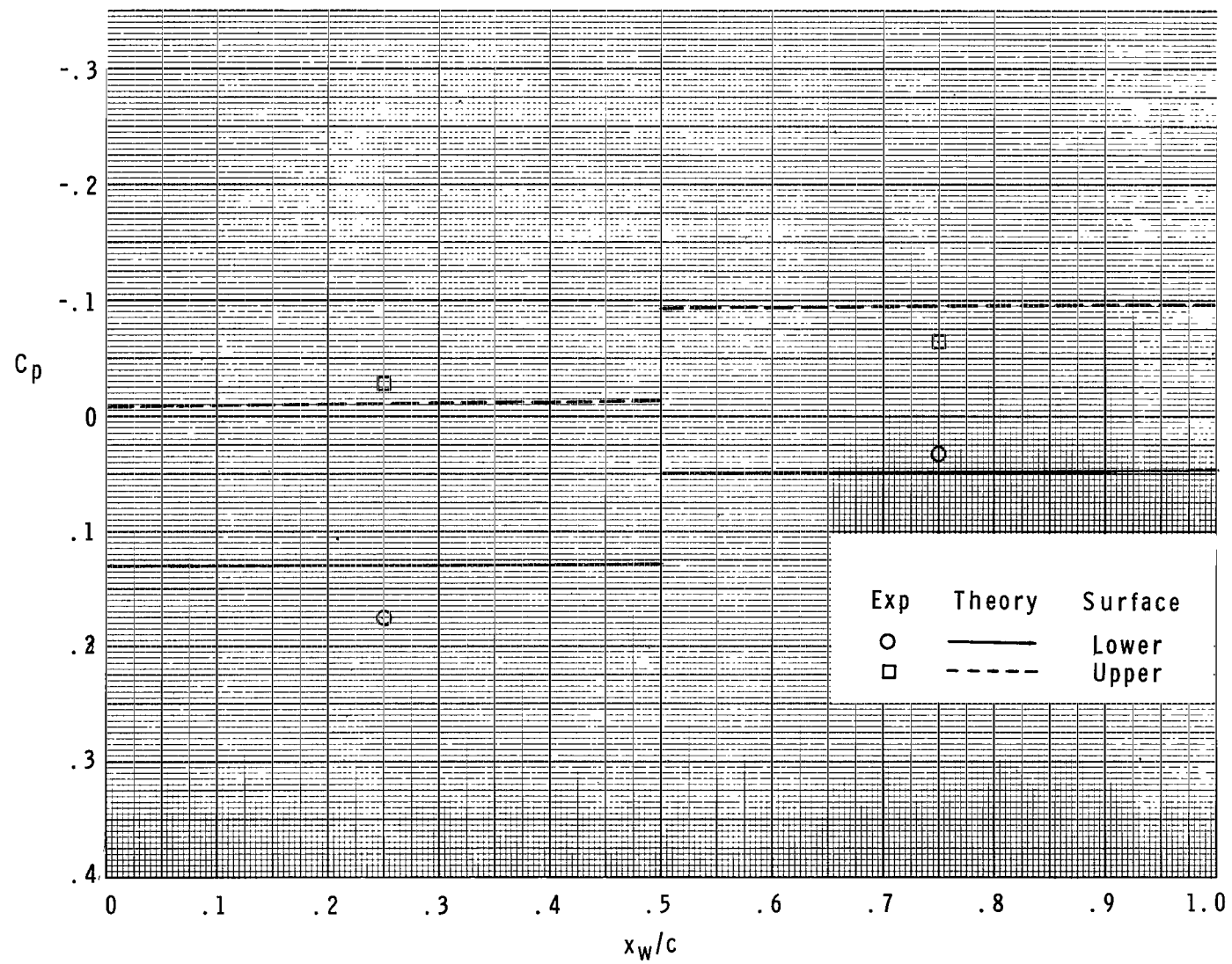
(b) $\frac{y}{b/2} = 0.444$.

Figure 14.- Continued.



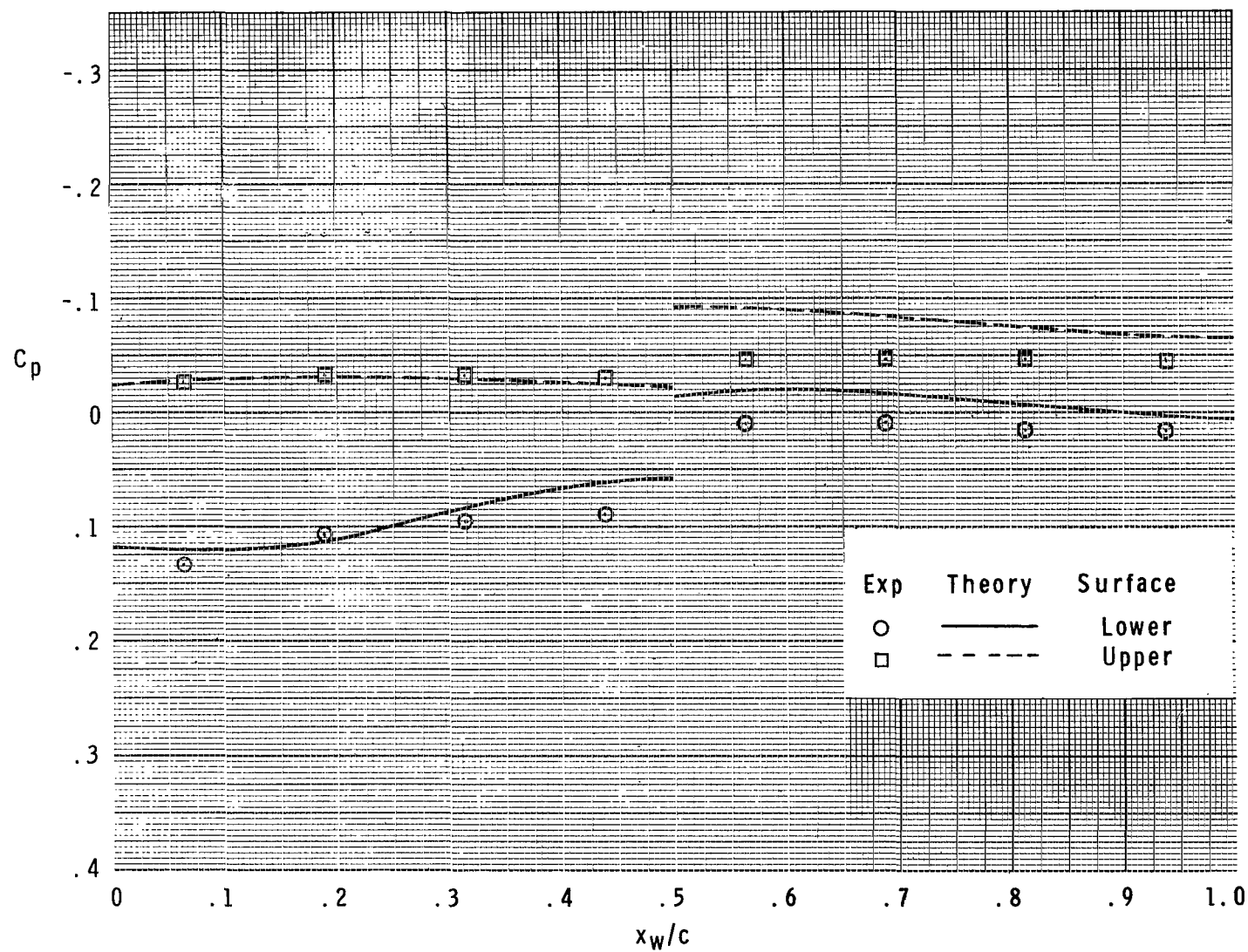
(c) $\frac{y}{b/2} = 0.629$.

Figure 14.- Continued.



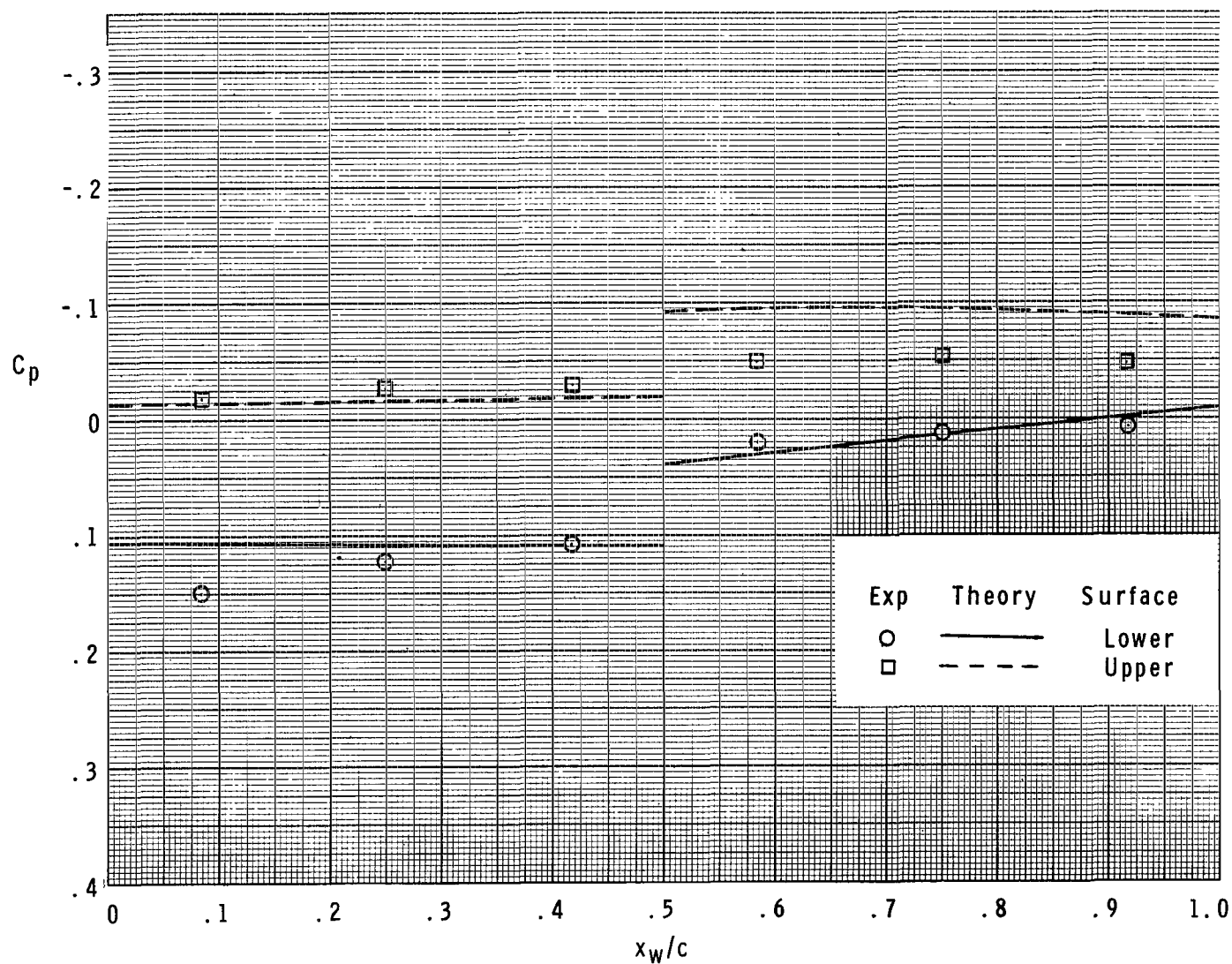
(d) $\frac{y}{b/2} = 0.815$.

Figure 14.- Concluded.



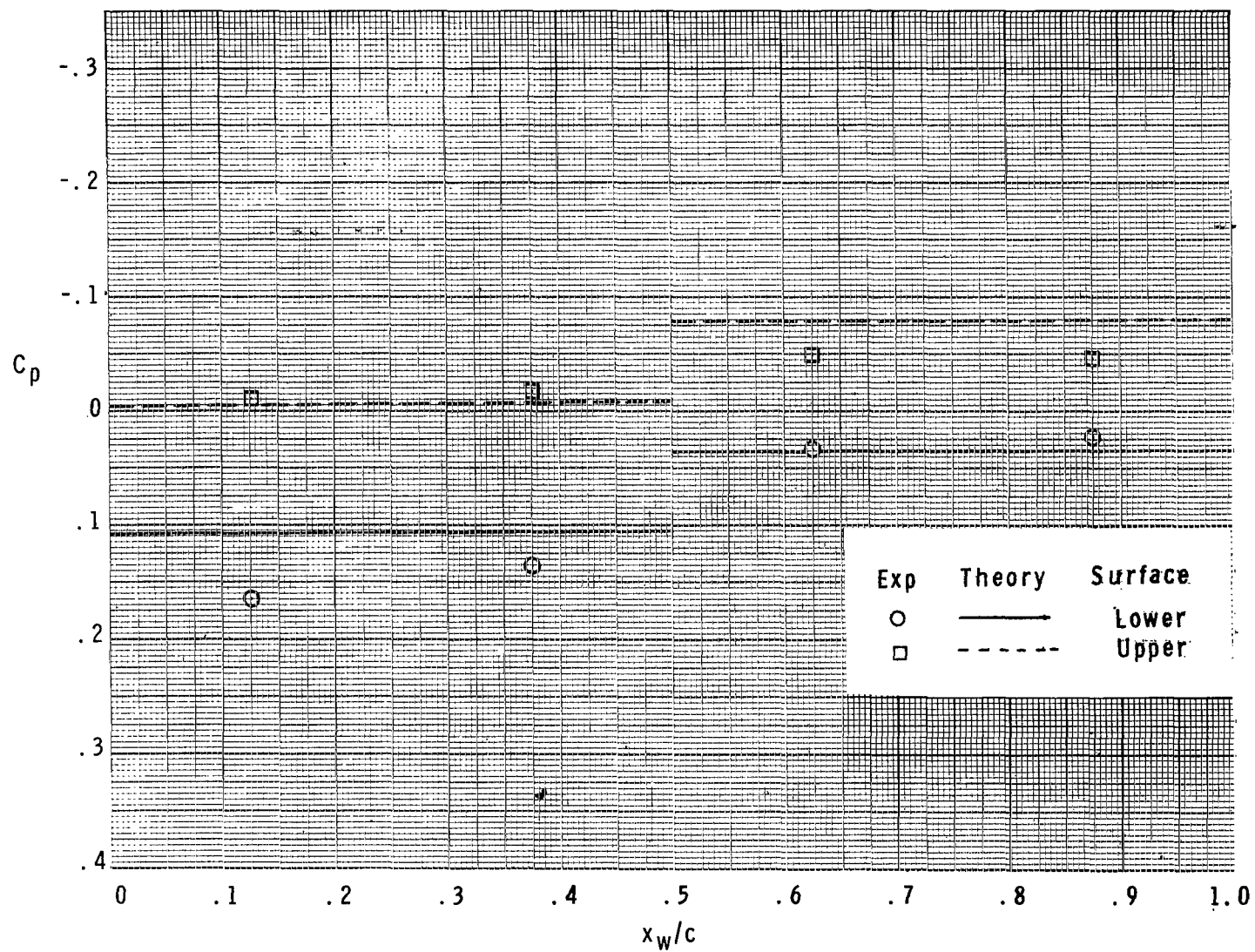
(a) $\frac{y}{b/2} = 0.258$.

Figure 15.- Comparison of wing experimental data with linear-theory method; $\alpha = 6.2^\circ$; $M = 4.63$.



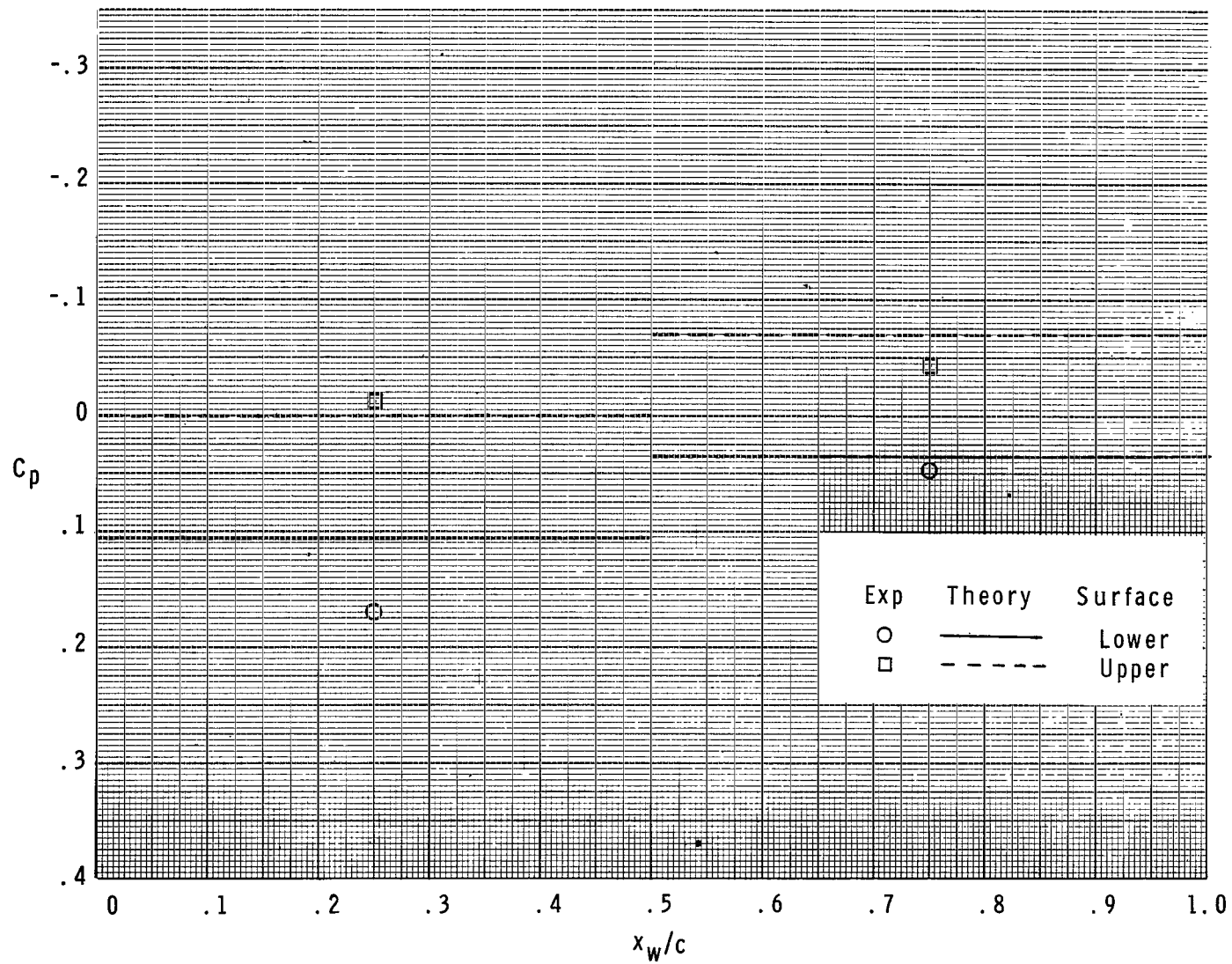
(b) $\frac{y}{b/2} = 0.444.$

Figure 15.- Continued.



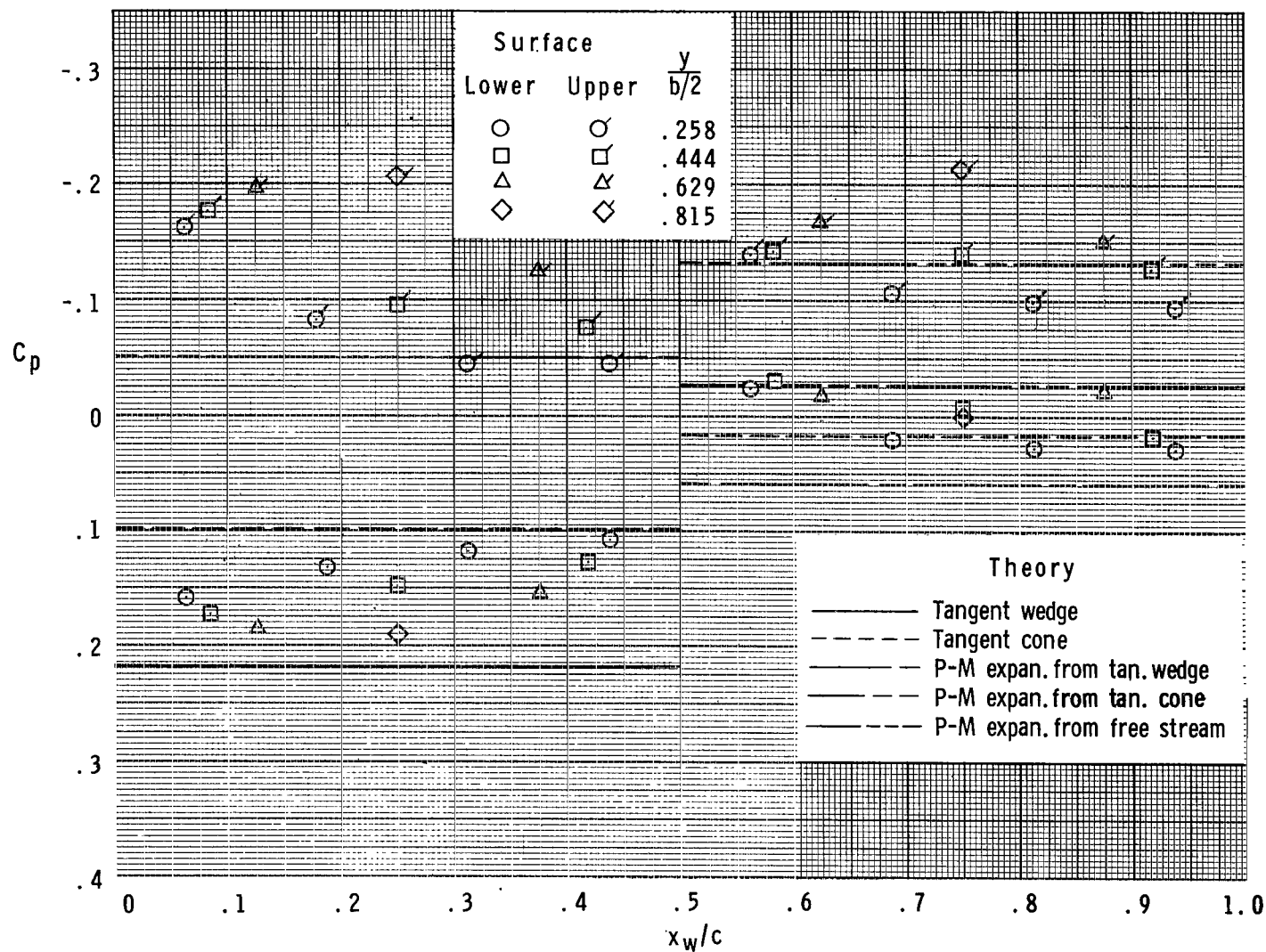
(c) $\frac{y}{b/2} = 0.629$.

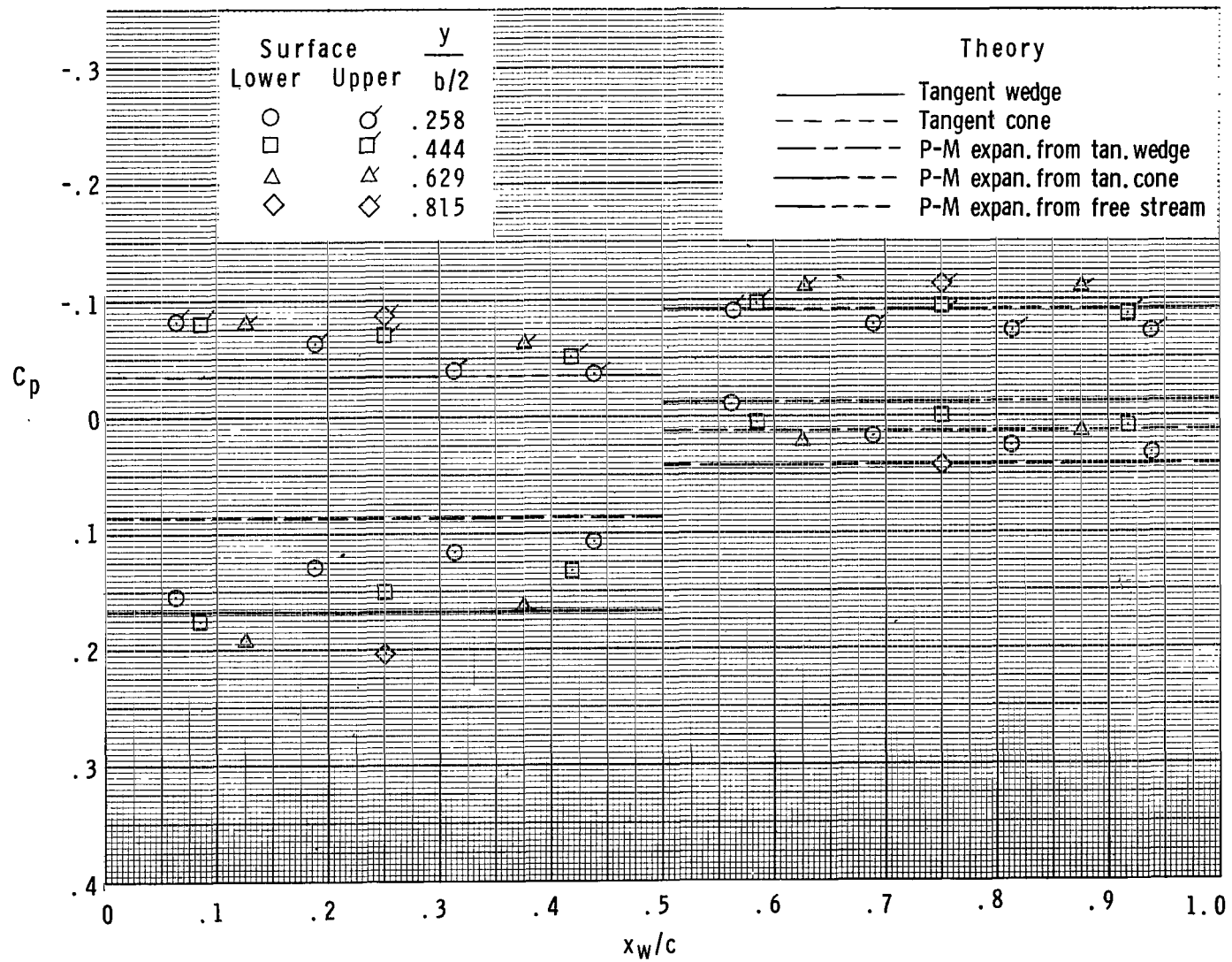
Figure 15.- Continued.



(d) $\frac{y}{b/2} = 0.815$.

Figure 15.- Concluded.

(a) $M = 2.30$.Figure 16.- Comparison of wing experimental data with various theories; $\alpha \approx 6^\circ$.



(b) $M = 2.96$.

Figure 16.- Continued.

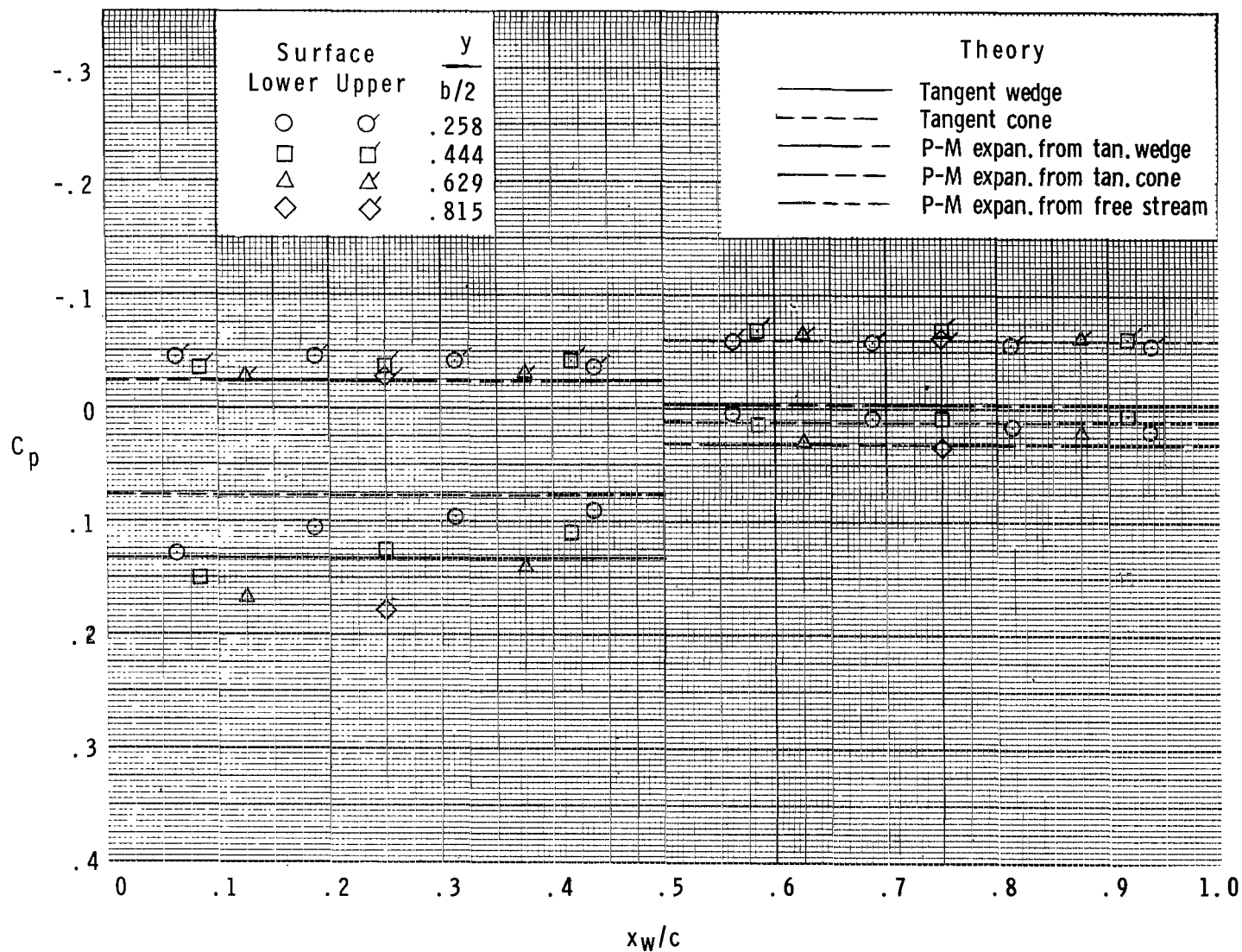
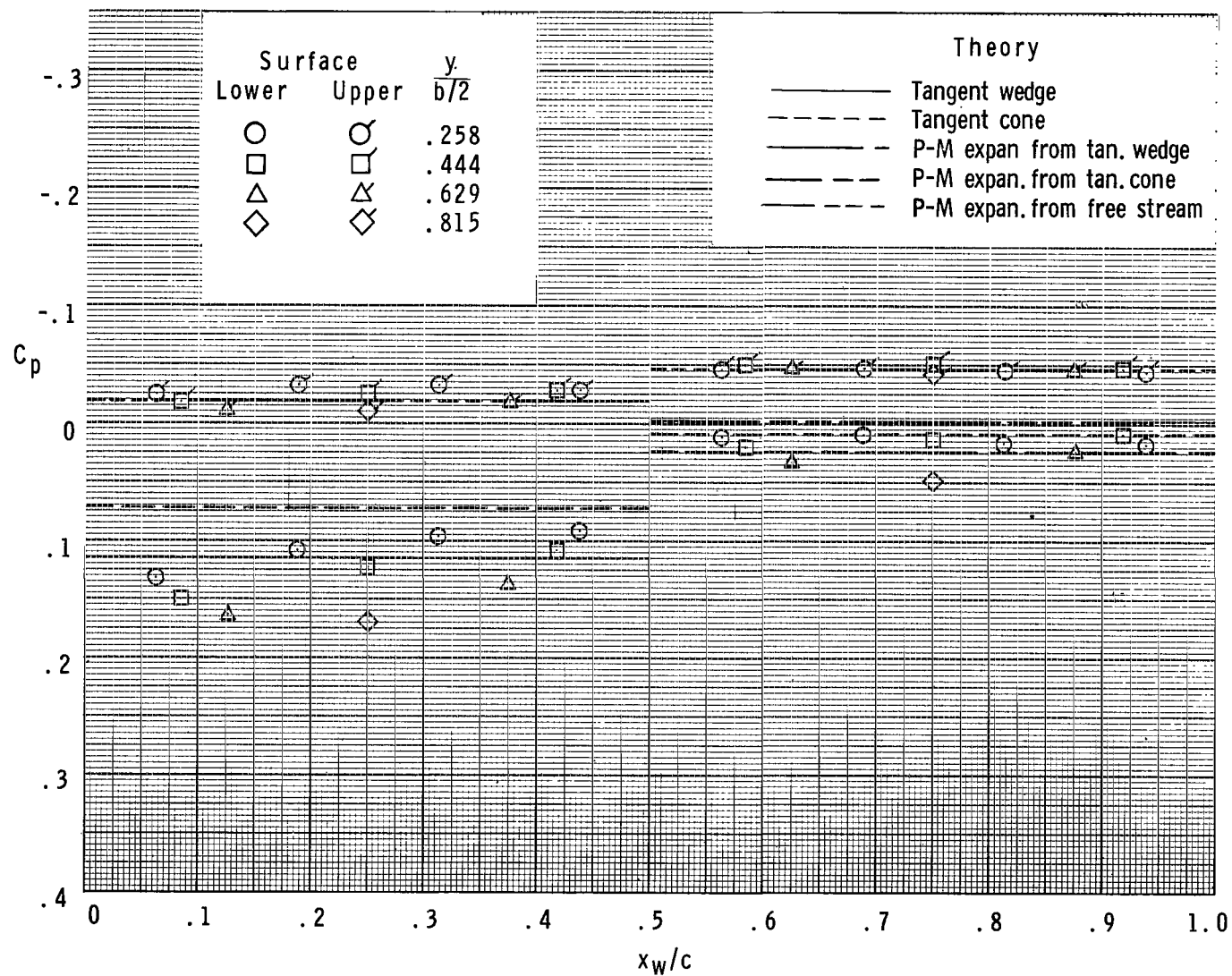
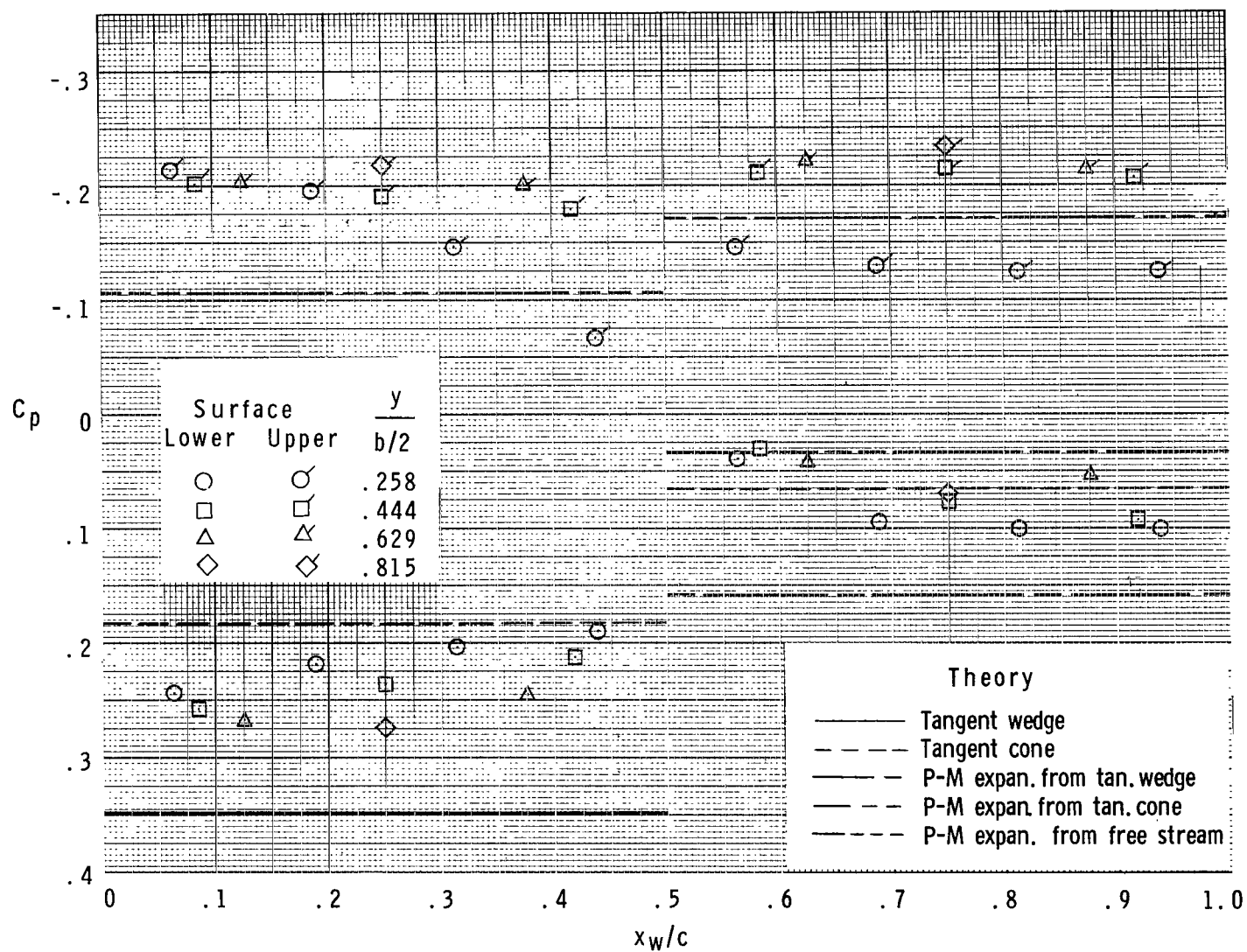
(c) $M = 3.95$.

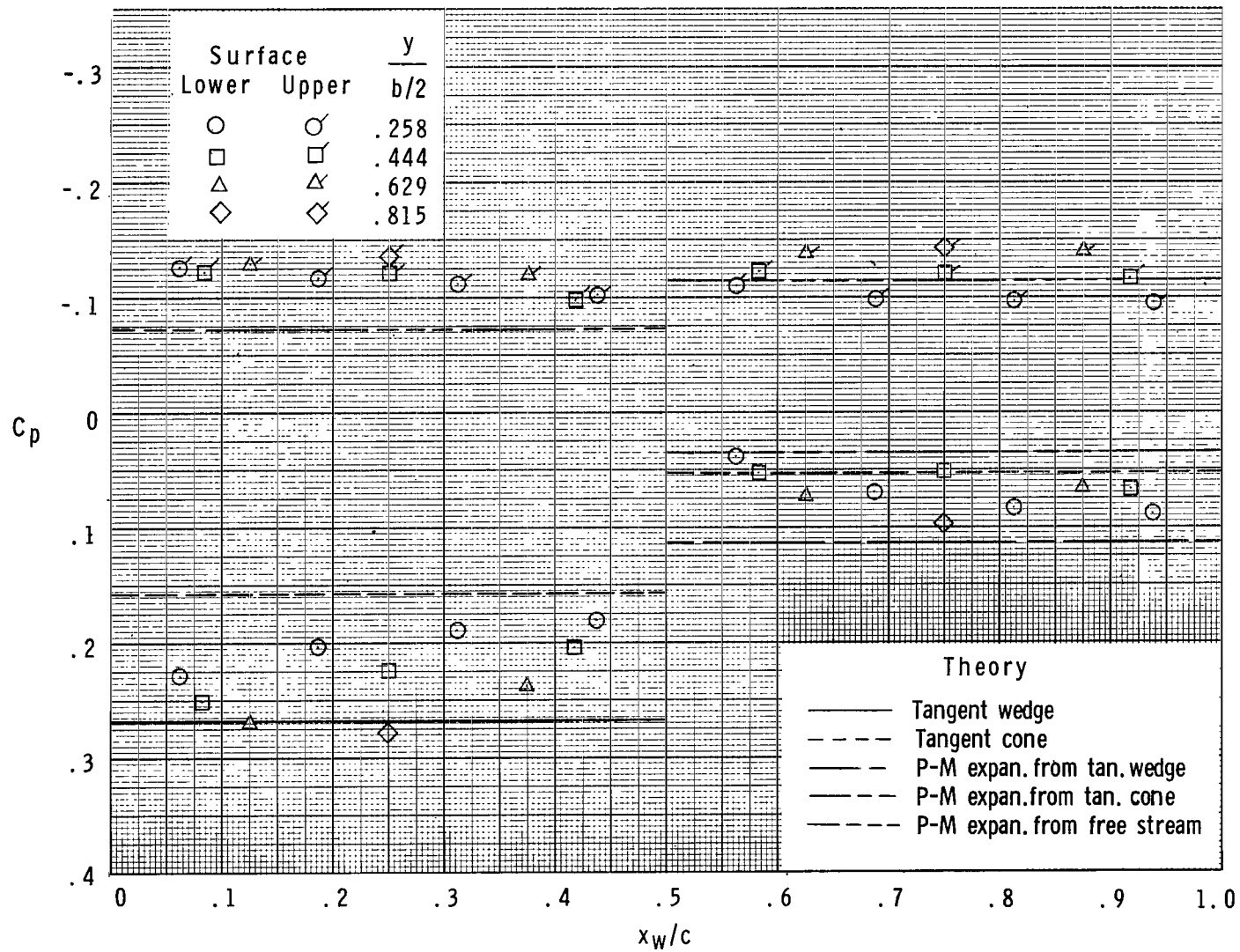
Figure 16.- Continued.



(d) $M = 4.63$.

Figure 16.- Concluded.

(a) $M = 2.30$.Figure 17.- Comparison of wing experimental data with various theories; $\alpha \approx 11^\circ$.



(b) $M = 2.96$.

Figure 17.- Continued.

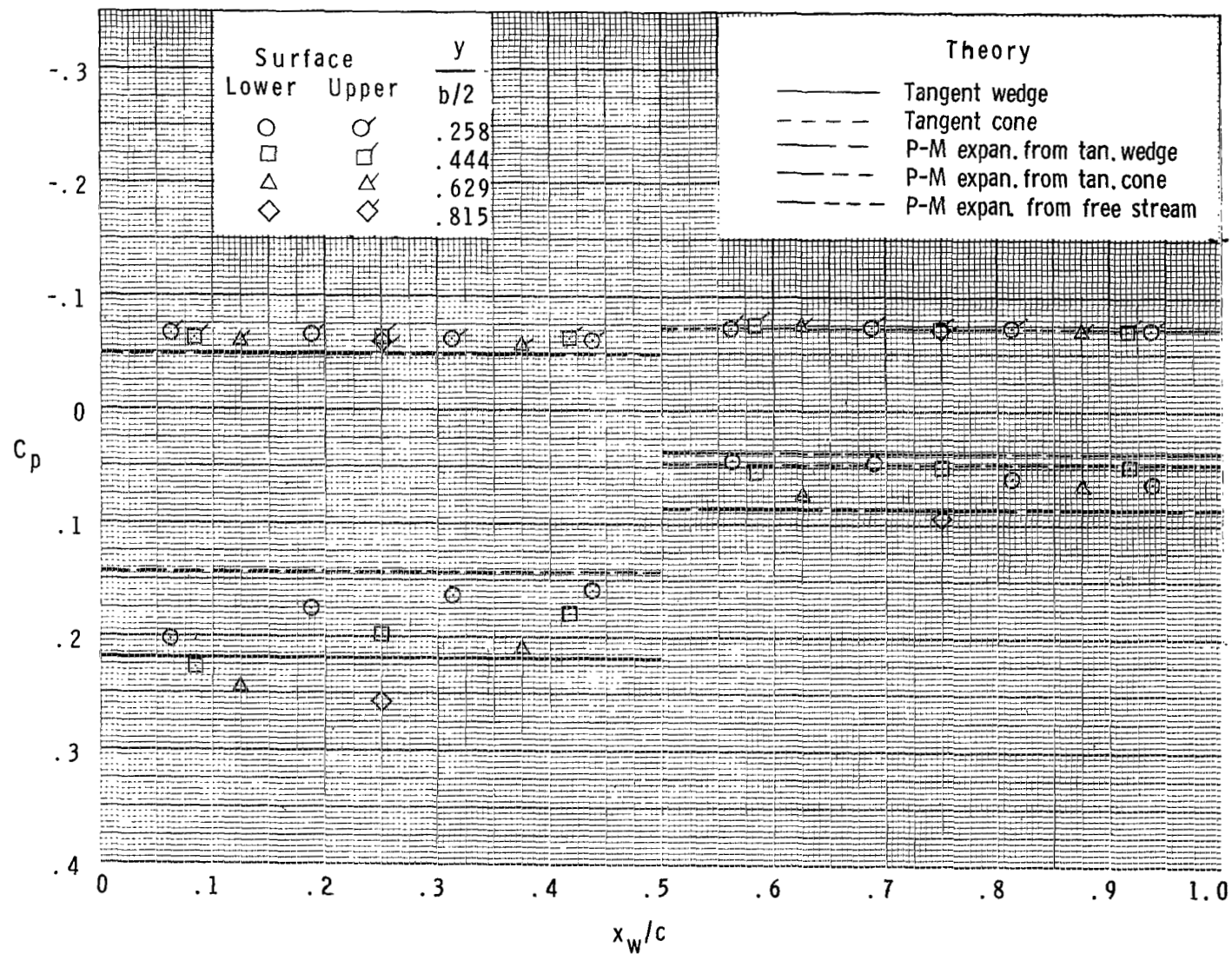
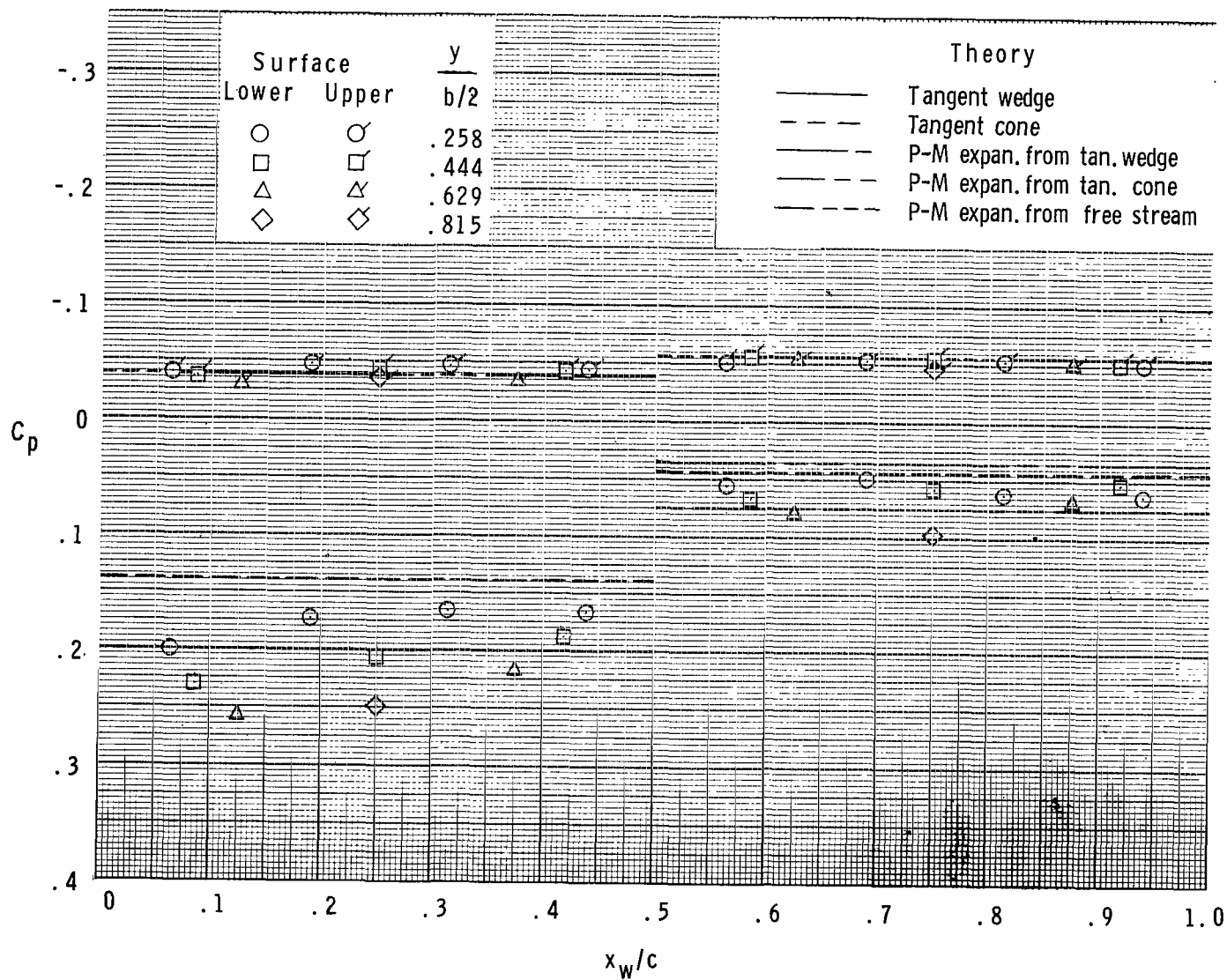
(c) $M = 3.95$.

Figure 17.- Continued.



(d) $M = 4.63$.

Figure 17.- Concluded.



020 001 C1 U 01 710917 S00903DS
DEPT OF THE AIR FORCE
AF SYSTEMS COMMAND
AF WEAPONS LAB (WL0L)
ATTN: E LOU BOWMAN, CHIEF TECH LIBRARY
KIRTLAND AFB NM 87117

POSTMASTER: If Undeliverable (Section 158
Postal Manual) Do Not Return

"The aeronautical and space activities of the United States shall be conducted so as to contribute . . . to the expansion of human knowledge of phenomena in the atmosphere and space. The Administration shall provide for the widest practicable and appropriate dissemination of information concerning its activities and the results thereof."

— NATIONAL AERONAUTICS AND SPACE ACT OF 1958

NASA SCIENTIFIC AND TECHNICAL PUBLICATIONS

TECHNICAL REPORTS: Scientific and technical information considered important, complete, and a lasting contribution to existing knowledge.

TECHNICAL NOTES: Information less broad in scope but nevertheless of importance as a contribution to existing knowledge.

TECHNICAL MEMORANDUMS: Information receiving limited distribution because of preliminary data, security classification, or other reasons.

CONTRACTOR REPORTS: Scientific and technical information generated under a NASA contract or grant and considered an important contribution to existing knowledge.

TECHNICAL TRANSLATIONS: Information published in a foreign language considered to merit NASA distribution in English.

SPECIAL PUBLICATIONS: Information derived from or of value to NASA activities. Publications include conference proceedings, monographs, data compilations, handbooks, sourcebooks, and special bibliographies.

TECHNOLOGY UTILIZATION PUBLICATIONS: Information on technology used by NASA that may be of particular interest in commercial and other non-aerospace applications. Publications include Tech Briefs, Technology Utilization Reports and Technology Surveys.

Details on the availability of these publications may be obtained from:

**SCIENTIFIC AND TECHNICAL INFORMATION OFFICE
NATIONAL AERONAUTICS AND SPACE ADMINISTRATION
Washington, D.C. 20546**